Robust Control of Transport Refrigeration System

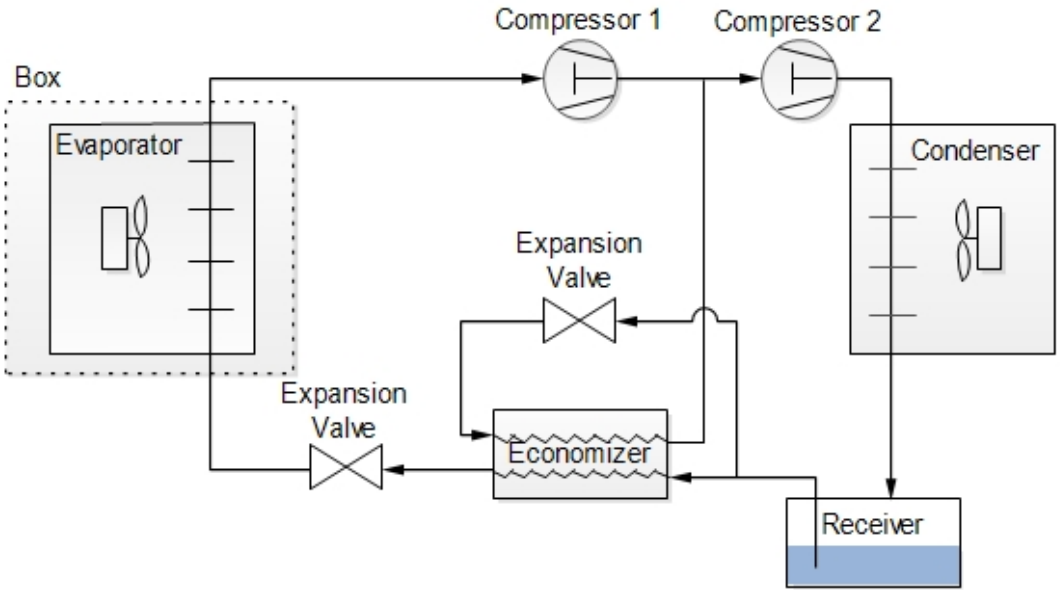

P10 Project - Ajdin Kovačević

Control and Automation

Aalborg University

January 8, 2020

AALBORG UNIVERSITET
STUDENTERRAPPORT

10. Semester - Control and Automation
Fredrik Bajers Vej 7
9220 Aalborg

Title:

Robust Control of Transport Refrigeration System

Project:

10. Semester project

Project period:

1. February 2019 - 8. January 2020

Participant:

Ajdin Kovačević

AAU Supervisors:
Kirsten Mølgaard Nielsen
Tom Søndergaard Pedersen

Company Supervisor:
Kresten Kjær Sørensen

Number of pages: 63
Pages in appendix: 21
Date of hand in: January 8, 2020

Synopsis:

The purpose of this project is to design a robust controller that can handle the dynamic changes in which appears when ice builds up on the evaporator coil. To be able to design such a controller, a model from the company is used. The model is initially a MIMO model of 14 states, 4 inputs and 2 outputs. But to make the controller design simple, it is decided to decouple the MIMO into two SISO systems.
The chosen robust controller is a H_∞ controller and the main goal is to have a stable superheat while ice builds up on the evaporator coil. To design a H_∞ controller some requirements needs to be achieved. These requirements are made for the nominal stability, nominal performance, robust stability and robust performance, which can be achieved by designing weight functions that fits with the conditions. The H_∞ controller is designed as a PID controller and through simulations it is proven to be functional. While it might be functional theoretically. When it is implemented on the real system, it has proven to be difficult to be nominal stable. All in all this project has proven that the solution, to the ice appearance on the evaporator coil issue, might not be a robust control, which therefore gives opportunity to investigate other solutions to this problem.

Table of content

Nomenclature

Units used in section 2.2:

$COP_{Cooling}$	is the coefficient of performance for cooling	$[\cdot]$
T_{Cold}	is the temperature just before the evaporator	[K]
T_{Hot}	is the temperature just after the second stage of the compressor	[K]

Units used in section 2.3:

Q_{Air}	is the heat energy supplied to the pipe from the ambient air	[J]
$\dot{m}_{in}$	is the mass-flow of refrigerant at the inlet of the evaporator	$\left[\frac{\text{Kg}}{\text{s}}\right]$
$\dot{m}_{lm}$	is the mass-flow of refrigerant at the saturated liquid curve	$\left[\frac{\text{Kg}}{\text{s}}\right]$
$\dot{m}_{mg}$	is the mass-flow of the refrigerant at the saturated vapor curve	$\left[\frac{\text{Kg}}{\text{s}}\right]$
$\dot{m}_{out}$	is the mass-flow of refrigerant at the outlet of the evaporator	$\left[\frac{\text{Kg}}{\text{s}}\right]$
T_{in}	is the temperature of the refrigerant at the inlet of the evaporator	[K]
T_{lm}	is the temperature of the refrigerant at saturated liquid curve	[K]
T_{lm}	is the temperature of the refrigerant at saturated vapor curve	[K]
T_{out}	is the temperature of the refrigerant at the outlet of the evaporator	[K]

Units used in section 5.1:

$L_{ev,1}$	is the length of the mixed zone of the evaporator	[m]
P_{ev}	is the pressure of the refrigerant in the evaporator	[bar]
$h_{ev,out}$	is the enthalpy of the refrigerant at the outlet of the evaporator	$\left[\frac{\text{J}}{\text{kg}}\right]$
$h_{ev,in}$	is the enthalpy of the refrigerant at the inlet of the evaporator	$\left[\frac{\text{J}}{\text{kg}}\right]$
$T_{ev,w,m}$	is the temperature of pipe-wall at the mixed zone	[K]
$T_{ev,w,sh}$	is the temperature of the pipe-wall at the superheated zone	[K]
$T_{ev,amb}$	is the ambient temperature at the evaporator	[K]

$\dot{m}_{ev,in}$	is the mass flow of the refrigerant at the inlet of the evaporator	$\left[\frac{\text{kg}}{\text{s}}\right]$
$\dot{m}_{ev,out}$	is the mass flow of the refrigerant at the outlet of the evaporator	$\left[\frac{\text{kg}}{\text{s}}\right]$
$\dot{m}_{in}$	is the mass flow at the inlet of the GMB model	$\left[\frac{\text{kg}}{\text{s}}\right]$
h_{in}	is the enthalpy at the inlet of the GMB model	$\left[\frac{\text{J}}{\text{kg}}\right]$
$\dot{m}_{out}$	is the mass flow at the outlet of the GMB model	$\left[\frac{\text{kg}}{\text{s}}\right]$
T_{amb}	is the ambient temperature at the GMB model	[K]
L_1, L_2	are the length of the different zones in the GMB model	[m]
P	is the pressure of the GMB model	[bar]
$T_{w,m}$, $T_{w,sh}$	are the pipe-wall temperature at different zones of the GMB model	[K]
h_{out}	is the enthalpy at the outlet of the GMB model	$\left[\frac{\text{J}}{\text{kg}}\right]$
$\dot{m}_{mg}$	is the mass flow in between the zones of the GMB model	$\left[\frac{\text{kg}}{\text{s}}\right]$

Units used in section 5.3:

$\rho_{ev,mg}$	is the density of the refrigerant at the saturated curve	$\left[\frac{\text{kg}}{\text{m}^3}\right]$
$\rho_{ev,l}$	is the density of the refrigerant at the sub cooled saturation curve	$\left[\frac{\text{kg}}{\text{m}^3}\right]$
$\rho_{ev,sh}$	is the mean density of the refrigerant at the superheat zone	$\left[\frac{\text{kg}}{\text{m}^3}\right]$
P_{ev}	is the pressure of the refrigerant	[bar]
t	is the time	[s]
$\dot{m}_{ev,in}$	is the mass flow of the refrigerant at the inlet of the evaporator	$\left[\frac{\text{kg}}{\text{s}}\right]$
$\dot{m}_{ev,mg}$	is the mass flow of the refrigerant at the saturated curve	$\left[\frac{\text{kg}}{\text{s}}\right]$
$\dot{m}_{ev,out}$	is the mass flow at the outlet of the evaporator	$\left[\frac{\text{kg}}{\text{s}}\right]$
$\bar{T}_{ev,m}$	is the temperature of the refrigerant in the mixed zone	[K]
$\bar{T}_{w,ev,m}$	is the temperature of the metal pipe	[K]
$\bar{T}_{ev,sh}$	is the temperature of the refrigerant at the superheat zone	[K]
$T_{w,ev,sh}$	is the temperature of the metal pipe at the superheat zone	[K]
$T_{ev,a}$	is the ambient temperature at the evaporator	[K]
$h_{ev,mg}$	is the enthalpy at the saturation curve	$\left[\frac{\text{J}}{\text{kg}}\right]$
$h_{ev,l}$	is the enthalpy at the sub cooled saturation curve	$\left[\frac{\text{J}}{\text{kg}}\right]$
$h_{ev,sh}$	is the mean enthalpy at the superheat zone	$\left[\frac{\text{J}}{\text{kg}}\right]$
$h_{ev,out}$	is the enthalpy of the refrigerant at the outlet of the evaporator	$\left[\frac{\text{J}}{\text{kg}}\right]$

$\alpha_{i,ev,m}$	is the transfer heat coefficient from pipe to refrigerant at the mixed zone	$\left[\frac{\mathrm{W}}{\mathrm{m^2K}}\right]$
$\alpha_{i,ev,sh}$	is the transfer heat coefficient from pipe to refrigerant at the superheat zone	$\left[\frac{\mathrm{W}}{\mathrm{m^2K}}\right]$
$\alpha_{o,ev,m}$	is the transfer heat coefficient from ambient air to refrigerant at mixed zone	$\left[\frac{\mathrm{W}}{\mathrm{m^2K}}\right]$
$\alpha_{o,ev,sh}$	is the transfer heat coefficient from ambient air to refrigerant at superheated zone	$\left[\frac{\mathrm{W}}{\mathrm{m^2K}}\right]$
P_c	is the condenser pressure	[bar]
$\rho_{c,sh}$	is the mean density at the superheated zone	$\left[\frac{\mathrm{kg}}{\mathrm{m^3}}\right]$
$\rho_{c,mg}$	is the density at the superheated saturation curve	$\left[\frac{\mathrm{kg}}{\mathrm{m^3}}\right]$
$\rho_{c,m}$	is the mean density of the refrigerant at the mixed zone	$\left[\frac{\mathrm{kg}}{\mathrm{m^3}}\right]$
$\rho_{c,ml}$	is the density of the refrigerant at the sub-cooled saturation curve	$\left[\frac{\mathrm{kg}}{\mathrm{m^3}}\right]$
$h_{c,sh}$	is the mean enthalpy at the superheated zone	$\left[\frac{\mathrm{J}}{\mathrm{kg}}\right]$
$h_{c,mg}$	is the enthalpy at the superheated saturation curve	$\left[\frac{\mathrm{J}}{\mathrm{kg}}\right]$
$h_{c,ml}$	is the enthalpy of the refrigerant at the sub-cooled saturation curve	$\left[\frac{\mathrm{J}}{\mathrm{kg}}\right]$
$h_{c,out}$	is the enthalpy of the refrigerant at the outlet of the condenser	$\left[\frac{\mathrm{J}}{\mathrm{kg}}\right]$
$\dot{m}_{c,in}$	is the mass flow going into the condenser	$\left[\frac{\mathrm{kg}}{\mathrm{s}}\right]$
$\dot{m}_{c,mg}$	is the mass flow at the superheated saturation curve	$\left[\frac{\mathrm{kg}}{\mathrm{s}}\right]$
$\dot{m}_{c,ml}$	is the mass flow of the refrigerant at the sub-cooled saturation curve	$\left[\frac{\mathrm{kg}}{\mathrm{s}}\right]$
$T_{w,c,sh}$	is the temperature of the metal pipe	[K]
$T_{c,sh}$	is the temperature of the refrigerant in the superheat zone	[K]
$T_{w,c,m}$	is the temperature of the pipe at the mixed zone	[K]
$T_{c,m}$	is the mean temperature of the refrigerant at the mixed zone	[K]
$T_{w,c,l}$	is the temperature of the wall at the sub-cooled zone	[K]
$T_{c,l}$	is the mean temperature of the refrigerant at the sub-cooled zone	[K]
$T_{c,a}$	is the ambient temperature at the condenser	[K]
$\alpha_{i,c,sh}$	is the heat transfer coefficient from refrigerant to pipe at the superheated zone	$\left[\frac{\mathrm{W}}{\mathrm{m^2K}}\right]$
$\alpha_{i,c,m}$	is the transfer heat coefficient from refrigerant to pipe at the mixed zone	$\left[\frac{\mathrm{W}}{\mathrm{m^2K}}\right]$
$\alpha_{i,c,l}$	is the transfer heat coefficient from refrigerant to pipe at the sub-cooled zone	$\left[\frac{\mathrm{W}}{\mathrm{m^2K}}\right]$

$\alpha_{o,c,sh}$	is the transfer heat coefficient from pipe to ambient air at the superheated zone	$\left[\frac{\mathrm{W}}{\mathrm{m^2K}}\right]$
$\alpha_{o,c,m}$	is the transfer heat coefficient from pipe to ambient air at the mixed zone	$\left[\frac{\mathrm{W}}{\mathrm{m^2K}}\right]$
$\alpha_{o,c,l}$	is the transfer heat coefficient from pipe to ambient air at the sub-cooled zone	$\left[\frac{\mathrm{W}}{\mathrm{m^2K}}\right]$
$\dot{m}_v$	is the mass flow rate of the refrigerant through the valve	$\left[\frac{\mathrm{kg}}{\mathrm{s}}\right]$
C_v	is the discharge coefficient	$[\cdot]$
A_V	is the opening area	$\left[\mathrm{m^2}\right]$
ρ_v	is the density of the refrigerant at the inlet of the valve	$\left[\frac{\mathrm{kg}}{\mathrm{m^3}}\right]$
ΔP	is the pressure drop across the valve	[bar]
$h_{exp,in}$	are the enthalpy before the expansion valve	$\left[\frac{\mathrm{J}}{\mathrm{kg}}\right]$
$h_{exp,out}$	are the enthalpy after the expansion valve	$\left[\frac{\mathrm{J}}{\mathrm{kg}}\right]$
$\dot{m}_{cpr}$	is the mass flow of the refrigerant at the compressor	$\left[\frac{\mathrm{kg}}{\mathrm{s}}\right]$
ω	is the compressor speed	[Hz]
V_{cpr}	is the volume of the compressor	$\left[\mathrm{m^3}\right]$
ρ_{cpr}	is the density of the refrigerant at the compressor	$\left[\frac{\mathrm{kg}}{\mathrm{m^3}}\right]$
C_{cpr}	s the constant followed by the ideal gas law	$[\cdot]$
P_c	is the pressure at the condenser	[bar]
n	is the polytropic coefficient	$[\cdot]$
$h_{cpr,out}$	is the enthalpy of the refrigerant at the outlet of the compressor	$\left[\frac{\mathrm{J}}{\mathrm{kg}}\right]$
$h_{cpr,out,ist}$	is the enthalpy of the refrigerant at the outlet of the compressor during isentropic process	$\left[\frac{\mathrm{J}}{\mathrm{kg}}\right]$
$h_{cpr,in}$	is the enthalpy of the refrigerant the inlet of the compressor	$\left[\frac{\mathrm{J}}{\mathrm{kg}}\right]$
η_{cpr}	is the efficiency coefficient of the compressor	$[\cdot]$

Units used in section 6.4:

cpr.mdot	is the massflow at the compressor	$\left[\frac{\mathrm{kg}}{\mathrm{s}}\right]$
evap.pout	is the pressure at the outlet of the evaporator	[bar]
evap.hout	is the enthalpy at the outlet of the evaporator	$\left[\frac{\mathrm{J}}{\mathrm{kg}}\right]$
evap.mdotin	is the mass flow at the inlet of the evaporator	$\left[\frac{\mathrm{kg}}{\mathrm{s}}\right]$
evap.sigma	is the boundary between liquid/gas mix and superheated gas region	$[\cdot]$
*evap.m*1	is the mass of liquid/gas mix in the mixed zone of the evaporator	[kg]
*evap.m*2	is the mass of superheated gas in the superheated zone of the evaporator	[kg]

$evap.Tm1$	is the temperature of the metal at the mixed zone of the evaporator	[°C]
$evap.Tm2$	is the temperature of the metal at the superheated zone of the evaporator	[°C]
$evap.Tsup$	is the temperature of the supplied air to the evaporator	[°C]
$evap.Tsuc$	is the temperature at the inlet of the compressor	[°C]
$evap.Tsupm1$	is the temperature of the supplied air from the first fan blowing the air	[°C]
$evap.Tsupm2$	is the temperature of the supplied air from the second fan blowing the air	[°C]
$evap.mdotair$	is the mass flow of the air blown to the evaporator	$\left[\frac{\text{kg}}{\text{s}}\right]$
$ctrl.cpr.spe$	is the compressor frequency	[Hz]
$ctrl.evap.ve$	is the expansion valve opening degree value	[%]
$ctrl.vfan.ev$	is the fans speed	$[\cdot]$
$ctrl.Tret$	is the temperature insider of the container	[°C]

Preface 1

The project and report is conducted by Ajdin Kovacevic, attending master project of Control and Automation at Lodam electronics in the Spring semester of 2019. The report consists of nine chapters and [n] appendices.

Some requisites are required in order to fully understand the report: The essentials of robust control theory and thermodynamic modelling.

Harward method is used for referencing in the report. The reference pages can be found in the list of reference, and will referred to with citations written as [index number].

The matlab code used in the project specifically for the modelling and robust control part can be found in the submitted attached file. It will be in the folder named: *"Matlab"*. To run the scripts it is necessary to install LET-Toolbox and xSteam-toolbox.

Continuation of last semester project

The report [1] will be referenced throughout the modelling section of this project, since that report is also conducted by Ajdin Kovacevic, and it is about the modelling of the same system.

This thesis project is a continuation from previous semester work [1]. Since the previous work was focused on making the state space moving boundary model for the system, the control system will be focused in this thesis project. Throughout this project some of the previous work will be cited as [1] and some of the stuff will be copied to the appendix as it will help the reader to understand some parts of the project.

Part I

Introduction

Introduction To The Project 2

2.1 The Transport-Refrigeration System

Refrigeration systems is widely used in many different ways. There are refrigeration systems in stores, at homes and also in transportation of food. The transport-refrigeration system, such as reefer containers, are operating under different condition which can be complicated to control with classical methods without worsening the performance. The main issue that can appear in such system is that ice builds up on the evaporator coil and will block the cooling effect which the evaporator has.

One of the worst cargo to transport is garlic, since it has difficult requirements to keep it cooled. After the garlic is stored at near 0 $^{\circ}C$, it produces a lot of water moisture and heat to the air. This is the reason for ice building up on the evaporator coil as the amount of water moisture allowed in the low air temperature is lowered. This will be explained through some Hx-diagrams later in this Part of the report.

It will therefore be focused to buildup a robust control system to this refrigeration system that might potentially improve the system.

The Transport-Refrigeration system that is used in this project will be the reefer container available at Lodam Electronics A/S, which looks like as seen in Figure 2.1[2].

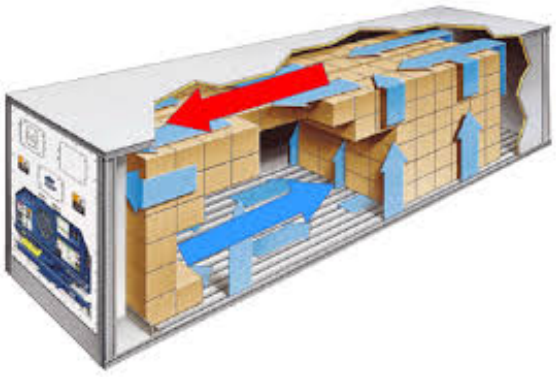

Figure 2.1: A figure showing the reefer container and the arbitrary airflow inside of the container

The transport-refrigeration system can be seen as a block diagram in Figure 2.2. This figure is easier to interpret, what components are used in the system and how each are

connected to each other[2].

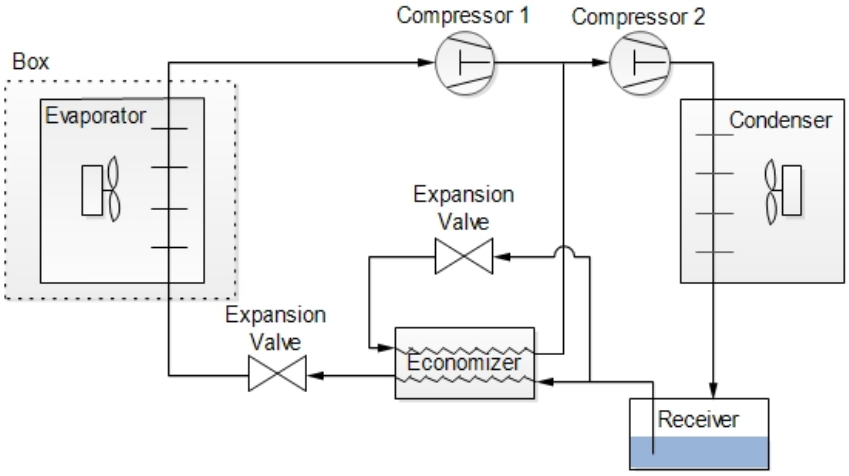

Figure 2.2: This figure shows a block diagram of the refrigeration system setup used in this project.

This system can be comparable to a general vapor compression system. In this case the only difference is that there is a dual compressor system and an extra expansion valve that is used to control the economizer. The added receiver works as a buffer which is only used if suddenly more cooling capacity is needed. The economizer also helps to deal with the same problem by cooling the refrigerant more before it enters the evaporator expansions valve, but also has the feature to cool some of the refrigerant after the first stage compressor (compressor 1, in Figure 2.2).

2.2 PH-Diagram For The Refrigeration System

Since there are some added changes in the refrigeration system compared to a general vapor compression system, the Pressure-Enthalpy diagram for this will also be changed. As seen in Figure 2.3, the added component to the system as the dual compressor and the economizer, makes the system more efficient in cooling. This can be interpreted by looking at point (b) in Figure 2.3. If only one compressor is used, the refrigerant at point (b) will be more to the right, which means that the temperature of the refrigerant at this point would be more hot compared to if a dual compressor system is used. The pros of this kind of system is that the coefficient of performance, COP, for cooling will be ensured, so that it will not get a worse COP when more cooling capacity is needed. This in fact can increase the COP in these cases because of the temperature difference decrease. To be more precise the COP for cooling can be calculated as seen in Equation 2.1. And the only con for the added component are the expenses.

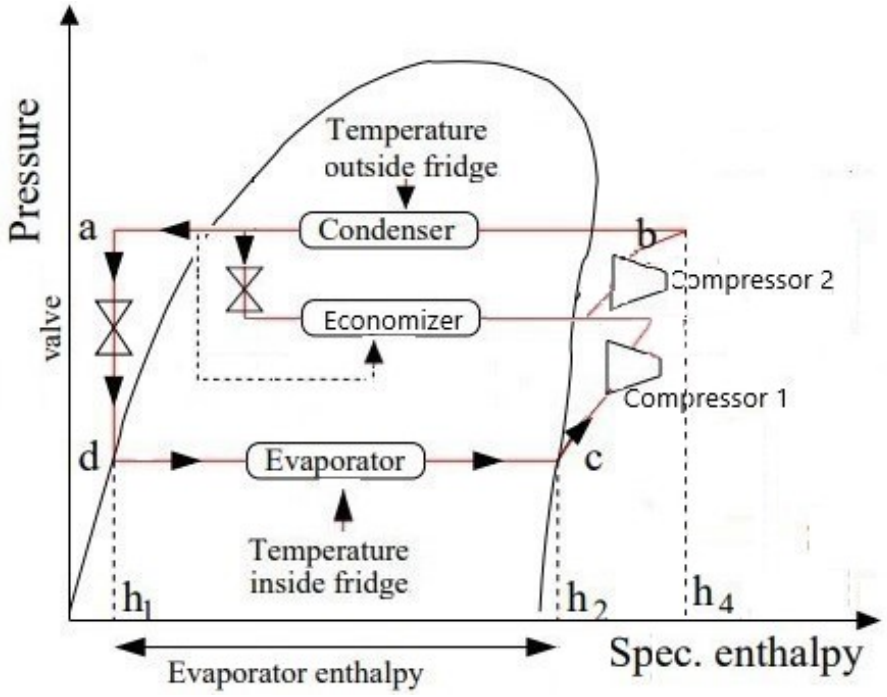

Figure 2.3: This figure shows the PH diagram for the refrigeration system used in this project

$$COP_{Cooling} = \frac{T_{Cold}}{T_{Hot} - T_{Cold}} \tag{2.1}$$

Where:

$COP_{Cooling}$	is the coefficient of performance for cooling	[·]
T_{Cold}	is the temperature just before the evaporator	[K]
T_{Hot}	is the temperature just after the second stage of the compressor	[K]

2.3 Evaporator, Superheat

In this section an important variable will be explained which is the superheat, TSH for short. An evaporator has three phases, the subcooled zone (liqiud), mixed zone (liqiud+gas) and superheated zone(gas). The superheat is determined by the temperature difference between the outlet temperature of the evaporator and the boiling point at a specific pressure of the refrigerant, which is the point (c) in Figure 2.3. This temperature difference, TSH, is not allowed to reach 0 ℃. If it happens then some liquid might enter the compressor and destroy it. To prevent this from happening, a control system is necessary. To give an easier interpretation of the three phases of an evaporator see Figure 2.4 and to see how superheat is calculated see Equation 2.2.

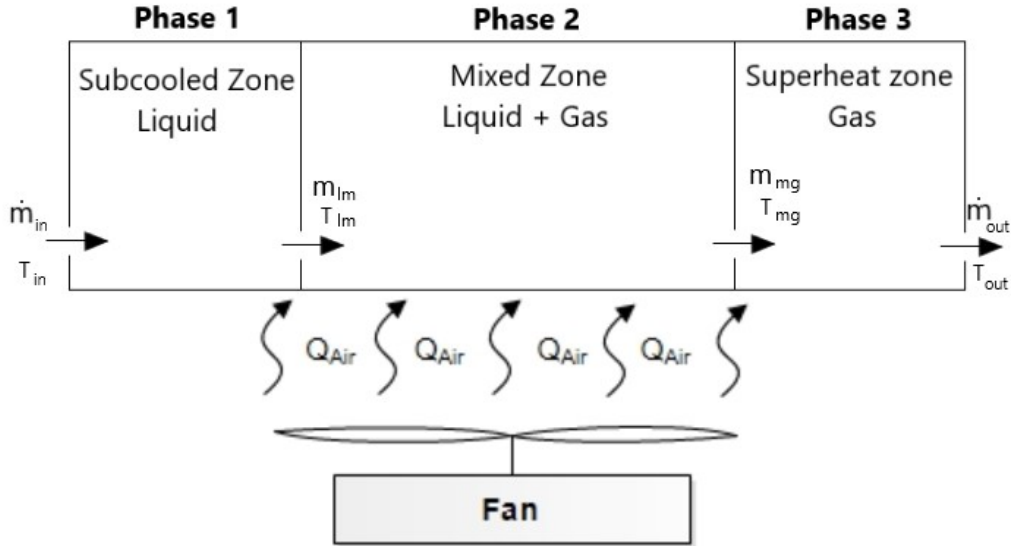

Figure 2.4: This figure shows the flow of an evaporator.

Where:

Q_{Air}	is the heat energy supplied to the pipe from the ambient air	[J]
$\dot{m}_{in}$	is the mass-flow of refrigerant at the inlet of the evaporator	$\left[\frac{\text{Kg}}{\text{s}}\right]$
$\dot{m}_{lm}$	is the mass-flow of refrigerant at the saturated liquid curve	$\left[\frac{\text{Kg}}{\text{s}}\right]$
$\dot{m}_{mg}$	is the mass-flow of the refrigerant at the saturated vapor curve	$\left[\frac{\text{Kg}}{\text{s}}\right]$
$\dot{m}_{out}$	is the mass-flow of refrigerant at the outlet of the evaporator	$\left[\frac{\text{Kg}}{\text{s}}\right]$
T_{in}	is the temperature of the refrigerant at the inlet of the evaporator	[K]
T_{lm}	is the temperature of the refrigerant at saturated liquid curve	[K]
T_{lm}	is the temperature of the refrigerant at saturated vapor curve	[K]
T_{out}	is the temperature of the refrigerant at the outlet of the evaporator	[K]

$$TSH = T_{out} - T_{mg} \tag{2.2}$$

Evaporator, Ice buildup problem 3

In this chapter it will be focused on the issue in this project which is about the ice buildup, that occurs on the evaporator in special cases.

3.1 Absolute- and Relative Humidity, H-X Diagram

As explained in section 2.1 ice builds up on the evaporator when food, that emits a lot of water moisture and heat to the air, needs to be stored at 0 ℃. To understand the relation between the air temperature and the relative humidity an H-X diagram will be used as seen in Figure 3.1. A way to look at this figure is first to understand what the different expressions are.

In open air there will always be some water particles in it. This is what absolute humidity is used for. The absolute humidity shows the amount of water in air with the unit $\frac{kg(water)}{kg(air)}$. The relative humidity shows how much of the air is condensed in relative to the air temperature. This means that when the relative humidity reaches at 100 %, some of the water can be frozen. Figure 3.1 illustrates that the higher air temperature there is, the more air can contain water until the air is fully condensed [3].

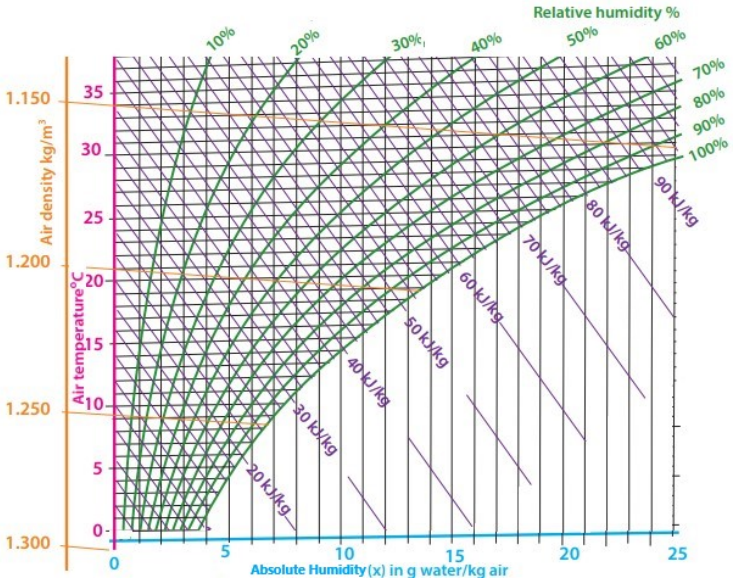

Figure 3.1: This figure shows the H-X diagram [3].

Comparing it to the problem where food needs to be stored at 0 ℃, it can be seen, on the figure, that approximately 3.8 g of water in 1 kg air is enough to fully condense the air. And while some food emits a lot of water moisture and heat to the air, the problem happens to be unavoidable. A more visual representation of how it is connected to the refrigeration unit(evaporator) see Figure 3.2

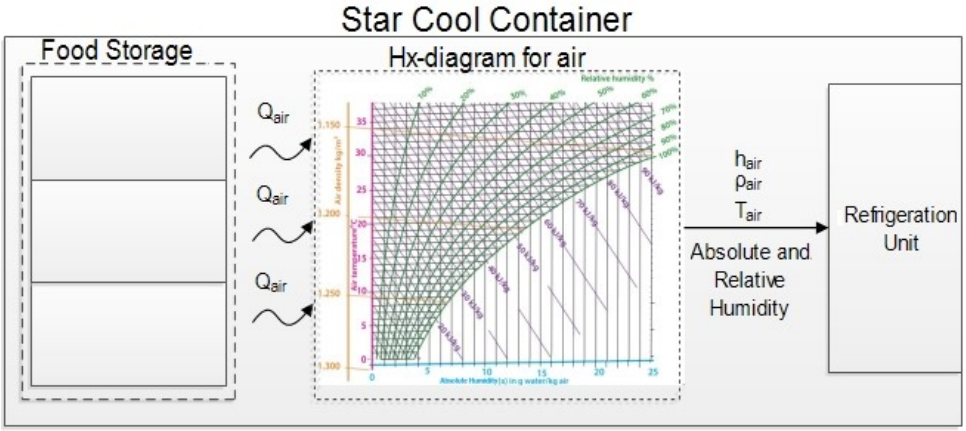

Figure 3.2: This figure shows the flow in a star cool container using H-X diagram

3.2 Defrosting

Since the problem is unavoidable, a solution that is used on the container is as seen in Figure 3.3. This block diagram is almost the same as before in Figure 2.2, modified to handle ice is buildup at a certain point. The modification is that a connection between the outlet of the dual compressor and the inlet of the evaporator is made. This way, the system can use some of the heat produced from the dual compressor and melt the ice with heat from the inside of the evaporator.

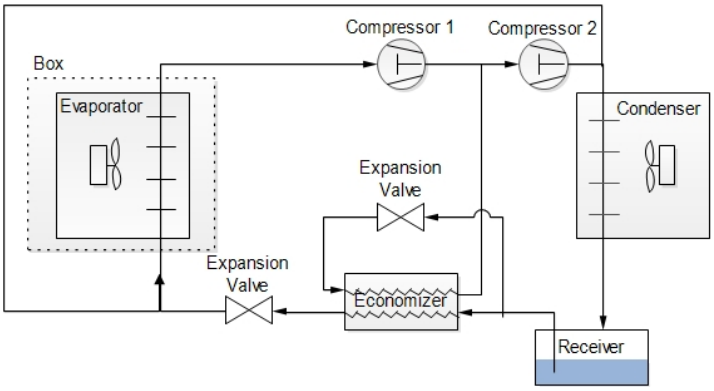

Figure 3.3: This figure shows the block diagram of the container system in defrosting state.

In this project a different approach will be focused on. Instead of using the current method of defrosting, a specific design of a controller will be experimented with, which is a robust control.

Requirements for the system 4

In this chapter the requirements for both the nominal system and the robust design requirements will be explained.

4.1 Requirements For The Nominal System

Since it is desired to design a robust controller, it is necessary to know what the controller needs to be robust against. This requirement section will therefore help this project to design a robust controller. The controller will require to operate at a specific operating point, which will be 0 $^{\circ}C$ air temperature. This is the temperature needed to keep the worst case cargo cooled.

In the refrigeration system, a superheat of 0 $^{\circ}C$ in the evaporator would be the most efficient. However this is practically impossible since the superheat will oscillate and let some of the liquid from the the evaporator to get to the compressor in which it then will destroy the compressor in the system. From tests of the existing controller in the system, it is measured that the possible operating superheat area will be for this project in the interval of 4 $^{\circ}C$ - 8 $^{\circ}C$.

Since the operating area is around 0 $^{\circ}C$ air temperature, ice can buildup on the evaporator coil depending on the humidity level. This means that the nominal system needs to be stable in regards to the evaporator dynamic changes because of the amount of ice blockage. It needs to be stable in regards to changes of the amount of load in the system. And it needs to be stable in regards to the humidity level of the air. The energy that the dry air generator of the system can provide is a load from 0 [kW] - 8000 [kW] and for the humid air generator from 0 [kW] - 9000 [kW]. By a rule of thumb so that the system does not go out of control, the load of the dry air generator needs to be double the amount compared to the humid air generator.

It is possible to control certain components in the system, which will be essential for designing the controller. These components are the valves, compressor, and the fans in the system. The compressor can run at different speeds in the interval from 20 [Hz] - 110 [Hz]. The expansion valves can be opened from 0 % - 100 %. The fans has three settings, where each setting corresponds to an air velocity from the fans.

In order to see improvement of the system, a comparison between the currently used controller to the robust controller in this project will determine the improvements and

vice versa by calculating the COP for cooling.

The aim of this master thesis is to create a controller, which is nominal stable in the operating area given earlier and at the same time being robust towards the change in the transfer heat coefficients for the evaporator. These requirements are summed up in Table 4.1.

	Requirement	**Unit**
Air temperature	0	[°C]
System load	0 to 8000	[kW]
Humidity generator	0 to 4000	[kW]
Working area for compressor frequency	20 to 110	[Hz]
Superheat operating area	4 to 8	[°C]

Table 4.1: The nominal system requirements for this project.

4.2 Robust Requirements, uncertainties For Control Design

Throughout the design of the robust controller, some uncertainties needs to be considered. When ice buildup happens, some parameters becomes uncertain. These parameters are specifically related to the heat transfer coefficient, because the heat from the fans for the evaporator gets blocked by the ice. This will become the uncertain parameter though out the robust control design. The requirements for the controller design will be set to handle the worst case scenario of the heat transfer coefficient. This worst case value is set to be 1225 $\frac{W}{m^2K}$, which is a value that the company supervisor Kresten Sørensen provided with.

Part II

Modelling

In this part the model of the system will be explained. The total model includes the evaporator, condenser, expansion valve and the compressor which are modelled and explained in the part. The evaporator and condenser are modelled with help of moving boundary method. This ensures a model with a low order that can be used to design a controller. The model is a continuation of a previous report that was written last semester which can be read in [1]. From previous work, some changes in the model is done. The model of the economizer is not a part of the total model, it will not be used in tests either. Throughout simulation of the established moving boundary model it can be concluded that it is not a viable model to design a controller since there are some errors in the matlab scripts for the model. Hence the existing model from the company will be used and explained.

Modelling of The System 5

To design a controller for a system as the vapor-compression system at Lodam electronics, a low order of each component model is needed. Since there are two main components of the system, evaporator and condenser, that can have a big order, the general moving boundary will be used to reduce that order. The modelling has been done in last semester project, which can be found in Appendix A and for the whole report [1]. In this chapter only the essentials will be shown explained while the more detailed version can be read on Appendix A.

5.1 The General Moving Boundary Method

The two mentioned components are both with distributed parameters and can be described using partial differential equation. Solving the partial differential equations by approximating them to a lumped parameter model may result in a large order system. Instead the so called moving boundary concept is used, this results in lower order models. The way that the general moving boundary works is that it takes the dynamics of the evaporator into consideration. In an evaporator, in this case a dry expansion evaporator, there will be two zones: the mixed zone and the superheated zone, as seen in Figure 5.1.

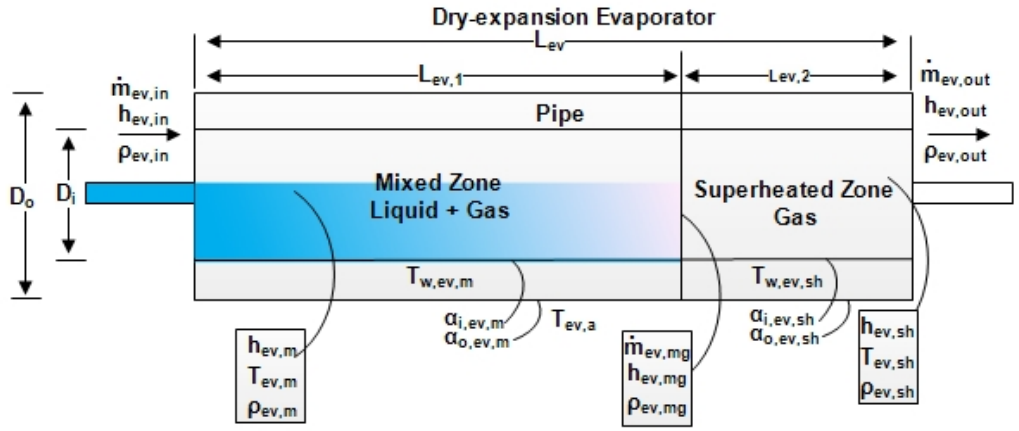

Figure 5.1: This figure shows a dry-expansion evaporator model

From Figure 5.1, a model can be produced where the designed inputs/output can be seen in Figure 5.2 and the model equations are evaluated in Appendix A, which was done in last semester project. The model for the evaporator will result 5 state variables: $\{L_{ev,1}, P_{ev}, h_{ev,out}, T_{ev,w,m}, T_{ev,w,sh}\}$, 4 inputs :$\{\dot{m}_{ev,in}, h_{ev,in}, \dot{m}_{ev,out}, T_{ev,amb}\}$.

Where:

$L_{ev,1}$	is the length of the mixed zone of the evaporator	[m]
P_{ev}	is the pressure of the refrigerant in the evaporator	[bar]
$h_{ev,out}$	is the enthalpy of the refrigerant at the outlet of the evaporator	$\left[\frac{\text{J}}{\text{kg}}\right]$
$h_{ev,in}$	is the enthalpy of the refrigerant at the inlet of the evaporator	$\left[\frac{\text{J}}{\text{kg}}\right]$
$T_{ev,w,m}$	is the temperature of pipe-wall at the mixed zone	[K]
$T_{ev,w,sh}$	is the temperature of the pipe-wall at the superheated zone	[K]
$T_{ev,amb}$	is the ambient temperature at the evaporator	[K]
$\dot{m}_{ev,in}$	is the mass flow of the refrigerant at the inlet of the evaporator	$\left[\frac{\text{kg}}{\text{s}}\right]$
$\dot{m}_{ev,out}$	is the mass flow of the refrigerant at the outlet of the evaporator	$\left[\frac{\text{kg}}{\text{s}}\right]$

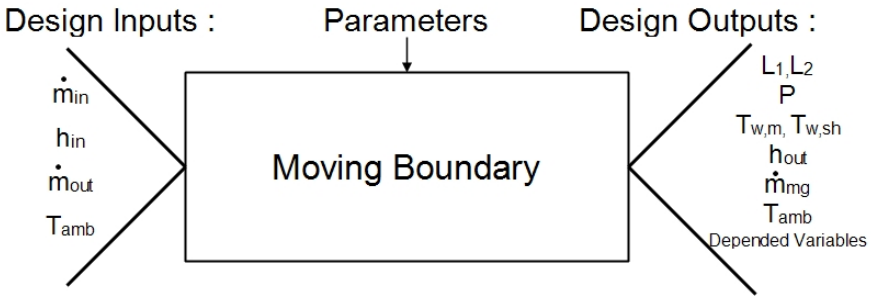

Figure 5.2: The General Moving Boundary (GMB) Design Model

Where:

$\dot{m}_{in}$	is the mass flow at the inlet of the GMB model	$\left[\frac{\text{kg}}{\text{s}}\right]$
h_{in}	is the enthalpy at the inlet of the GMB model	$\left[\frac{\text{J}}{\text{kg}}\right]$
$\dot{m}_{out}$	is the mass flow at the outlet of the GMB model	$\left[\frac{\text{kg}}{\text{s}}\right]$
T_{amb}	is the ambient temperature at the GMB model	[K]
L_1, L_2	are the length of the different zones in the GMB model	[m]
P	is the pressure of the GMB model	[bar]
$T_{w,m}$, $T_{w,sh}$	are the pipe-wall temperature at different zones of the GMB model	[K]
h_{out}	is the enthalpy at the outlet of the GMB model	$\left[\frac{\text{J}}{\text{kg}}\right]$

$\dot{m}_{mg}$	is the mass flow in between the zones of the GMB model	$\left[\frac{\text{kg}}{\text{s}}\right]$

This general moving boundary has been used for the condenser as well as it gives good representation of the dynamics of the component and at the same time keeping the model in low order. All the models are evaluated in the Appendix A.

5.2 Linearization Method For All Models

To use the model, a linearization of the models are necessary. The method used in this project is the Taylor series expansion method. This method takes the steady state solution with small dynamic deviations from a fixed operating point into account. Since vapor compression systems are usually designed to operate at specific points, it gives more reason to use this method. The linearization of the evaporator model will be used as an example of how the other models are done.

$$x_{ev}(t) = x_{ev}^{ss} + \delta x_{ev}(t), u_{ev}(t) = u_{ev}^{ss} + \delta u_{ev}(t) \tag{5.1}$$

where: $x_{ev}^{ss} = \begin{bmatrix} L_{ev,1}^{ss} & P_{ev}^{ss} & h_{ev,out}^{ss} & T_{w,ev,m}^{ss} & T_{w,ev,sh}^{ss} \end{bmatrix}^T$ and $u_{ev}^{ss} = \begin{bmatrix} \dot{m}_{ev,in}^{ss} & h_{ev,in}^{ss} & \dot{m}_{ev,out}^{ss} & T_{ev,a}^{ss} \end{bmatrix}^T$ are the steady state solution and both $\delta x_{ev}(t)$ and $\delta u_{ev}(t)$ are small dynamic deviations from the fixed operating point. The Taylor series expansion will be used to describe the linear model of the dynamic deviations as seen in

$$\delta \dot{x}_{ev} = A_{ev}\delta x_{ev} + B_{ev}\delta u_{ev} \tag{5.2}$$

where $A_{ev} = D_{ev}^{-1}\frac{\delta f(x_{ev},u_{ev})}{\delta x_{ev}} = D_{ev}^{-1}A'_{ev}$ and $B_{ev} = D_{ev}^{-1}\frac{\delta f(x,u)}{\delta u} = D_{ev}^{-1}B'_{ev}$. The Taylor series expansions A_{ev}' and B_{ev}' can be seen in Equation A.16, and the element expressions can be found in **Appendix B**.

$$A'_{ev} = \begin{bmatrix} a_{ev,11} & a_{ev,12} & 0 & a_{ev,14} & 0 \\ a_{ev,21} & a_{ev,22} & a_{ev,23} & 0 & a_{ev,25} \\ 0 & 0 & 0 & 0 & 0 \\ a_{ev,41} & a_{ev,42} & 0 & a_{ev,44} & 0 \\ a_{ev,51} & a_{ev,52} & a_{ev,53} & 0 & a_{ev,55} \end{bmatrix}, B'_{ev} = \begin{bmatrix} b_{ev,11} & b_{ev,12} & 0 & 0 \\ 0 & 0 & b_{ev,23} & 0 \\ b_{ev,31} & 0 & b_{ev,33} & 0 \\ 0 & 0 & 0 & b_{v44} \\ 0 & 0 & 0 & b_{ev,54} \end{bmatrix} \tag{5.3}$$

Following the same instructions as just before, the linearized form of the condenser model

$$\delta \dot{x}_c = A_c\delta x_c + B_c\delta u_c \tag{5.4}$$

$$where, \quad A_c = D_c^{-1}\frac{\delta f(x_c,u_c)}{\delta x_c} = D_c^{-1}A'_c \quad and \quad B_{ev} = D_c^{-1}\frac{\delta f(x_c,u_c)}{\delta u} = D_c^{-1}B'_c.$$

The Taylor series expansions A_c' and B_c' can be seen in Equation 5.5, and the element expressions can be found in **Appendix C**. .

$$A_c' = \begin{bmatrix} a_{c11} & & a_{c13} & 0 & a_{c15} & 0 & 0 \\ 0 & a_{c22} & a_{c23} & 0 & 0 & a_{c26} & 0 \\ a_{c31} & a_{c32} & a_{c33} & a_{c34} & 0 & 0 & 0 \\ 0 & 0 & 0 & 0 & 0 & 0 & 0 \\ 0 & 0 & a_{c53} & 0 & a_{c55} & 0 & 0 \\ 0 & 0 & a_{c63} & 0 & 0 & a_{c66} & 0 \\ 0 & 0 & a_{c73} & a_{c74} & 0 & 0 & a_{c77} \end{bmatrix}, B_c' = \begin{bmatrix} b_{c11} & b_{c12} & 0 & 0 \\ 0 & 0 & b_{c23} & 0 \\ 0 & 0 & b_{c33} & 0 \\ b_{c41} & 0 & b_{c43} & 0 \\ 0 & 0 & 0 & b_{c54} \\ 0 & 0 & 0 & b_{c64} \\ 0 & 0 & 0 & b_{c74} \end{bmatrix} \tag{5.5}$$

5.3 Results of The Model

In this section only the results of the models will be shown. The evaluation of each equations can be found in appendix from previous work of the project [1].

5.3.1 Evaporator Model equations

The model achieved from the moving boundary method for the evaporator:

$$D_{ev}\dot{x}_{ev} = f(x_{ev}, u_{ev}) \rightarrow \dot{x}_{ev} = D_{ev}^{-1} f(x_{ev}, u_{ev}) \tag{5.6}$$

where,

$$f(x_{ev}, u_{ev}) = \begin{bmatrix} \dot{m}_{ev,in}h_{ev,in} - \dot{m}_{ev,in}h_{ev,mg} + \pi D_i L_{ev,1}\alpha_{i,ev,m}(T_{w,ev,m} - \bar{T}_{ev,m}) \\ \dot{m}_{ev,out}h_{ev,mg} - \dot{m}_{ev,out}h_{ev,out} + \pi D_i(L_{ev} - L_{ev,1})\alpha_{i,ev,sh}(T_{w,ev,sh} - \bar{T}_{ev,sh}) \\ \dot{m}_{ev,in} - \dot{m}_{ev,out} \\ \pi D_o L_{ev,1}\alpha_{o,ev,m}(T_{ev,a} - T_{w,ev,m}) - \pi D_i L_{ev,1}\alpha_{i,ev,m}(T_{w,ev,m} - \bar{T}_{ev,m}) \\ \pi D_o(L_{ev} - L_{ev,1})\alpha_{o,ev,sh}(T_{ev,a} - T_{w,ev,sh}) - \pi D_i(L_{ev} - L_{ev,1})\alpha_{i,ev,sh}(T_{w,ev,sh} - \bar{T}_{ev,sh}) \end{bmatrix} \tag{5.7}$$

and

$$D_{ev} = \begin{bmatrix} d_{ev,11} & d_{ev,12} & 0 & 0 & 0 \\ d_{ev,21} & d_{ev,22} & d_{ev,23} & 0 & 0 \\ d_{ev,31} & d_{ev,32} & d_{ev,33} & 0 & 0 \\ 0 & 0 & 0 & d_{ev,44} & 0 \\ 0 & 0 & 0 & 0 & d_{ev,55} \end{bmatrix}, x_{ev} = \begin{bmatrix} L_{ev,1} \\ P_{ev} \\ h_{ev,out} \\ T_{w,ev,m} \\ T_{w,ev,sh} \end{bmatrix}, u_{ev} = \begin{bmatrix} \dot{m}_{ev,in} \\ h_{ev,in} \\ \dot{m}_{ev,out} \\ T_{ev,a} \end{bmatrix} \tag{5.8}$$

Where:

A	is the cross sectional area of the inner tube of the pipe	$[\mathrm{m}^2]$
D_i	is the inner diameter of the metal pipe	[m]
$\bar{\gamma}$	is the average void fraction	$[\cdot]$
$\rho_{ev,mg}$	is the density of the refrigerant at the saturated curve	$\left[\frac{\mathrm{kg}}{\mathrm{m}^3}\right]$
$\rho_{ev,l}$	is the density of the refrigerant at the sub cooled saturation curve	$\left[\frac{\mathrm{kg}}{\mathrm{m}^3}\right]$

$\rho_{ev,sh}$	is the mean density of the refrigerant at the superheat zone	$\left[\frac{\text{kg}}{\text{m}^3}\right]$
P_{ev}	is the pressure of the refrigerant	[bar]
t	is the time	[s]
$\dot{m}_{ev,in}$	is the mass flow of the refrigerant at the inlet of the evaporator	$\left[\frac{\text{kg}}{\text{s}}\right]$
$\dot{m}_{ev,mg}$	is the mass flow of the refrigerant at the saturated curve	$\left[\frac{\text{kg}}{\text{s}}\right]$
$\dot{m}_{ev,out}$	is the mass flow at the outlet of the evaporator	$\left[\frac{\text{kg}}{\text{s}}\right]$
$\bar{T}_{ev,m}$	is the temperature of the refrigerant in the mixed zone	[K]
$\bar{T}_{w,ev,m}$	is the temperature of the metal pipe	[K]
$\bar{T}_{ev,sh}$	is the temperature of the refrigerant at the superheat zone	[K]
$T_{w,ev,sh}$	is the temperature of the metal pipe at the superheat zone	[K]
$T_{ev,a}$	is the ambient temperature at the evaporator	[K]
$h_{ev,mg}$	is the enthalpy at the saturation curve	$\left[\frac{\text{J}}{\text{kg}}\right]$
$h_{ev,l}$	is the enthalpy at the sub cooled saturation curve	$\left[\frac{\text{J}}{\text{kg}}\right]$
$h_{ev,sh}$	is the mean enthalpy at the superheat zone	$\left[\frac{\text{J}}{\text{kg}}\right]$
$h_{ev,out}$	is the enthalpy of the refrigerant at the outlet of the evaporator	$\left[\frac{\text{J}}{\text{kg}}\right]$
$\alpha_{i,ev,m}$	is the transfer heat coefficient from pipe to refrigerant at the mixed zone	$\left[\frac{\text{W}}{\text{m}^2\text{K}}\right]$
$\alpha_{i,ev,sh}$	is the transfer heat coefficient from pipe to refrigerant at the superheat zone	$\left[\frac{\text{W}}{\text{m}^2\text{K}}\right]$
$\alpha_{o,ev,m}$	is the transfer heat coefficient from ambient air to refrigerant at mixed zone	$\left[\frac{\text{W}}{\text{m}^2\text{K}}\right]$
$\alpha_{o,ev,sh}$	is the transfer heat coefficient from ambient air to refrigerant at superheated zone	$\left[\frac{\text{W}}{\text{m}^2\text{K}}\right]$

5.3.2 Condenser Model equations

The model achieved from the moving boundary method for the condenser:

$$D_c\dot{x}_c = f(x_c, u_c) \rightarrow \dot{x}_c = D_c^{-1} f(x_c, u_c) \tag{5.9}$$

where,

$$f(x_c, u_c) = \begin{bmatrix} \dot{m}_{c,in}h_{c,in} - \dot{m}_{c,in}h_{c,mg} + \pi D_i L_{c,1}\alpha_{i,c,sh}(T_{w,c,sh} - T_{c,sh}) \\ \dot{m}_{c,out}h_{c,mg} - \dot{m}_{c,out}h_{c,l} + \pi D_i L_{c,2}\alpha_{i,c,m}(T_{w,c,m} - T_{c,m}) \\ \dot{m}_{c,out}h_{c,l} - \dot{m}_{c,out}h_{c,out} + \pi D_i L_{c,3}\alpha_{i,c,m}(T_{w,c,l} - T_{c,l}) \\ \dot{m}_{c,in} - \dot{m}_{c,out} \\ \alpha_{o,c,sh}\pi D_o(T_{c,a} - T_{w,c,sh}) - \alpha_{i,c,sh}\pi D_i(T_{w,c,sh} - T_{c,m}) \\ \alpha_{o,c,m}\pi D_o(T_{c,a} - T_{w,c,m}) - \alpha_{i,c,m}\pi D_i(T_{w,c,m} - T_{c,m}) \\ \alpha_{o,c,l}\pi D_o(T_{c,a} - T_{w,c,l}) - \alpha_{i,c,l}\pi D_i(T_{w,c,l} - T_{c,l}) \end{bmatrix} \tag{5.10}$$

,

$$D_c = \begin{bmatrix} d_{c,11} & 0 & d_{c,c,13} & 0 & 0 & 0 & 0 \\ d_{c,21} & d_{c,22} & d_{c,23} & 0 & 0 & 0 & 0 \\ d_{c,31} & d_{c,32} & d_{c,33} & d_{c,34} & 0 & 0 & 0 \\ d_{c,41} & d_{c,42} & d_{c,43} & 0 & 0 & 0 & 0 \\ d_{c,51} & 0 & 0 & 0 & d_{55} & 0 & 0 \\ 0 & 0 & 0 & 0 & 0 & d_{c,66} & 0 \\ d_{c,71} & d_{c,72} & 0 & 0 & 0 & 0 & d_{c,77} \end{bmatrix}, x_c = \begin{bmatrix} L_{c,1} \\ L_{c,2} \\ P_c \\ h_{c,out} \\ T_{w,c,sh} \\ T_{w,c,m} \\ T_{w,c,l} \end{bmatrix}, u_c = \begin{bmatrix} \dot{m}_{c,in} \\ h_{c,in} \\ \dot{m}_{c,out} \\ T_{c,a} \end{bmatrix} \tag{5.11}$$

Where:

P_c	is the condenser pressure	[bar]
$\rho_{c,sh}$	is the mean density at the superheated zone	$\left[\frac{\text{kg}}{\text{m}^3}\right]$
$\rho_{c,mg}$	is the density at the superheated saturation curve	$\left[\frac{\text{kg}}{\text{m}^3}\right]$
$\rho_{c,m}$	is the mean density of the refrigerant at the mixed zone	$\left[\frac{\text{kg}}{\text{m}^3}\right]$
$\rho_{c,ml}$	is the density of the refrigerant at the sub-cooled saturation curve	$\left[\frac{\text{kg}}{\text{m}^3}\right]$
$h_{c,sh}$	is the mean enthalpy at the superheated zone	$\left[\frac{\text{J}}{\text{kg}}\right]$
$h_{c,mg}$	is the enthalpy at the superheated saturation curve	$\left[\frac{\text{J}}{\text{kg}}\right]$
$h_{c,ml}$	is the enthalpy of the refrigerant at the sub-cooled saturation curve	$\left[\frac{\text{J}}{\text{kg}}\right]$
$h_{c,out}$	is the enthalpy of the refrigerant at the outlet of the condenser	$\left[\frac{\text{J}}{\text{kg}}\right]$
$\dot{m}_{c,in}$	is the mass flow going into the condenser	$\left[\frac{\text{kg}}{\text{s}}\right]$
$\dot{m}_{c,mg}$	is the mass flow at the superheated saturation curve	$\left[\frac{\text{kg}}{\text{s}}\right]$
$\dot{m}_{c,ml}$	is the mass flow of the refrigerant at the sub-cooled saturation curve	$\left[\frac{\text{kg}}{\text{s}}\right]$

$T_{w,c,sh}$	is the temperature of the metal pipe	[K]
$T_{c,sh}$	is the temperature of the refrigerant in the superheat zone	[K]
$T_{w,c,m}$	is the temperature of the pipe at the mixed zone	[K]
$T_{c,m}$	is the mean temperature of the refrigerant at the mixed zone	[K]
$T_{w,c,l}$	is the temperature of the wall at the sub-cooled zone	[K]
$T_{c,l}$	is the mean temperature of the refrigerant at the sub-cooled zone	[K]
$T_{c,a}$	is the ambient temperature at the condenser	[K]
$\alpha_{i,c,sh}$	is the heat transfer coefficient from refrigerant to pipe at the superheated zone	$\left[\frac{\mathrm{W}}{\mathrm{m^2K}}\right]$
$\alpha_{i,c,m}$	is the transfer heat coefficient from refrigerant to pipe at the mixed zone	$\left[\frac{\mathrm{W}}{\mathrm{m^2K}}\right]$
$\alpha_{i,c,l}$	is the transfer heat coefficient from refrigerant to pipe at the sub-cooled zone	$\left[\frac{\mathrm{W}}{\mathrm{m^2K}}\right]$
$\alpha_{o,c,sh}$	is the transfer heat coefficient from pipe to ambient air at the superheated zone	$\left[\frac{\mathrm{W}}{\mathrm{m^2K}}\right]$
$\alpha_{o,c,m}$	is the transfer heat coefficient from pipe to ambient air at the mixed zone	$\left[\frac{\mathrm{W}}{\mathrm{m^2K}}\right]$
$\alpha_{o,c,l}$	is the transfer heat coefficient from pipe to ambient air at the sub-cooled zone	$\left[\frac{\mathrm{W}}{\mathrm{m^2K}}\right]$

5.3.3 Expansion Valve Model equations

$$\dot{m}_v = T_{on,cev} \cdot K_{c,ev} \sqrt{\rho_v \cdot (P_c - P_{ev})} \tag{5.12}$$

$$h_{exp,out} = h_{exp,in} = h_{c,out}$$

Where:

$\dot{m}_v$	is the mass flow rate of the refrigerant through the valve	$\left[\frac{\mathrm{kg}}{\mathrm{s}}\right]$
C_v	is the discharge coefficient	$[\cdot]$
A_V	is the opening area	$[\mathrm{m^2}]$
ρ_v	is the density of the refrigerant at the inlet of the valve	$\left[\frac{\mathrm{kg}}{\mathrm{m^3}}\right]$
ΔP	is the pressure drop across the valve	[bar]
$h_{exp,in}$	are the enthalpy before the expansion valve	$\left[\frac{\mathrm{J}}{\mathrm{kg}}\right]$
$h_{exp,out}$	are the enthalpy after the expansion valve	$\left[\frac{\mathrm{J}}{\mathrm{kg}}\right]$

The small dynamic deviation for the linearized model of the expansion valve between condenser and evaporator can be expressed as :

$$\delta\dot{m}_v = \delta T_{on,cev} \cdot K_{c,ev}\sqrt{\rho_v \cdot (\delta P_c - \delta P_{ev})} = C_{11}\delta x_{ev2} + C_{12}\delta x_{c3} + C_{13}\delta u_3 \tag{5.13}$$

$$\delta h_{exp,cev} = \delta x_{c4} \tag{5.14}$$

5.3.4 Compressor Model equations

$$\dot{m}_{cpr} = \omega V_{cpr}\rho_{cpr}(1 + C_{cpr} - C_{cpr}(\frac{P_c}{P_{ev}})^{\frac{1}{n}}) \tag{5.15}$$

and

$$h_{cpr,out} = \frac{h_{cpr,out,ist} - h_{cpr,in}}{\eta_{cpr}} + h_{cpr,in} \tag{5.16}$$

Where:

$\dot{m}_{cpr}$	is the mass flow of the refrigerant at the compressor	$\left[\frac{\text{kg}}{\text{s}}\right]$
ω	is the compressor speed	[Hz]
V_{cpr}	is the volume of the compressor	$\left[\text{m}^3\right]$
ρ_{cpr}	is the density of the refrigerant at the compressor	$\left[\frac{\text{kg}}{\text{m}^3}\right]$
C_{cpr}	s the constant followed by the ideal gas law	$[\cdot]$
P_c	is the pressure at the condenser	[bar]
n	is the polytropic coefficient	$[\cdot]$
$h_{cpr,out}$	is the enthalpy of the refrigerant at the outlet of the compressor	$\left[\frac{\text{J}}{\text{kg}}\right]$
$h_{cpr,out,ist}$	is the enthalpy of the refrigerant at the outlet of the compressor during isentropic process	$\left[\frac{\text{J}}{\text{kg}}\right]$
$h_{cpr,in}$	is the enthalpy of the refrigerant the inlet of the compressor	$\left[\frac{\text{J}}{\text{kg}}\right]$
η_{cpr}	is the efficiency coefficient of the compressor	$[\cdot]$

Since the are some changes from previous model, as the economizer is removed, the linearization constants are changed for the model of the compressor as seen in Equation 5.17 and Equation 5.18.

$$\delta\dot{m}_{cpr,ev,c} = \delta\omega_{cpr}V_{cpr}\rho_{cpr}(1+C_{cpr}-C_{cpr}(\frac{\delta P_c}{\delta P_{ev}})^{\frac{1}{n}}) = C_{71}\delta x_{ev,2}+C_{72}\delta x_{c,3}+C_{73}\delta u_1 \tag{5.17}$$

$$h_{cpr,out} = \frac{\delta h_{cpr,out,ist} - \delta h_{ev,out}}{\eta_{cpr}} + \delta h_{ev,out} = C_{74}\delta x_{ev,2} + C_{75}\delta x_{c,3} + C_{76}\delta x_{ev,3} \tag{5.18}$$

5.4 The Total Model

This model of the whole system without the economizer will give 4 inputs with 12 state variables and to summarize it, the equations are listed from Equation 5.19 to Equation 5.25.

The inputs for the total model are:

$$u_1 = \omega_{cpr}, \quad u_2 = T_{cev,on}, \quad u_3 = v_e, \quad u_4 = v_c \tag{5.19}$$

Model for the evaporator can be described by the states x_{ev} seen in Equation 5.8, the mass flows around the evaporator and the enthalpy of the refrigerant going into the evaporator :

$$\dot{x}_{s,ev} = g(x_{ev}, \dot{m}_{ev,in}, h_{ev,in}, \dot{m}_{ev,out}, u_3) \tag{5.20}$$

Model for the condenser can be described by the states x_c seen in Equation 5.11, the mass flows around the condenser and the enthalpy of the refrigerant going into the condenser :

$$\dot{x}_{s,c} = g(x_c, \dot{m}_{c,in}, h_{c,in}, \dot{m}_{c,out}, u_4) \tag{5.21}$$

The variables $\dot{m}_{ev,in}, h_{ev,in}, \dot{m}_{ev,out}, \dot{m}_{ev,in}, h_{ev,in}, \dot{m}_{ev,out}$ are the ones that are used to bind the whole system together. From the linearization of the expansion valve in Equation 5.13 and Equation 5.14 and the linearization of the compressor in Equation 5.17 and Equation 5.18, the mass flow and enthalpy around the evaporator and condenser can be described from the states in x_{ev}, x_c and the new inputs from Equation 5.19. The variables can be calculated as seen from Equation 5.22 to Equation 5.25 and an illustration as shown in Figure 5.3 to see how the variables connects the models together.

$$\dot{m}_v = \dot{m}_{ev,in} = \dot{m}_{c,out} = u_2 \cdot K_{c,ev}\sqrt{\rho_v \cdot (x_{c,3} - x_{ev,2})} = T_{cev,on} \cdot K_{c,ev}\sqrt{\rho_v \cdot (P_c - P_{ev})} \tag{5.22}$$

$$\dot{m}_{cpr} = \dot{m}_{ev,out} = \dot{m}_{c,in} = f(\frac{x_{c,3}}{x_{ev,2}}, u_1, \rho) = f(\frac{P_c}{P_{ev}}, \omega_{cpr}, \rho) \tag{5.23}$$

$$h_{exp,out} = h_{ev,in} = x_{c,4} = h_{c,out} \tag{5.24}$$

$$h_{cpr,out} = h_{c,in} = C_{74}x_{ev,2} + C_{75}x_{c,3} + C_{76}x_{ev,3} = C_{74}P_{ev} + C_{75}P_c + C_{76}h_{ev,out} \tag{5.25}$$

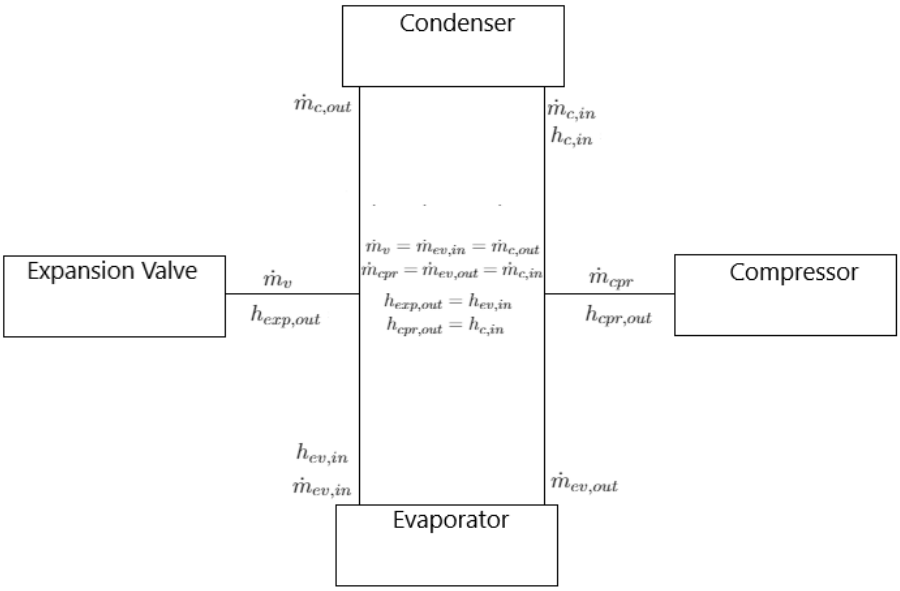

Figure 5.3: This figure shows which variables from which components are connected to each-other

By the established the equations from Equation 5.19 to Equation 5.25, the model of the whole system, without the economizer, is determined as seen in the states space form on Equation 5.26.

$$\dot{x}_s = g(x_s, u_s) \tag{5.26}$$

where,

$$x_s = \{x_{ev} \quad x_c\}^T \tag{5.27}$$

$$u_s = \{u_1 \quad u_2 \quad u_3 \quad u_4\}^T \tag{5.28}$$

This means that the state space model of the whole system is now as seen from Equation 5.29 to Equation 5.32.

$$\dot{x}_s = A_s x_s + B_s u_s \tag{5.29}$$

$$y_s = C_s x_s \tag{5.30}$$

$$\begin{bmatrix} D_{ev}\delta\dot{x}_{s,ev} \\ D_c\delta\dot{x}_{s,c} \end{bmatrix} = \begin{bmatrix} A'_{ev,ev} & A'_{ev,c} \\ A'_{c,ev} & A'_{c,c} \end{bmatrix} \begin{bmatrix} \delta x_{ev} \\ \delta x_c \end{bmatrix} + \begin{bmatrix} B'_{s,ev} \\ B'_{s,c} \end{bmatrix} \delta u_s \tag{5.31}$$

$$\begin{bmatrix} \delta\dot{x}_{s,ev} \\ \delta\dot{x}_{s,c} \end{bmatrix} = \begin{bmatrix} D_{ev}^{-1}A'_{ev,ev} & D_{ev}^{-1}A'_{ev,c} \\ D_c^{-1}A'_{c,ev} & D_c^{-1}A'_{c,c} \end{bmatrix} \begin{bmatrix} \delta x_{ev} \\ \delta x_c \end{bmatrix} + \begin{bmatrix} D_{ev}^{-1}B'_{s,ev} \\ D_c^{-1}B'_{s,c} \end{bmatrix} \delta u_s$$

$$\begin{bmatrix} \delta\dot{x}_{s,ev} \\ \delta\dot{x}_{s,c} \end{bmatrix} = \begin{bmatrix} A_{ev,ev} & A_{ev,c} \\ A_{c,ev} & A_{c,c} \end{bmatrix} \begin{bmatrix} \delta x_{ev} \\ \delta x_c \end{bmatrix} + \begin{bmatrix} B_{s,ev} \\ B_{s,c} \end{bmatrix} \delta u_s \tag{5.32}$$

where,

$$A'_{ev,ev} = \begin{bmatrix} a_{ev,11} & a_{ev,12} + b_{ev,11}C_{11} & 0 & a_{ev,14} & 0 \\ a_{ev,21} & a_{ev,22} + b_{ev,23}C_{71} & a_{ev,23} & 0 & a_{ev,25} \\ 0 & b_{ev,31}C_{11} + b_{ev,33}C_{71} & 0 & 0 & 0 \\ a_{ev,41} & a_{ev,42} & 0 & a_{ev,44} & 0 \\ a_{ev,51} & a_{ev,52} & a_{ev,53} & 0 & a_{ev,55} \end{bmatrix}$$

$$, A'_{ev,c} = \begin{bmatrix} 0 & 0 & b_{ev,11}C_{12} & b_{ev,12} & 0 & 0 & 0 \\ 0 & 0 & b_{ev,23}C_{72} & 0 & 0 & 0 & 0 \\ 0 & 0 & b_{ev,31}C_{12} + b_{ev,33}C_{72} & 0 & 0 & 0 & 0 \\ 0 & 0 & 0 & 0 & 0 & 0 & 0 \\ 0 & 0 & 0 & 0 & 0 & 0 & 0 \\ 0 & 0 & 0 & 0 & 0 & 0 & 0 \\ 0 & 0 & 0 & 0 & 0 & 0 & 0 \end{bmatrix}, B'_{s,ev} = \begin{bmatrix} 0 & b_{ev,11}C_{13} & 0 & 0 \\ b_{ev,23}C_{73} & 0 & 0 & 0 \\ b_{ev,33}C_{73} & b_{ev,31}C_{13} & 0 & 0 \\ 0 & 0 & b_{ev,44} & 0 \\ 0 & 0 & b_{ev,54} & 0 \end{bmatrix}$$

and,

$$A'_{c,ev} = \begin{bmatrix} 0 & B_{c,11}C_{71} + b_{c,12}C_{74} & b_{c,12}C_{76} & 0 & 0 \\ 0 & b_{c,23}C_{11} & 0 & 0 & 0 \\ 0 & b_{c,33}C_{11} & 0 & 0 & 0 \\ 0 & b_{c,41}C_{71} + b_{c,43}C_{11} & 0 & 0 & 0 \\ 0 & 0 & 0 & 0 & 0 \end{bmatrix}, B'_{s,c} = \begin{bmatrix} b_{c,11}C_{73} & 0 & 0 & 0 \\ 0 & b_{c,23}C_{13} & 0 & 0 \\ 0 & b_{c,33}C_{13} & 0 & 0 \\ b_{c,41}C_{73} & b_{c,43}C_{13} & 0 & 0 \\ 0 & 0 & 0 & b_{c,54} \\ 0 & 0 & 0 & b_{c,64} \\ 0 & 0 & 0 & b_{c,74} \end{bmatrix}$$

$$, A'_{c,c} = \begin{bmatrix} a_{c,11} & 0 & a_{c,13} + b_{c,11}C_{72} + b_{c,12}C_{75} & 0 & a_{c,15} & 0 & 0 \\ 0 & a_{c,22} & a_{c,23} + b_{c,23}C_{12} & 0 & 0 & a_{c,26} & 0 \\ a_{c,31} & a_{c,32} & a_{c,33} + b_{c,33}C_{12} & a_{c,34} & 0 & 0 & 0 \\ 0 & 0 & b_{c,41}C_{72} + b_{c,43}C_{12} & 0 & 0 & 0 & 0 \\ 0 & 0 & a_{c,53} & 0 & a_{c,55} & 0 & 0 \\ 0 & 0 & a_{c,63} & 0 & 0 & a_{c,66} & 0 \\ 0 & 0 & a_{c,73} & a_{c,74} & 0 & 0 & a_{c,77} \end{bmatrix}$$

The model of the whole system is now derived, and now ready to be verified in the next chapter.

Simulation of The Model 6

Having developed a state space system describing the model in the previous chapter it is now necessary to verify the model. This is done through linear simulations and data comparisons.

6.1 Linear simulation

To see if the model is presenting the system acceptable, some arbitrary values are used to use the Matlab command; "lsim". lsim can simulate a time response of continuous linear systems fro, arbitrary inputs. To try this command out, it will be used only on the evaporator model, to see if that holds. With the help of the supervisor from the company, the arbitrary values are chosen to be : $[\dot{m}_{ev,in}, \quad h_{ev,in}, \quad \dot{m}_{ev,out}, \quad T_{ev,amb}] = [0.027 \quad 210000 \quad 0.027 \quad 5]$ and the estimated value of the states that the lsim should converge to are: $[\dot{L}_{ev,1}, \quad h_{ev,out}, \quad \dot{P}_{ev}, \quad T_{w,ev,m}, \quad T_{w,ev,sh}] \approx [10.5, \quad 400000, \quad 2, \quad -2, \quad 5]$. From these arbitrary inputs, the linear simulation response can be seen in Figure 6.1.

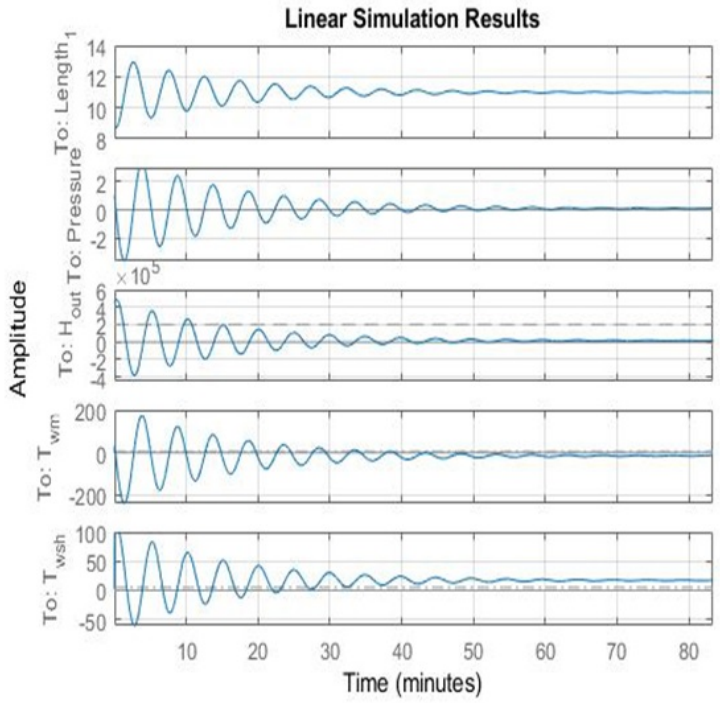

Figure 6.1: The linear simulation of the dry-expansion evaporator model

The simulation seen Figure 6.1, is a simulation of the linear system in which shows what happens if you move a little around from the operating point. The states are converging towards a value after some oscillations, which means that there is a pole in the complex plane, but still is a stable system. The issue with this simulation is that it oscillates in an total time of one hour before it is stable, this might come from that the input to the model is mass flow where both input and output mass flow are equal. This will never be the case in reality. So instead of only using the model of the evaporator, the whole model, as described in Equation 5.32, will be used, since the inputs to that system reflects the real system more.

6.2 Parameter estimation

Before looking at the response of the linear simulations, lsim, an estimation of the unknown parameters of the whole system will be done. The used estimation method is called greyest which shows improvements and the number of iterations as seen in Figure 6.2. This uses the concept of ODE solver, and the parameters that needs to be estimated are: $[\alpha_{i,ev,m}, \alpha_{o,ev,m}, \alpha_{i,ev,sh}, \alpha_{o,ev,sh}, \alpha_{i,c,sh}, \alpha_{o,c,sh}, \alpha_{i,c,m}, \alpha_{o,c,m}, \alpha_{i,c,sc}, \alpha_{o,c,sc}, \gamma]$.

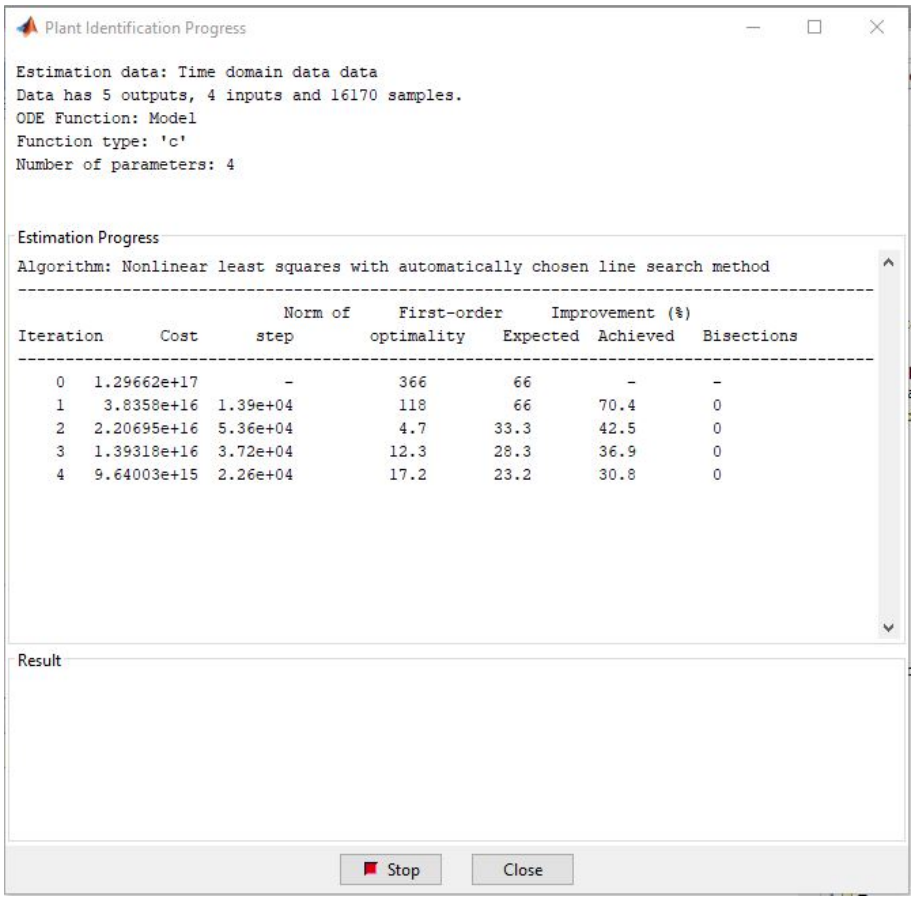

Figure 6.2: The estimation process for the unknown parameters

Throughout some test data, the unknown parameters are estimated, and the results of the

lsim can be seen in Figure 6.3 and Figure 6.4.

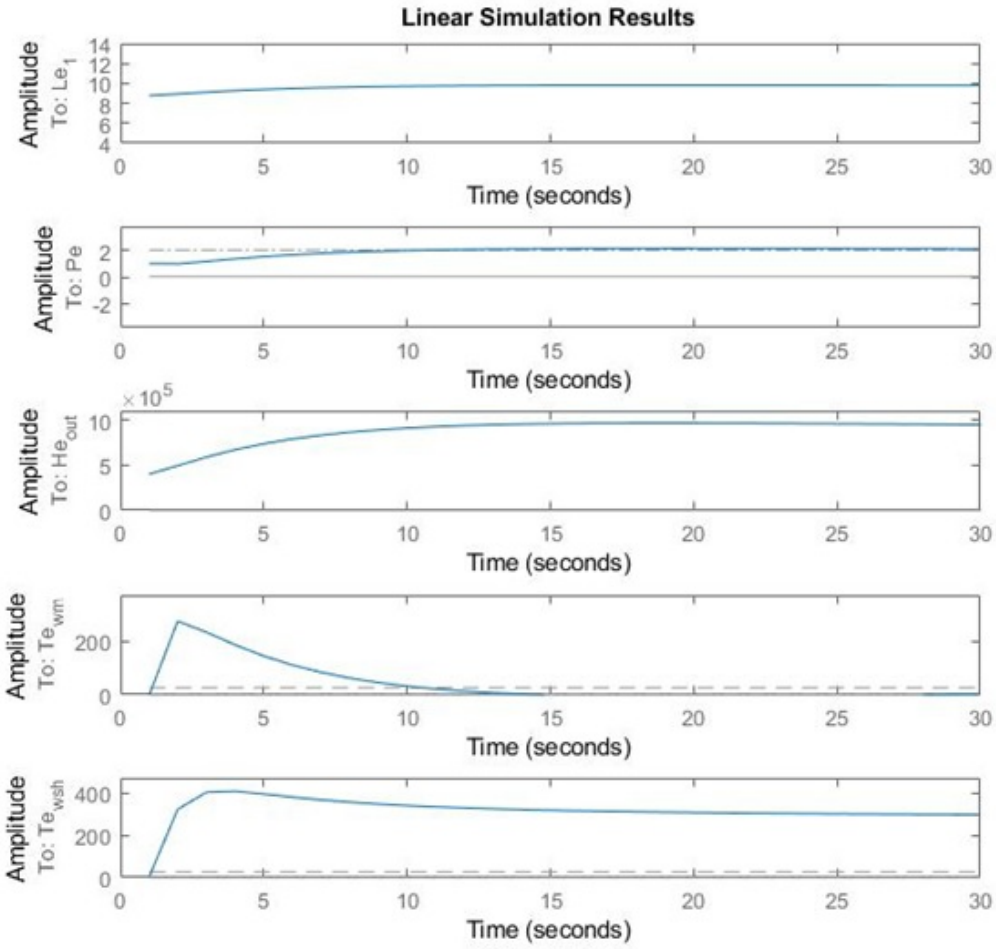

Figure 6.3: The linear simulation of whole system model, the evaporator states

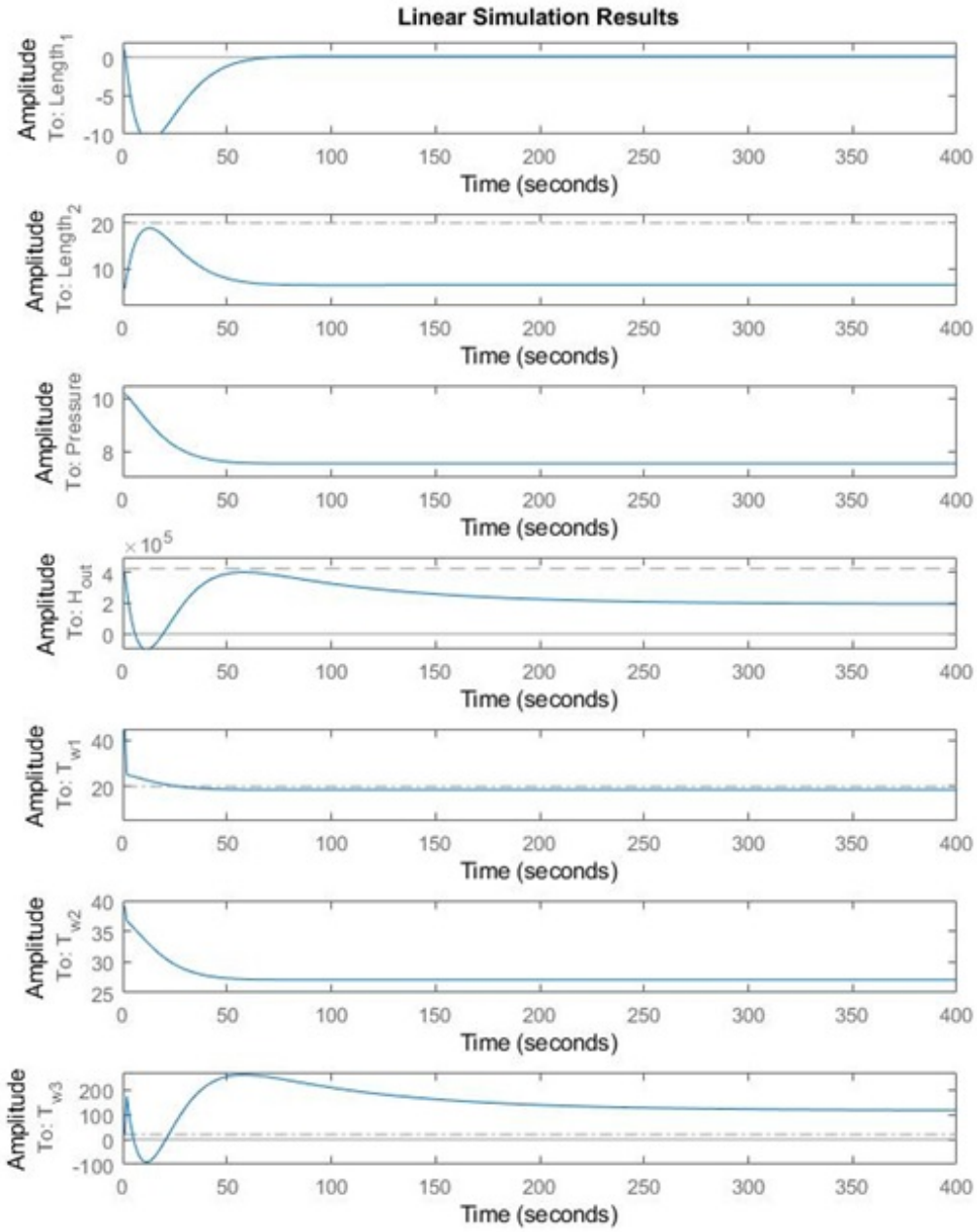

Figure 6.4: The linear simulation of whole system model, the condenser states

As before arbitrary values are used to simulate the response, and as before the states are converging, and this time response has become quicker and more smooth, which in this case will be an acceptable result.

6.3 System Verification, Data Comparison

Since the model is finished, a comparison to the open-loop data will show how good the dynamics are estimated. The comparison can be seen on Figure 6.5, where the grey line is the data, and the blue line is the model simulation. As seen in the figure the model does not follow the data quite, but by further inspecting the figure, it can be seen that the model contains the dynamics, but with an error to the data. The reason that the model does not follow it entirely, could be that the test has too many samples and too little steps.

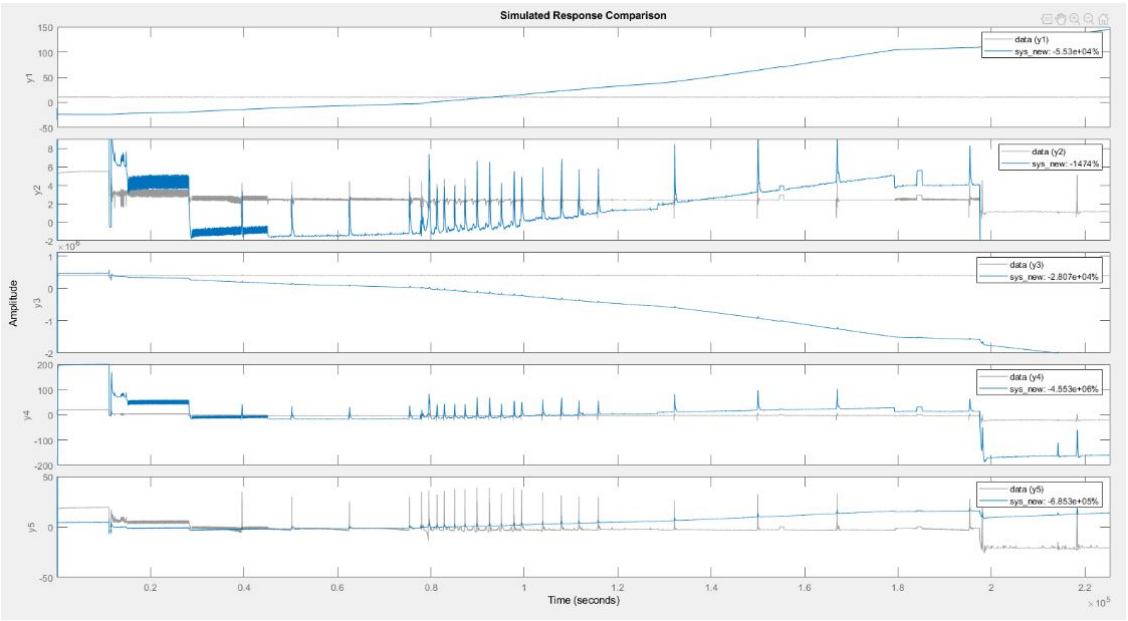

Figure 6.5: First try to compare data and estimated model, Openloop

Another try, with more iterations of the unknown parameters, less samples and more steps has been conducted on the system which then gives the model comparison as seen in Figure 6.6.

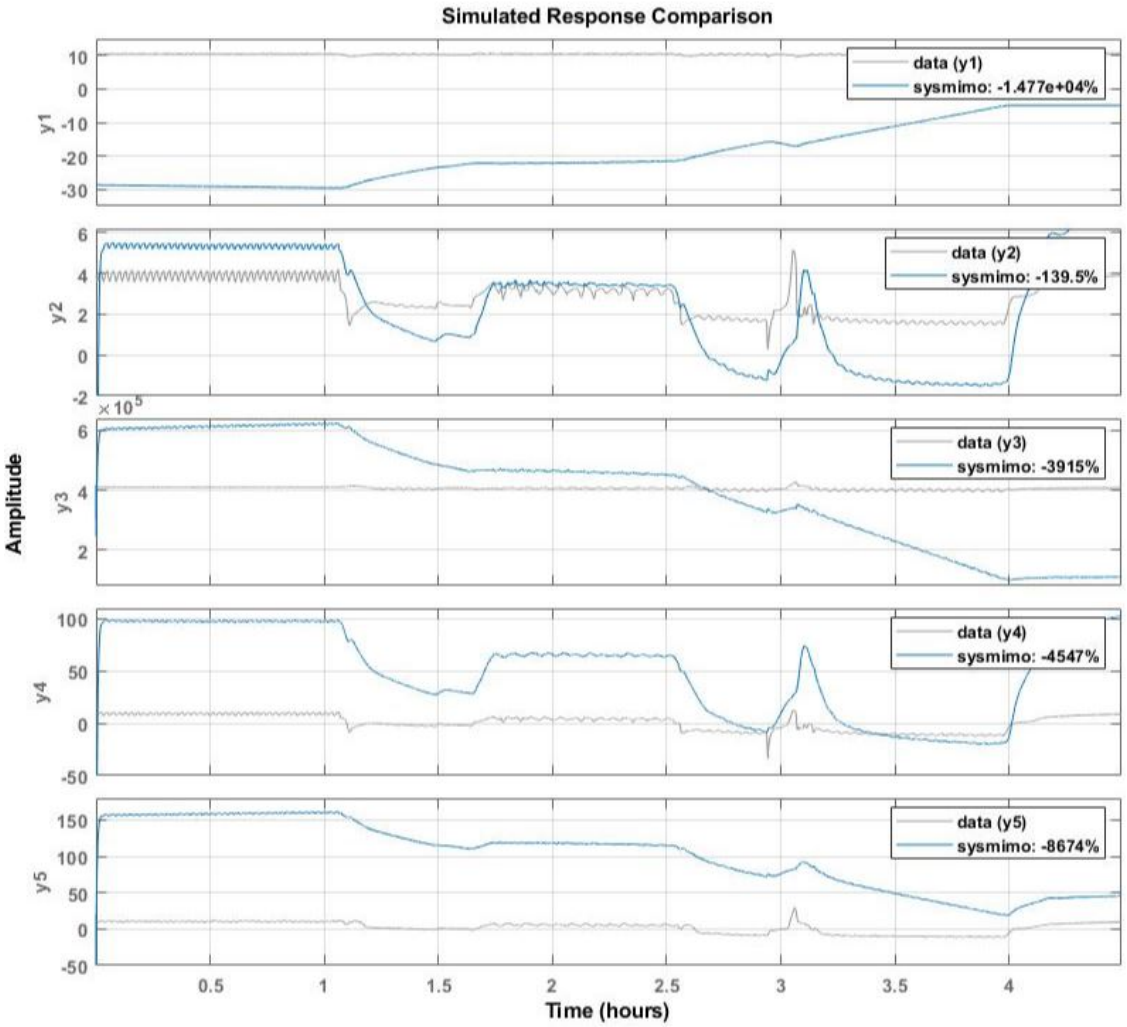

Figure 6.6: Second try to compare data and estimated model, Openloop

The new estimation of the unknown parameters gives a better estimated model than the first try. There are still big errors to the real data for some states, but the one state that needs to be close is the one noted as y2, which is the the evaporator pressure, and it is not good enough to be used for control. Having verified the model through simulations and data comparisons it is possible to determine that the initial model is flawed when comparing the model to the given data. As mentioned the evaporator pressure states does not fit satisfyingly and even through the model was thoroughly examined the error was not located. Due to time constraints on the project the model provided by Kresten Sørensen and Lodam will be used for control scheme development.

6.4 MIMO Model Provided From The Company

In this section the model, provided by the supervisor will be described and analysed. The provided model has 14 states, 4 inputs and 2 outputs corresponding to the Figure 6.8 and the theory behind it is similar to the MIMO created earlier, but it can be read in more

details in [2].

A =

	cpr.mdot	evap.pout	evap.hout	evap.mdotin	evap.sigma	evap.ml	evap.m2
cpr.mdot	-1	1.488	-0.09503	0	0	0	0
evap.pout	-0.5746	-12.57	0.05332	0.02628	1.146	0.8409	2.298
evap.hout	0	0.176	-0.4545	0	-0.3434	0	-0.0005102
evap.mdotin	0	-0.04845	0	-1	0	0	0
evap.sigma	0	-0.5985	0	0	-1	0.4205	0
evap.ml	0	0.5602	0	0.03125	-0.06532	0	0
evap.m2	-0.25	-4.482	0	0	0.5226	0	0
evap.Tml	0	1.731	0	0	-0.2036	0	0
evap.Tm2	0	0.07195	0.3218	0	0.2553	0	0
evap.Tsup	0	0	0	0	0	0	0
evap.Tsuc	0	0	0	0	0	0	0
evap.Tsupml	0	0	0	0	0	0	0
evap.Tsupm2	0	0	0	0	0	0	0
evap.mdotair	0	0	0	0	0	0	0

	evap.Tml	evap.Tm2	evap.Tsup	evap.Tsuc	evap.Tsupml	evap.Tsupm2	evap.mdotair
cpr.mdot	0	0	0	0	0	0	0
evap.pout	0.6809	0	0	0	0	0	0
evap.hout	-0.01447	0.1512	0	0	0	0	0
evap.mdotin	0	0	0	0	0	0	0
evap.sigma	0	0	0	0	0	0	0
evap.ml	-0.03881	0	0	0	0	0	0
evap.m2	0.3105	0	0	0	0	0	0
evap.Tml	-0.1717	0.2033	0	0	0	0	0.04858
evap.Tm2	0.008361	-0.7732	0	0	0	0	0.01165
evap.Tsup	0.25	0	-1	0	0	0	0
evap.Tsuc	0	0	0	-0.01	0	0	-2.857e-05
evap.Tsupml	0	0	0.08	0	-0.01	0	0
evap.Tsupm2	0	0	0.04	0	0	-0.01	0
evap.mdotair	0	0	0	0	0	0	-0.1

Figure 6.7: Model of the system Kresten Provided

Where:

cpr.mdot	is the massflow at the compressor	$\left[\frac{\text{kg}}{\text{s}}\right]$
evap.pout	is the pressure at the outlet of the evaporator	[bar]
evap.hout	is the enthalpy at the outlet of the evaporator	$\left[\frac{\text{J}}{\text{kg}}\right]$
evap.mdotin	is the mass flow at the inlet of the evaporator	$\left[\frac{\text{kg}}{\text{s}}\right]$
evap.sigma	is the boundary between liquid/gas mix and superheated gas region	$[\cdot]$
*evap.m*1	is the mass of liquid/gas mix in the mixed zone of the evaporator	[kg]
*evap.m*2	is the mass of superheated gas in the superheated zone of the evaporator	[kg]
*evap.Tm*1	is the temperature of the metal at the mixed zone of the evaporator	[°C]
*evap.Tm*2	is the temperature of the metal at the superheated zone of the evaporator	[°C]
evap.Tsup	is the temperature of the supplied air to the evaporator	[°C]
evap.Tsuc	is the temperature at the inlet of the compressor	[°C]
*evap.Tsupm*1	is the temperature of the supplied air from the first fan blowing the air	[°C]
*evap.Tsupm*2	is the temperature of the supplied air from the second fan blowing the air	[°C]
evap.mdotair	is the mass flow of the air blown to the evaporator	$\left[\frac{\text{kg}}{\text{s}}\right]$

B =

	ctrl.cpr_spe	ctrl.evap_ve	ctrl.vfan_ev	ctrl.Tret
cpr.mdot	1.505	0	0	0
evap.pout	0	0	0	0
evap.hout	0	0	0	0
evap.mdotin	0	2.205	0	0
evap.sigma	0	0	0	0
evap.ml	0	0	0	0
evap.m2	0	0	0	0
evap.Tml	0	0	0	0
evap.Tm2	0	0	0.4602	4.951
evap.Tsup	0	0	0	0
evap.Tsuc	0	0	0.007437	0.08
evap.Tsupml	0	0	0	0
evap.Tsupm2	0	0	0	0
evap.mdotair	0	0	17.93	-0.04084

C =

	cpr.mdot	evap.pout	evap.hout	evap.mdotin	evap.sigma	evap.ml	evap.m2
SysMon.QCool	0	0	0	0	0	0	0
SysMon.Tsh	0	-0.4475	0	0	0	0	0

	evap.Tml	evap.Tm2	evap.Tsup	evap.Tsuc	evap.Tsupml	evap.Tsupm2	evap.mdotair
SysMon.QCool	0	0	0	0	-7.413	-14.83	0
SysMon.Tsh	0	0	0	0.125	0	0	0

D =

	ctrl.cpr_spe	ctrl.evap_ve	ctrl.vfan_ev	ctrl.Tret
SysMon.QCool	0	0	5565	932.9
SysMon.Tsh	0	0	0	0

Figure 6.8: Model of the system Kresten Provided

Where:

$ctrl.cpr.spe$	is the compressor frequency	[Hz]
$ctrl.evap.ve$	is the expansion valve opening degree value	[%]
$ctrl.vfan.ev$	is the fans speed	[·]
$ctrl.Tret$	is the temperature insider of the container	[°C]

To see if the model is controllable the controllability matrix will be checked for full rank. If the rank of the controllability matrix is the same as the rank as the A matrix of the model, $rank(Ctrb(A, B)) = rank(A)$, then it is controllable. As seen in Figure 6.9 it is not controllable.

```
>> % Checking Controllability
rankA = rank(A)
rankCtrbAB = rank(ctrb(A,B))
rankA =
    14
rankCtrbAB =
    11
```

Figure 6.9: Controllability check

Uncontrollable State

Since the model can not be controlled, it will be necessary to find which state can not be controlled. As seen in Figure 6.10 there is 1 uncontrollable state. This state corresponds to either the state evap.Tsup1 or evap.Tsup2 as shown in Figure 6.11. Since both states has the same poleplacement, one of them will be removed firstly, and at the same time see if the model behaviour changes or remains the same. And then secondly remove the second state aswell and see the the changes again.

```
uncon = tzero(A,B,[],[]) %When you provide A and B matrices to tzero, but no C and D matrices, the
                         %command returns the eigenvalues of the uncontrollable states of the model.

unobs = tzero(A,[],C,[]) %When you provide A and C matrices, but no B and D matrices, the command
                         %returns the eigenvalues of the unobservable modes. The empty result
                         %shows that the model contains no unobservable states.
ans =
     1
uncon =
  -0.010000000000207
unobs =
  0×1 empty double column vector
```

Figure 6.10: The uncontrollable state of the model

```
>> eig(A)
ans =
 -0.010000000000207 + 0.000000000000000i evap.Tsup1
 -0.010000000000207 + 0.000000000000000i evap.Tsup2
 -0.999999999974647 + 0.000000000000000i
-11.684803662306555 + 0.000000000000000i
 -0.002623890962445 + 0.000000000000000i
 -0.056319591973733 + 0.000000000000000i
 -0.345676713995365 + 0.000000000000000i
 -0.852990494221271 + 0.000000000000000i
 -1.011730408039063 + 0.048801576975771i
 -1.011730408039063 - 0.048801576975771i
 -0.999999999998922 + 0.000000000000000i
 -0.999996533018999 + 0.000000000000000i
 -0.010000000000082 + 0.000000000000000i
 -0.099999999999957 + 0.000000000000000i
```

Figure 6.11: All poles in the model

Removing The Uncontrollable State

Now that one of the state is removed the changes of the model is slightly different as seen in Figure 6.12.

A =

	cpr.mdot	evap.pout	evap.hout	evap.mdotin	evap.sigma	evap.ml	evap.m2
cpr.mdot	-1	1.488	-0.09503	0	0	0	0
evap.pout	-0.5746	-12.57	0.05332	0.02628	1.146	0.8409	2.298
evap.hout	0	0.176	-0.4545	0	-0.3434	0	-0.0005102
evap.mdotin	0	-0.04845	0	-1	0	0	0
evap.sigma	0	-0.5985	0	0	-1	0.4205	0
evap.ml	0	0.5602	0	0.03125	-0.06532	0	0
evap.m2	-0.25	-4.482	0	0	0.5226	0	0
evap.Tml	0	1.731	0	0	-0.2036	0	0
evap.Tm2	0	0.07195	0.3218	0	0.2553	0	0
evap.Tsup	0	0	0	0	0	0	0
evap.Tsuc	0	0	0	0	0	0	0
evap.Tsupm2	0	0	0	0	0	0	0
evap.mdotair	0	0	0	0	0	0	0

	evap.Tml	evap.Tm2	evap.Tsup	evap.Tsuc	evap.Tsupm2	evap.mdotair
cpr.mdot	0	0	0	0	0	0
evap.pout	0.6809	0	0	0	0	0
evap.hout	-0.01447	0.1512	0	0	0	0
evap.mdotin	0	0	0	0	0	0
evap.sigma	0	0	0	0	0	0
evap.ml	-0.03881	0	0	0	0	0
evap.m2	0.3105	0	0	0	0	0
evap.Tml	-0.1717	0.2033	0	0	0	0.04858
evap.Tm2	0.008361	-0.7732	0	0	0	0.01165
evap.Tsup	0.25	0	-1	0	0	0
evap.Tsuc	0	0	0	-0.01	0	-2.857e-05
evap.Tsupm2	0	0	0.04	0	-0.01	0
evap.mdotair	0	0	0	0	0	-0.1

B =

	ctrl.cpr_spe	ctrl.evap_ve	ctrl.vfan_ev	ctrl.Tret
cpr.mdot	1.505	0	0	0
evap.pout	0	0	0	0
evap.hout	0	0	0	0
evap.mdotin	0	2.205	0	0
evap.sigma	0	0	0	0
evap.ml	0	0	0	0
evap.m2	0	0	0	0
evap.Tml	0	0	0	0
evap.Tm2	0	0	0.4602	4.951
evap.Tsup	0	0	0	0
evap.Tsuc	0	0	0.007437	0.08
evap.Tsupm2	0	0	0	0
evap.mdotair	0	0	17.93	-0.04084

C =

	cpr.mdot	evap.pout	evap.hout	evap.mdotin	evap.sigma	evap.ml	evap.m2
SysMon.QCool	0	0	0	0	0	0	0
SysMon.Tsh	0	-0.4475	0	0	0	0	0

	evap.Tml	evap.Tm2	evap.Tsup	evap.Tsuc	evap.Tsupm2	evap.mdotair
SysMon.QCool	0	0	0	0	-14.83	0
SysMon.Tsh	0	0	0	0.125	0	0

D =

	ctrl.cpr_spe	ctrl.evap_ve	ctrl.vfan_ev	ctrl.Tret
SysMon.QCool	0	0	5565	932.9
SysMon.Tsh	0	0	0	0

Figure 6.12: The same model with one removed state

Controllability matrix has full rank now. Removing the one uncontrollable state helped this problem as seen in Figure 6.13.

```
>> % Checking Controllability
rankA = rank(A1)
rankCtrbAB = rank(ctrb(A1,B1))
rankA =
    13
rankCtrbAB =
    13
```

Figure 6.13: Controllability check

Removing another State

Same procedure of removing a state, the second state with the same poleplacement is now removed and the model is again slightly changed as in Figure 6.14

A =

	cpr.mdot	evap.pout	evap.hout	evap.mdotin	evap.sigma	evap.ml	evap.m2
cpr.mdot	-1	0.744	-0.04751	0	0	0	0
evap.pout	-1.149	-12.57	0.05332	0.02628	0.5731	0.4205	2.298
evap.hout	0	0.176	-0.4545	0	-0.1717	0	-0.0005102
evap.mdotin	0	-0.04845	0	-1	0	0	0
evap.sigma	0	-1.197	0	0	-1	0.4205	0
evap.ml	0	1.12	0	0.0625	-0.06532	0	0
evap.m2	-0.5	-4.482	0	0	0.2613	0	0
evap.Tml	0	0.8656	0	0	-0.05089	0	0
evap.Tm2	0	0.07195	0.3218	0	0.1276	0	0
evap.Tsup	0	0	0	0	0	0	0
evap.Tsuc	0	0	0	0	0	0	0
evap.mdotair	0	0	0	0	0	0	0

	evap.Tml	evap.Tm2	evap.Tsup	evap.Tsuc	evap.mdotair
cpr.mdot	0	0	0	0	0
evap.pout	1.362	0	0	0	0
evap.hout	-0.02893	0.1512	0	0	0
evap.mdotin	0	0	0	0	0
evap.sigma	0	0	0	0	0
evap.ml	-0.1552	0	0	0	0
evap.m2	0.6209	0	0	0	0
evap.Tml	-0.1717	0.1017	0	0	0.04858
evap.Tm2	0.01672	-0.7732	0	0	0.0233
evap.Tsup	0.25	0	-1	0	0
evap.Tsuc	0	0	0	-0.01	-0.0002286
evap.mdotair	0	0	0	0	-0.1

B =

	ctrl.cpr_spe	ctrl.evap_ve	ctrl.vfan_ev	ctrl.Tret
cpr.mdot	0.1882	0	0	0
evap.pout	0	0	0	0
evap.hout	0	0	0	0
evap.mdotin	0	0.5512	0	0
evap.sigma	0	0	0	0
evap.ml	0	0	0	0
evap.m2	0	0	0	0
evap.Tml	0	0	0	0
evap.Tm2	0	0	0.1151	1.238
evap.Tsup	0	0	0	0
evap.Tsuc	0	0	0.007437	0.08
evap.mdotair	0	0	2.242	-0.005104

C =

	cpr.mdot	evap.pout	evap.hout	evap.mdotin	evap.sigma	evap.ml	evap.m2
SysMon.QCool	0	0	0	0	0	0	0
SysMon.Tsh	0	-1.79	0	0	0	0	0

	evap.Tml	evap.Tm2	evap.Tsup	evap.Tsuc	evap.mdotair
SysMon.QCool	0	0	0	0	0
SysMon.Tsh	0	0	0	0.125	0

D =

	ctrl.cpr_spe	ctrl.evap_ve	ctrl.vfan_ev	ctrl.Tret
SysMon.QCool	0	0	5565	932.9
SysMon.Tsh	0	0	0	0

Figure 6.14: The same model with two removed states

Controllability matrix has full rank again. Removing both states of the model, remained the model to be controllable as seen in Figure 6.15.

```
>> % Checking Controllability
rankA = rank(A2)
rankCtrbAB = rank(ctrb(A2,B2))
rankA =
    12
rankCtrbAB =
    12
```

Figure 6.15: Controllability check

To make sure that the model still retains the same behaviour, as the states are removed. Through simulations of bodeplots in Matlab the comparison can be seen in Figure 6.16.

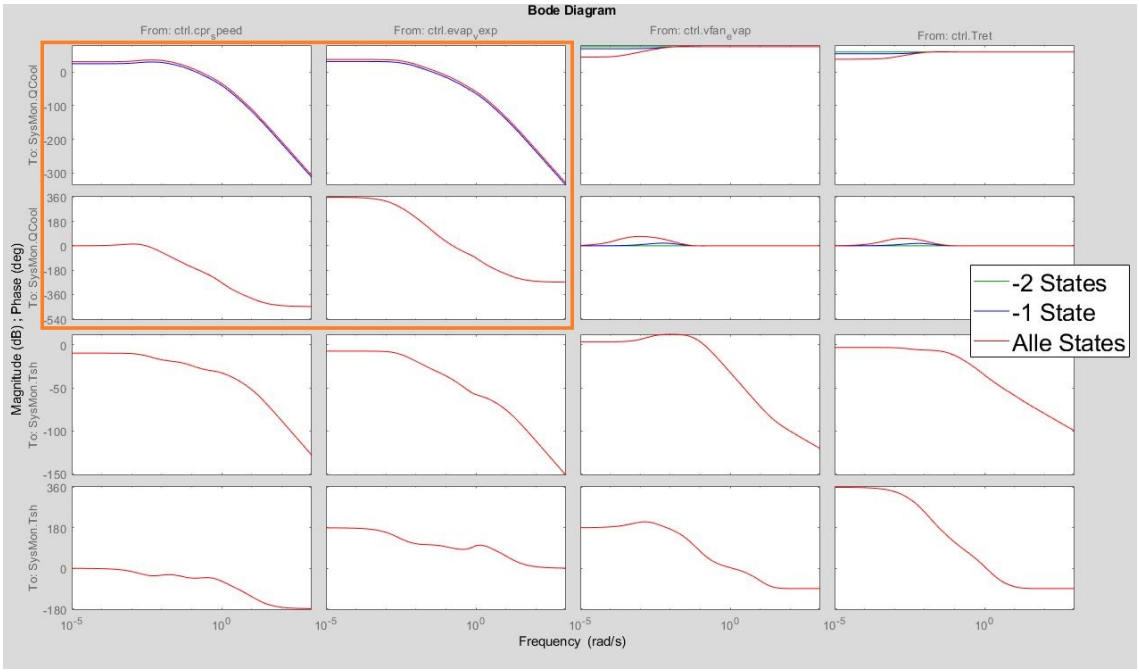

Figure 6.16: Bode with all three models

The only significant difference in the models are shown on the bode plots. In figure Figure 6.16 the results are the same for all models except for the orange marked box. In this marked area it shows that by removing two states the output; cooling capacity, is no longer depended on two inputs, as it it in the other two models. This means that the model that will be focused on will be the one where only one state is removed.

Part III

Control design

Introduction

In this part the design of a controller will be shown and explained. The MIMO model provided from the company is decoupled, so that a robust controller will be designed in a simpler manner. The proposed controller that will be designed is a robust H_∞ controller. This will then be explained and implemented on the system. Theoretically it shows promise, while the only con is that of the conservative of the controller. It will then be investigated if it works in the real system through some tests.

Decoupling of the model 7

Since the model of the system is a multiple input multiple output, MIMO, the complexity of controller design increases. To avoid the complexity a simplification of the model will be done. The simplification technique that is used is to decouple the system model. The decoupling allows the feature of dealing with two single input single output control systems instead of a MIMO control system. This simplification makes it easier to design, implement and tune control systems. The downside of using two SISO systems instead of a MIMO system is that the model loses the dependency of other variables. It is therefore chosen to decouple the MIMO system into two single inputs single outputs, SISO, systems.

7.1 Cross Coupling of MIMO Model

First to decouple the system model, the MIMO model is split into transfer functions with the help of Matlab commands 'tf' and 'minreal' to get the smallest order possible and as result of the feedback system is now as seen in Figure 7.1.

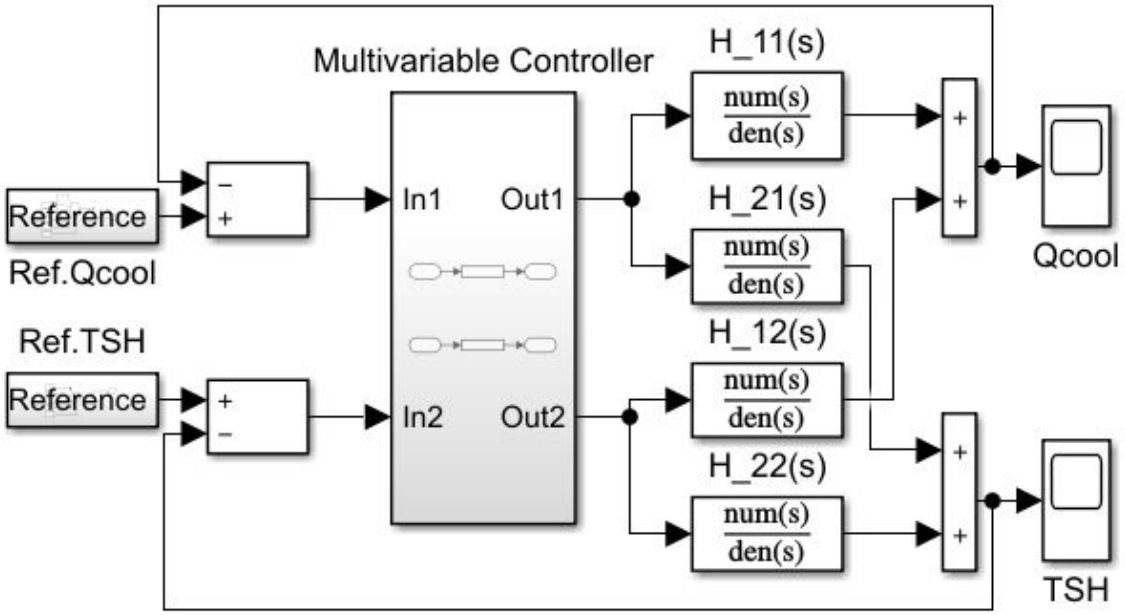

Figure 7.1: Multivariable control of MIMO Model of the system

As there are cross couplings in the model, it is necessary to test how much the cross coupling affects the output, before it is viable to decouple it. The procedure to test this,

is by first stepping on one of the reference and then after wards the other. This helps to visualise on how much the other output gets affected by this. As seen in Figure 7.2 a step in the superheat reference does not change much in superheat output, it gives a small variation of 5% of the output and stabilises. And as seen in Figure 7.3, the change in cooling capacity reference does not change the output for superheat much either. This also has a variation of approximately 5% and stabilises.

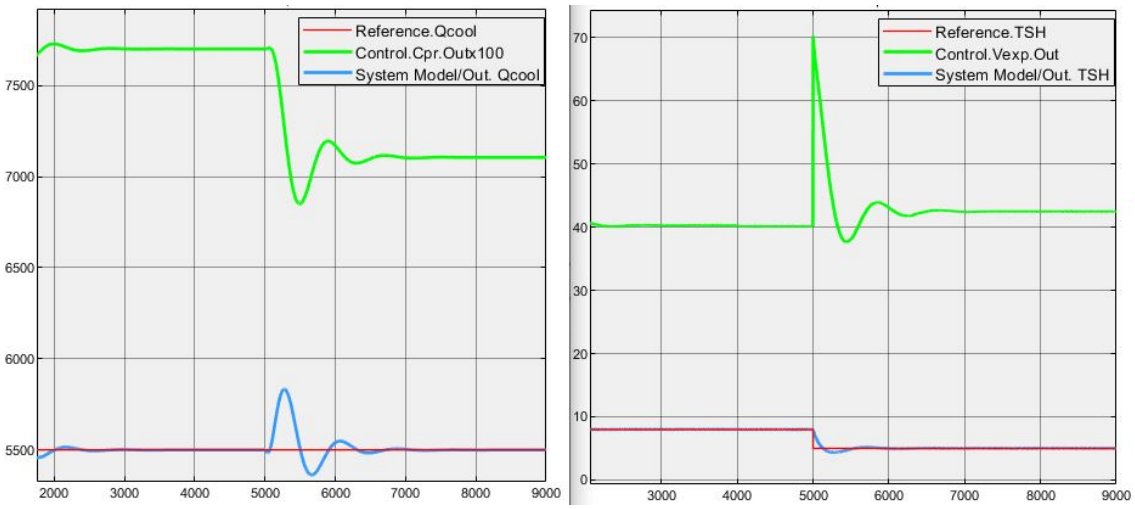

Figure 7.2: In this figure a step is given to the superheat reference

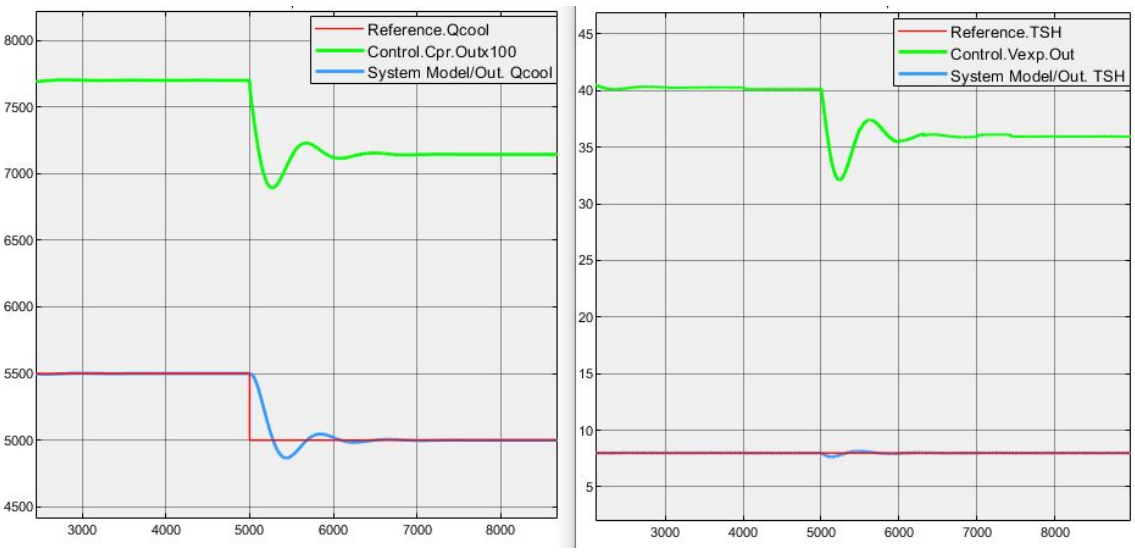

Figure 7.3: In this figure a step is given to the cooling capacity reference

This means that decoupling of this model is a reasonable choice since it simplifies the design phase of a controller.

7.2 Decoupling Transfer Function, Two SISO Systems

To cancel the cross couplings happening in Figure 7.1, compensator blocks, D1(s) and D2(s), are the transfer function calculated to decouple the system model as seen in Figure 7.4.

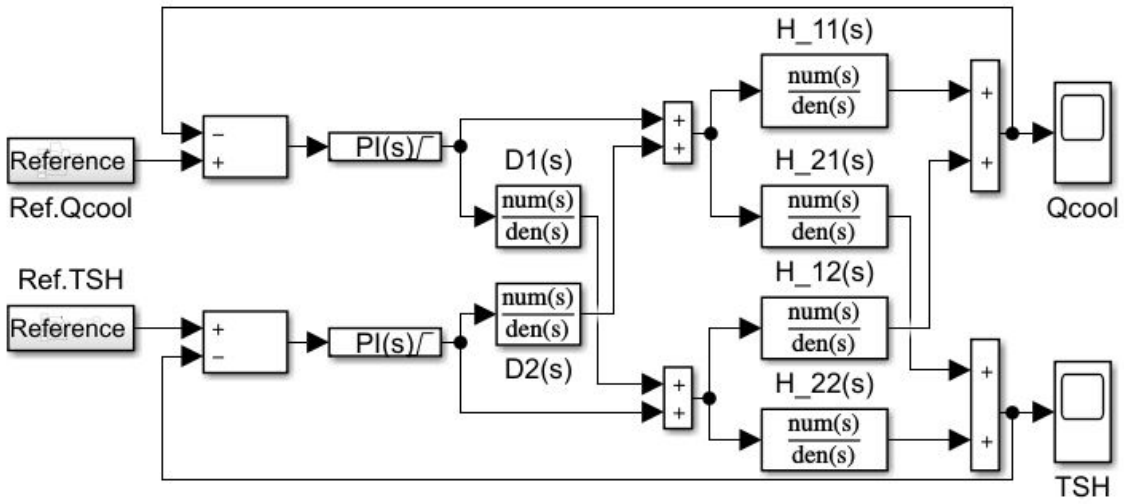

Figure 7.4: Decoupled MIMO Model of the system

From the Figure 7.4 the transfer functions can be found in Appendix D and the calculation for the decoupled transfer functions can be seen in Equation 7.1 and Equation 7.2.

$$D_1(s) = -\frac{H_{21}(s)}{H_{22}(s)} \tag{7.1}$$

$$D_2(s) = -\frac{H_{12}(s)}{H_{11}(s)} \tag{7.2}$$

These two decoupled transfer function gives the opportunity to split the system into two SISO system now, as seen in Figure 7.5.

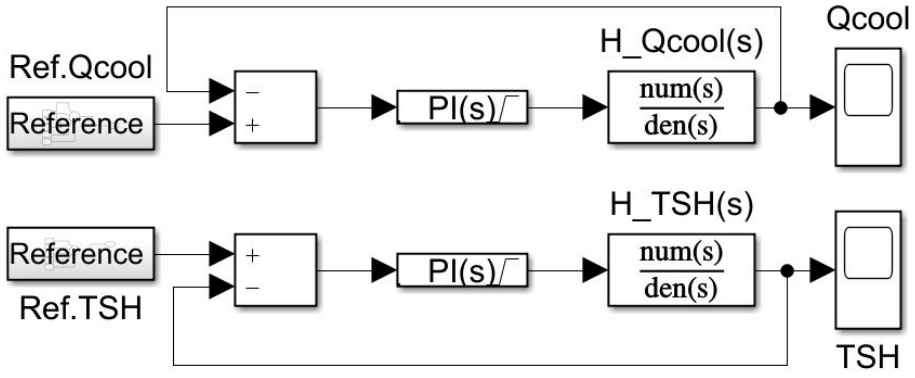

Figure 7.5: Control of two SISO Models of the system

From Figure 7.5, the transfer functions are calculated as seen in Equation 7.3 and Equation 7.4 and the zero, pole, gain form of it can be seen in Appendix D. .

$$H_{Qcool}(s) = H_{11}(s) - \frac{H_{12}(s)H_{21}(s)}{H_{22}(s)} = H_{11}(s) + H_{12}(s)D_1(s) \tag{7.3}$$

$$H_{TSH}(s) = H_{22}(s) - \frac{H_{21}(s)H_{12}(s)}{H_{11}(s)} = H_{22}(s) + H_{21}(s)D_2(s) \tag{7.4}$$

The feedback signals with simple PI-control of cooling capacity and superheat where both are now SISO systems can be seen in Figure 7.6.

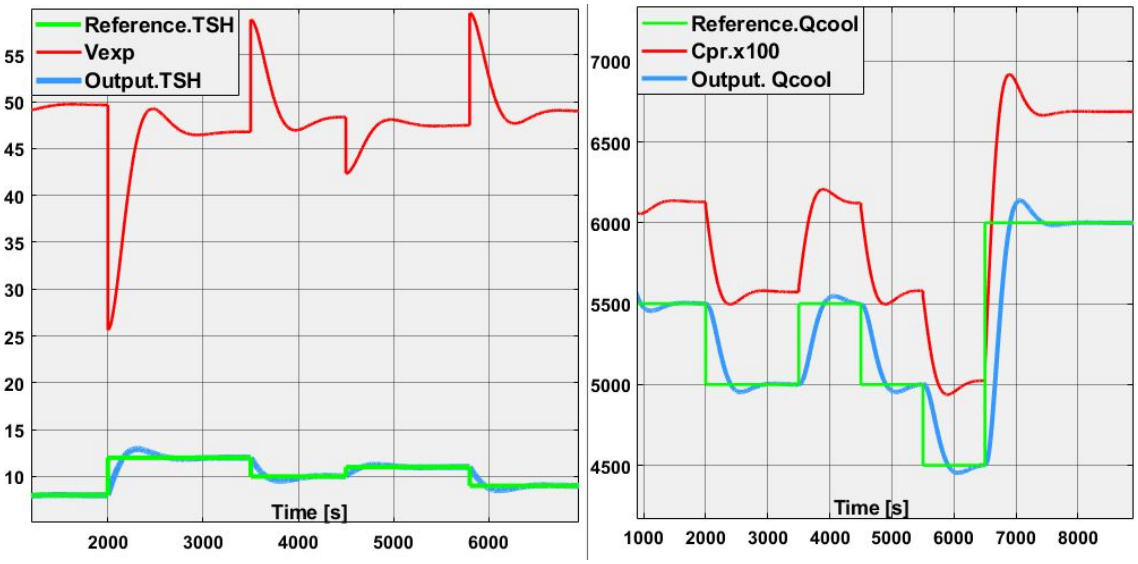

Figure 7.6: Control of both SISO systems; The left graph is control of cooling capacity, and the right graph is control of superheat

The transfer functions are simplified by reducing the model order with use of hankel singular values, and in matlab the function is called hankelsv(). The function measures the contribution of each state to the input/output behavior. As seen in Figure 7.7, a system order of one is more significant than others, which means that the model can be reduced to a first order system and the rest of the states can be discarded by using the matlab function balred().

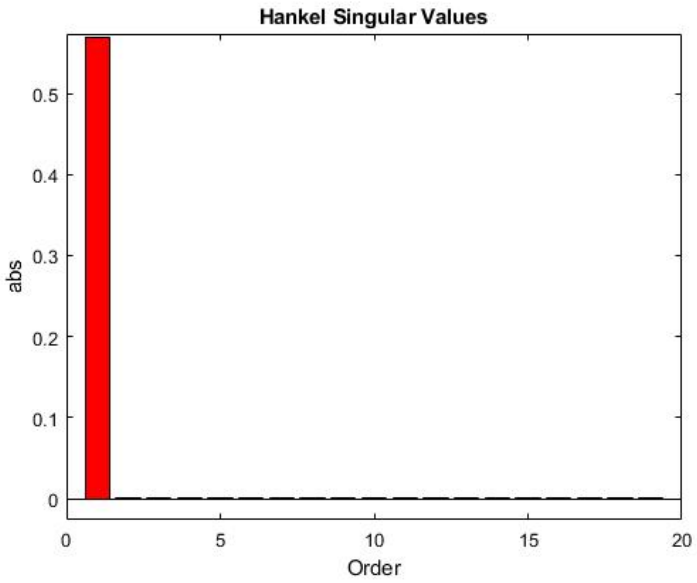

Figure 7.7: Hankel singular value graph, that shows the significance of each state in the superheat system

The first order model for superheat can be seen in Equation 7.5.

$$H_{tsh} = \frac{1,37565}{1022s+1} = \frac{0.001346}{(s+0.0009783)} \tag{7.5}$$

Similar procedure for the model of cooling capacity, where the Hankelsv can be seen in Figure 7.8

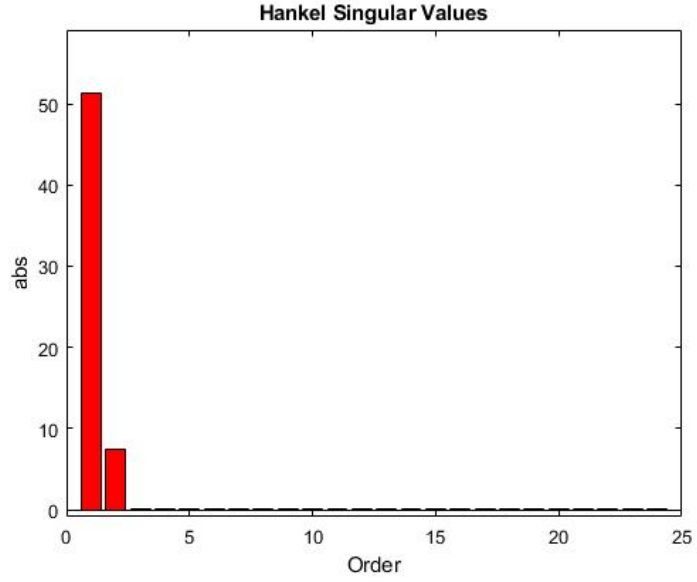

Figure 7.8: Hankel singular value graph, that shows the significance of each state in the cooling capacity system

From Figure 7.8 it can be seen that two poles are more significant than the rest, so this

model will be reduced to a second order system as seen in Equation 7.6.

$$H_{qcool} = \frac{-0,091509(s - 0,3395)}{(s + 0,03451)(s + 0,01025)} \tag{7.6}$$

In this chapter the MIMO system has been reduced to two SISO systems by decoupling; a system for the superheat and a system for the cooling capacity. These two models has been reduced further to a first order and a second order systems. This project will mainly focus on controlling the superheat, because it is important to not let any liquid into the compressor. Now that the model is ready, a specific control method is ready to be designed.

H_∞ Control Design and Implementation

8

For this chapter the general procedure to make a SISO robust controller will be explained. The superheat model will mainly be focused on and used to explain some parts in this chapter. The robust controller that will be focused on is a H_∞ - controller because it gives an opportunity to achieve the best performance available by designing weight functions. This will further be explained in section 8.4.

Since the chosen controller is an H_∞ controller, some requirements are to be upheld. These requirement relates to the nominal performance, robust stability and robust performance, and these topic will be covered in this chapter. The requirements that are to be upheld are as listed:

- Nominal performance $\rightarrow |S(j\omega)W_s(j\omega)| < 1.$
- Robust stability $\rightarrow |T(j\omega)l_m(\omega)| < 1.$
- Robust performance $\rightarrow |S(j\omega)W_s(j\omega)| + |T(j\omega)l_m(\omega)| < 1.$

The variables and the requirements will be explained throughout the chapter. A quick summary of the variables; S is the sensitivity function, Ws is the weight function for the sensitivity, T is the complementary function, lm is the uncertainty model.

8.1 Nominal Model

A nominal model is a model where either all of the parameters are known, or where the parameters are calculated as the mean of the deviations. A nominal model is always needed if control system needs to be implemented. The nominal model for this project was found earlier and is as seen in Equation 8.1.

$$G(s) = \frac{y(s)}{u(s)} = \frac{T_{sh}}{V_{exp}} = H_{tsh}(s) = \frac{1,37565}{1022s+1} = \frac{0.001346}{s+0.0009783} \tag{8.1}$$

The nominal model of the system is a reduced first order system for superheat. This means that the uncertainty model can now be designed.

8.2 Model uncertainty

In this section the uncertainty model will be explained and designed for the worst case scenario.

Definition of model uncertainty

It is necessary to create a uncertainty boundary to establish a robust controller later on. To explain how the uncertainty is described Figure 8.1 will be used. And as seen in Figure 8.1 there are two ways of defining the uncertainty, either in amplitude and phase in which indicates the edge boundaries of the uncertainty. This gives the shape as $g(w)$ in Figure 8.1 (a) or the norm bounded uncertainty in which contains the uncertainty at all frequencies by taking the worst case uncertainty and encircled with the maximal model uncertainty, $l_a(w)$ or $l_m(w)$ as seen in Figure 8.1 (b).

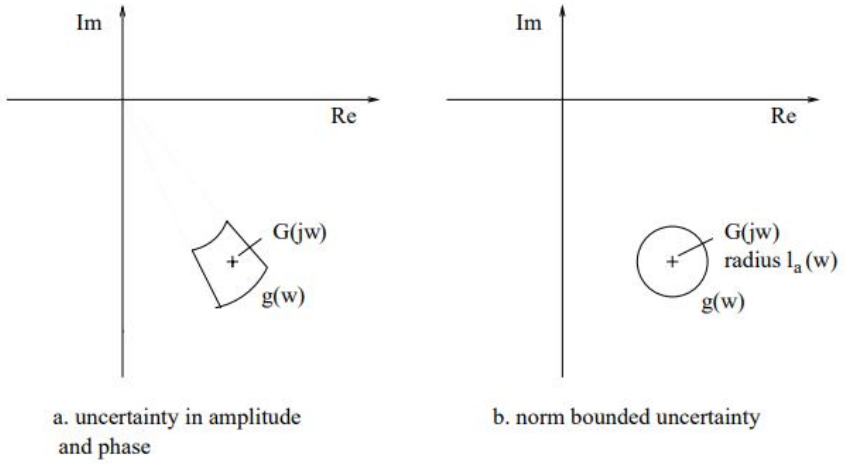

Figure 8.1

The norm bounded uncertainty region contains all the uncertainty models since the radius of the drawn circle is the maximum error. A way to define the radius is by using the method called additive, l_a, or multiplicative, l_m, uncertainty. In this project multiplicative uncertainty will be focused on. All of the models for the uncertainty method can be defined to the family of models,G_{models}, which can be described as seen in Equation 8.2. [4]

$$For Multiplicative: \quad G_{models,m} = \{G_\Delta : |G_\Delta(j\omega) - G_(j\omega)| \leq l_m(\omega)|G(j\omega)|\} \qquad (8.2)$$

In Equation 8.2 $G_(j\omega)$ is the nominal model defined earlier, $G_\Delta(j\omega)$ expresses the possible model which can be the real model and the $l_m(\omega)$ is the maximum multiplicative uncertainty.

The way to add the multiplicative uncertainty model to the known closed loop system is shown in Figure 8.2.

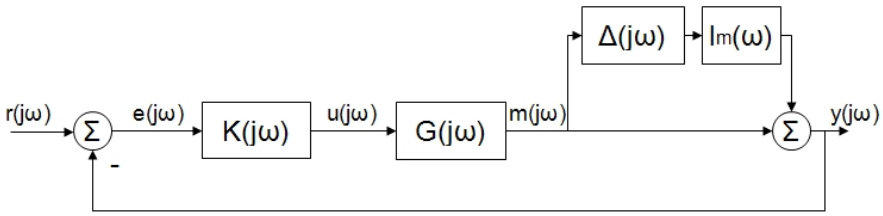

Figure 8.2: Closed Loop System with an multiplicative model uncertainty

From Figure 8.2 the maximum multiplicative model, $l_m(\omega)$, can be calculated as seen in **Equation 8.3**.

$$l_m(\omega) \cdot \Delta_m(j\omega) = \frac{G_\Delta(j\omega) - G(j\omega)}{G(j\omega)} \tag{8.3}$$

In Equation 8.3 the $\Delta_m(j\omega)$ is the multiplicative uncertainty which needs to be either equal to one or less than one.

Design of l_m

The uncertainty model as explained will be used to design the controller to handle all of the uncertainties of the system. While it is known that the worst case scenario appears when certain amount of ice appears on the evaporator it is said by the company supervisor that the coefficient of heat transfer in the model is halved. This means that energy from the fans are significantly lowered. Because of this change a new model is derived and reduced in order of one as seen in Equation 8.5, where $H_{tsh,red}$ is the new model by reducing the value of the transfer heat coefficient by 50% and as a comparison the nominal model found earlier can be seen in Equation 8.4.

$$G(s) = H_{tsh} = \frac{T_{sh}}{V_{exp}} = \frac{1,37565}{1022s + 1} \tag{8.4}$$

$$H_{tsh,red} = \frac{T_{sh}}{V_{exp}} = \frac{1,092585}{507s + 1} \tag{8.5}$$

From Equation 8.5 and Equation 8.4, the edge boundaries of the models can be calculated as seen in Equation 8.6.

$$\begin{aligned} G_{\Delta 1}(s) &= \frac{K_{min}}{\tau_{min}s + 1} \rightarrow G_{models,m,1} = \frac{G_{\Delta 1}(s) - G(s)}{G(s)} \\ G_{\Delta,2}(s) &= \frac{K_{min}}{\tau_{max}s + 1} \rightarrow G_{models,m,2} = \frac{G_{\Delta 2}(s) - G(s)}{G(s)} \\ G_{\Delta,3}(s) &= \frac{K_{max}}{\tau_{min}s + 1} \rightarrow G_{models,m,3} = \frac{G_{\Delta 3}(s) - G(s)}{G(s)} \end{aligned} \tag{8.6}$$

$$G_{\Delta,4}(s) = \frac{K_{max}}{\tau_{max}s + 1} \rightarrow G_{models,m,4} = \frac{G_{\Delta 4}(s) - G(s)}{G(s)}$$

From Equation 8.6, $G_\Delta(s)$ are the possible models inside of the edge boundaries and $G_{models,m}$ are the family of models for multiplicative uncertainty which defines the edge boundaries.

The edge boundaries of the models are plotted in Figure 8.3 which will help to design a maximal multiplicative uncertainty which includes all the edge boundaries.

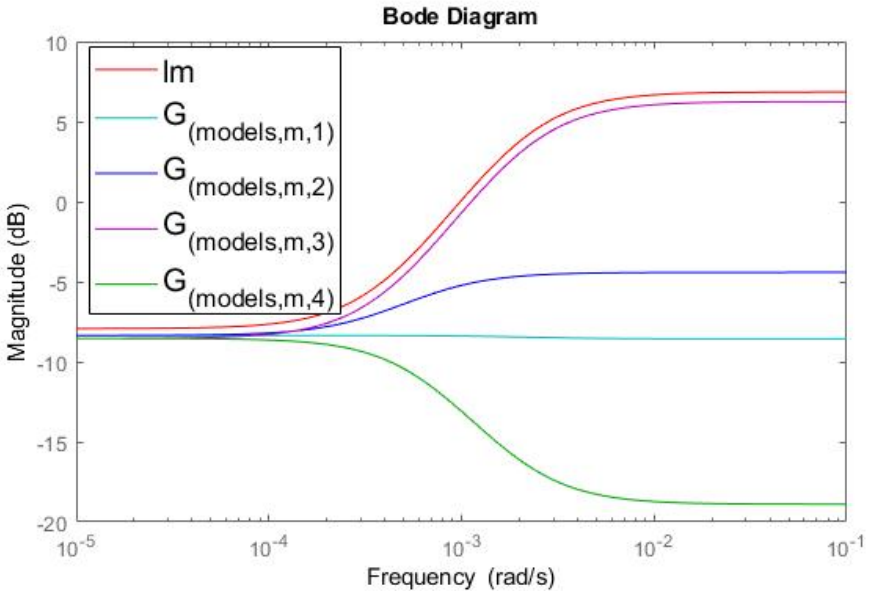

Figure 8.3: Model uncertainty and the designed worst case lm

In Figure 8.3 the lm is designed as a lead compensator where the cutoff frequencies were found by analysing the worst magnitude of the edge boundaries. lm is designed so that all uncertainties of the model at every frequency are included. The lead is designed as seen in Equation 8.7.

$$lm = 1,6 \cdot \frac{s + 2,85 \cdot 10^{-4}}{s + 2 \cdot 10^{-3}} \tag{8.7}$$

But as it already can be concluded from Figure 8.3, the controller will be very conservative since the magnitude ends up around 6 dB at low frequencies. This could mean that a robust control might not be optimal solution to the ice appearance problem. To testify this theory the procedure to design a robust controller will be continued and afterwards simulated.

8.3 Nominal Stability

For the system to be nominal stable the control system needs to be internally stable.

This means that by adding more inputs (r,u',d) and outputs (e,u,y) to the system as seen in Figure 8.4, it will give the opportunity to check the internal stability. If the system still is stable, then and only then the nominal stability is achieved.

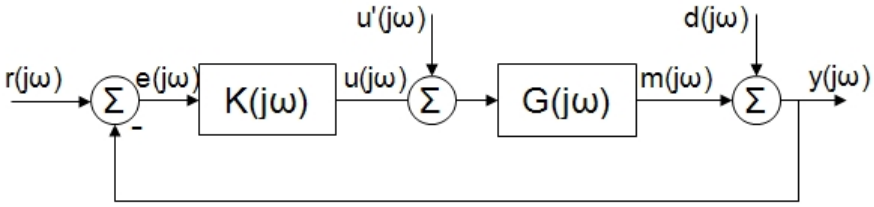

Figure 8.4: Closed Loop System with added inputs to analysis of internal stability

After adding extra inputs and outputs the internal stability can be determined if every elements in the new close loop equation, as seen in Equation 8.8, has no pole on the right half plane.

$$\begin{bmatrix} y(j\omega) \\ u(j\omega) \end{bmatrix} = \begin{bmatrix} \frac{GK(j\omega)}{1+GK(j\omega)} & \frac{G(j\omega)}{1+GK(j\omega)} \\ \frac{K(j\omega)}{1+GK(j\omega)} & \frac{-GK(j\omega)}{1+GK(j\omega)} \end{bmatrix} \begin{bmatrix} r(j\omega) \\ u'(j\omega) \end{bmatrix} \tag{8.8}$$

If it is known that G and K are stable, it is enough to analyse the characteristic equation 1+GK(s) = 0.

Since the nominal model was found earlier, and a control system was designed and tested in Figure 7.6 in chapter 7, and the poles were found to be in the left half plane, Therefore it is concluded that the system is nominal stable

8.4 Robust Stability, Nominal Performance and Weight Functions

Robust Stability

When looking at the robust stability of the controlled system, it means that the system is stable for all models in the family of models. In this case it is assumed that all of the models inside of the family of models contains equal amount of poles in the right half plan. Under the condition that it the system is to be robustly stable, the Nyquist criteria states that the Nyquist curve needs to encircle the Nyquist point (-1,0) counter-clockwise equally amount of times as how many poles there are in the right half plane [4].

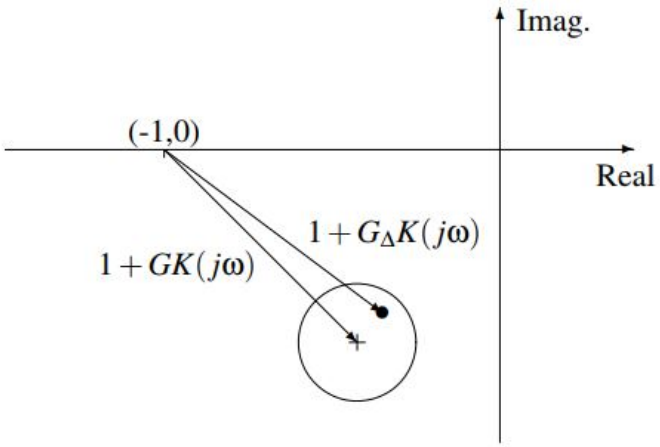

Figure 8.5: Nyquist plot for the nominal system and for an arbitrary model in the family of models [4].

From Figure 8.5 and the Nyquist criteria, it is interpreted that if the radius of the uncertainty region is smaller than the length between the Nyquist point and the center of the uncertainty region it will remain stable in all models in the family of models. This can be expressed mathematically as seen in Equation 8.9:

$$\begin{aligned} & & |1+GK(j\omega)| > |GK(j\omega)l_m(\omega)|, \forall \quad \omega & \\ rearranged \quad to: & \quad \frac{|GK(j\omega|)}{|1+GK(j\omega)|}l_m(\omega) < 1, & \forall \quad \omega & \quad (8.9) \\ or \quad to: & \quad |T(j\omega)l_m(\omega)| < 1, & \forall \quad \omega & \end{aligned}$$

The $T(j\omega)$ is the close loop system and also known as the complementary sensitivity function which describes how uncertainty affects the output. It is possible to define the complementary sensitivity function as seen in Equation 8.10:

$$T(j\omega) = \frac{y(j\omega)}{r(j\omega)} = \frac{|GK(j\omega)|}{|1+GK(j\omega)|} = \frac{|L(j\omega)|}{|1+L(j\omega)|} \quad (8.10)$$

In Equation 8.10 the $L(j\omega)$ is the open loop transfer function.

While at the topic of complementary sensitivity function, the sensitivity function can be explained as well. The sensitivity function defines the sensitivity to the disturbance of the system. The sensitivity is used as a reference tracking function, as it also is defined by the relation between error and reference as seen in Equation 8.11:

$$S(j\omega) = \frac{y(j\omega)}{d(j\omega)} = \frac{e(j\omega)}{r(j\omega)} = \frac{1}{|1+GK(j\omega)|} = \frac{1}{|1+L(j\omega)|} \quad (8.11)$$

While the sensitivity determines how well the closed loop system is to track the reference, the complementary sensitivity function determines how well the close loop system handles

the uncertainty of the system. As seen in Equation 8.12, a trade-off between reference tracking, and uncertainty handling which can be adjusted, depending on the performance requirements [4].

$$S(j\omega) + T(j\omega) = \frac{1}{|1 + L(j\omega)|} + \frac{|L(j\omega|}{|1 + L(j\omega)|} = 1 \tag{8.12}$$

Since it is a trade-off between performance and robustness, a way to adjust these priorities is by designing weight functions that will give the desired outcome of the controller.

Nominal Performance

The goal to achieve in a closed loop system is to minimise the error while the performance requirements are maintained. This can be related to the sensitivity function since the function determines the reference tracking. To achieve minimisation of the error the sensitivity, S, needs to be small, and the only way for now to achieve this is by having a larger L as seen in Equation 8.11.

Since the chosen controller method has been chosen to a H_∞ controller the nominal performance can be determined by the maintaining the condition as seen in Equation 8.13 [4].

$$Nominal\ Performance \rightarrow \quad |SW_s(j\omega)| < 1 \qquad \forall \quad \omega \tag{8.13}$$

In Equation 8.13 the W_s is the tunable weight function. This weight function will be designed that S will be minimised at specific frequencies. This will result in best possible reference tracking. Since the sensitivity needs to be close to zero the weight, Ws, need to be designed such that it has high gain in low frequencies and low gain at high frequencies. The design will be that of a lag compensator with the chosen cutoff frequencies as seen in Equation 8.14 and the magnitude plot is seen in Figure 8.6.

$$Ws = 0.69 \cdot \frac{s + 2 \cdot 10^{-4}}{s + 7 \cdot 10^{-7}} \tag{8.14}$$

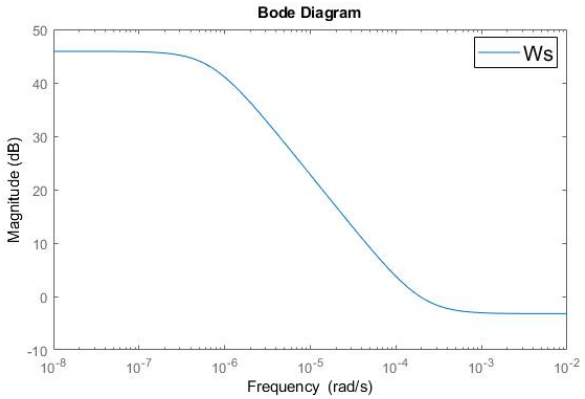

Figure 8.6: The Weight function seen in the magnitude plot of Bode

The sensitivity function, S and complementary sensitivity function, T includes a controller gain to achieve the requirements. This gain can be obtained by a matlab function, *hinfstruct*. This function uses an augmented plant which is defined by the nominal model, the weight for the reference, Ws and for the system output, Wt, to solve the H_∞ problem by minimising γ. A restriction condition to the function, *hinfstruct*, is given. The condition is set so that the controller gain will be created as a PID controller. In the matlab script **Add en reference til koden her** the PID is tunable, meaning that matlab will give the best PID controller, depended on the defined augmented plant. Since Ws is designed to keep reference tracking to the system the second weight Wt is added to keep robustness to system. The weight Wt is designed as an lead compensator with the chosen cutoff frequencies as seen Equation 8.15 and the magnitude can be seen on Figure 8.7.

$$Wt = 1.8 \cdot \frac{s + 7 \cdot 10^{-8}}{s + 9 \cdot 10^{-3}} \tag{8.15}$$

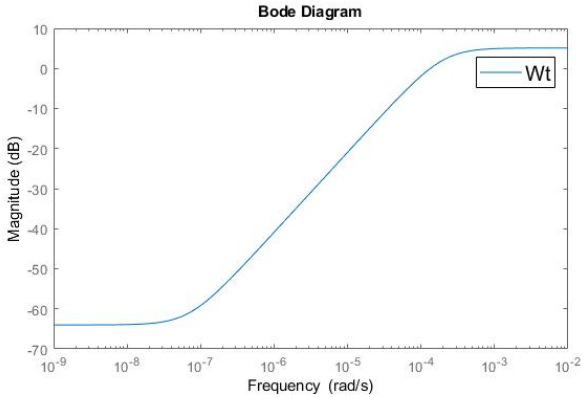

Figure 8.7: The Weight function seen in the magnitude plot of Bode

This will result in a nominal performance kept under 1 as seen in Figure 8.8 and for the robust stability the requirements given in Equation 8.9 are also maintained as seen in the same figure Figure 8.8

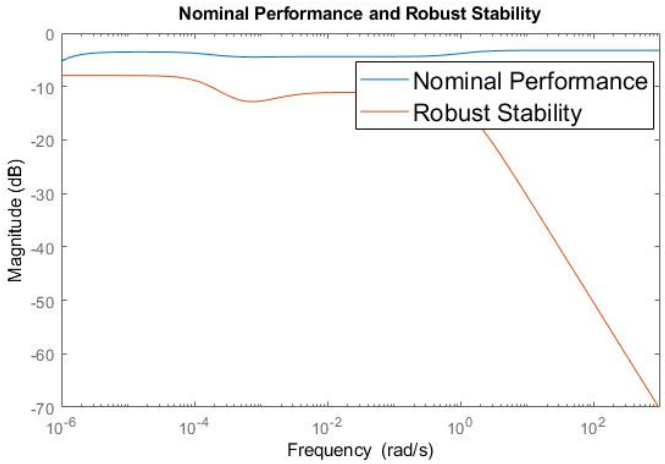

Figure 8.8: The figure shows that both nominal performance and robust stability are kept below 1

Now that the weights are defined, it is necessary to check if the it the function solve the H_∞ problem which can be concluded if the expression seen Equation 8.16 [4] in are maintained, and as seen in Figure 8.9.

$$\arg\min_{K\varepsilon\mathcal{K}} \begin{vmatrix} T(s)W_t(s) \\ S(s)W_s(s) \end{vmatrix} \leq \gamma \tag{8.16}$$

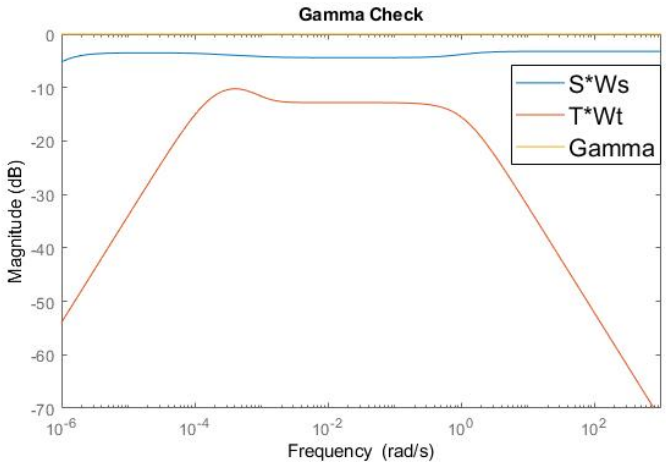

Figure 8.9: The figure shows that requirement are upheld

Now that the weight are designed and nominal performance and robust stability is achieved, the next next step is to achieve robust performance.

8.5 Robust Performance

To achieve a robust performance it means to design a compensator so that the error is minimized for all of the models in the family of models. As visual representation a Nyquist plot of this can be seen Figure 8.10 [4].

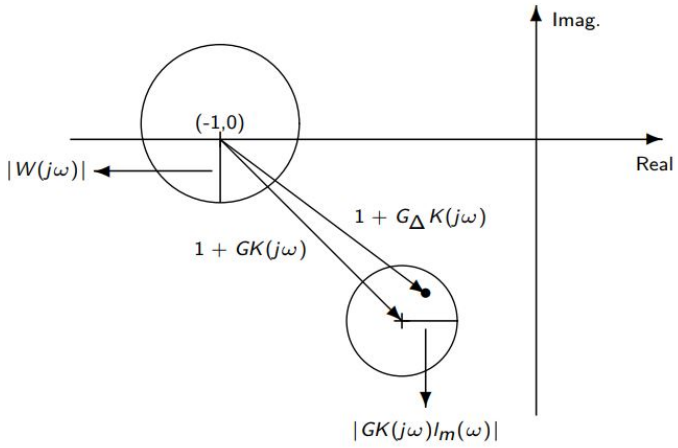

Figure 8.10: Nyquist plot for the geometrical perspective [4].

Including the robust performance in the system ensures the compensator that the error is bounded to all of the models in the family of models. Robust performance is defined by both the robust stability and nominal performance as seen in Equation 8.17 [4].

$$\begin{aligned} |S_\Delta(j\omega)| &= \frac{1}{|1 + G_\Delta K(j\omega)|} \\ &\leq \frac{1}{|1 + GK(j\omega)| - |GK(j\omega)l_m(\omega)|} \\ &= \frac{|S(j\omega)|}{1 - |T(j\omega)l_m(\omega)|} \end{aligned} \tag{8.17}$$

Inserting the definition of the pertubed sensitivity in Equation 8.17 in the expression of the nominal performance results as seen in Equation 8.18 [4].

$$\frac{|SW_s(j\omega)|}{|1 - |T(j\omega)l_m(\omega)||} < 1 \qquad \forall\omega \tag{8.18}$$

This can be further rewritten to :

$$|SW_s(j\omega)| + |T(j\omega)l_m(\omega)| < 1 \qquad \forall\omega \tag{8.19}$$

With the designed weight function shown earlier, the robust performance can be seen in Figure 8.11.

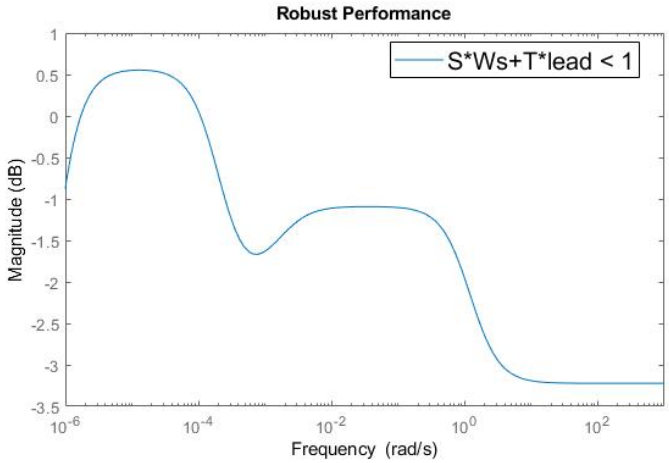

Figure 8.11: The figure shows that requirement for the robust performance are upheld

From the Figure 8.11 it can be seen that it meets the condition to achieve robust performance. The final controller ended up being a PID controller with the values Kp = 0.278, Ki = 0.00015, Kd = 108, Tf = 1.07.

$$K_{H_\infty}(s) = Kp + Ki \cdot \frac{1}{s} + Kd \cdot \frac{1}{Tf \cdot s + 1} \tag{8.20}$$

Now that the everything is designed it is ready to be implemented to the real system. But before that, a step response is made to proof the theory explained in section 8.2. As

seen in Figure 8.12 it takes around 40.000 seconds to stabilise the system, which mean approximately 11 hours.

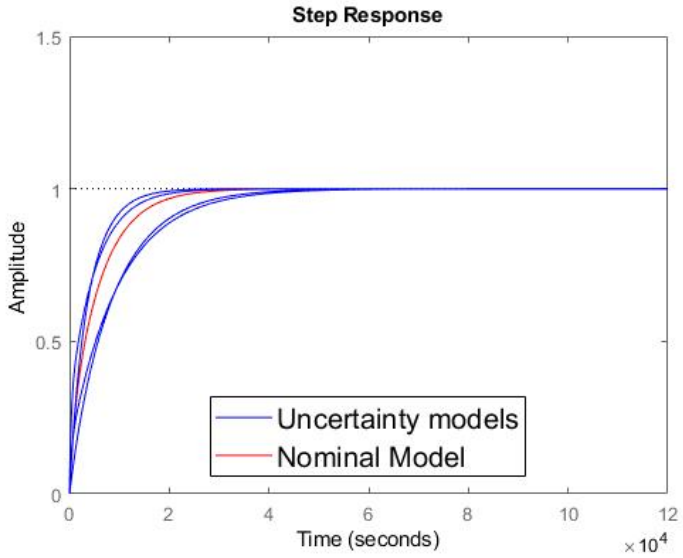

Figure 8.12: The figure shows the step response of the closed loop

As explained in section 8.2 the controller is going to be very conservative because of the uncertainty and this is proven in Figure 8.12. In a system that works on cooling, the thermodynamics changes slowly. But to be sure that the H_∞ is not designed too conservative, it will be tested on the real system.

8.6 Implementation of H_∞ controller and Test Results

In this section some tests will be shown, where the main goal is to implement the designed H_∞-controller into the real system. Before the implementation of the controller, it is necessary to understand how the system works, and how a controller can be implemented.

Control of the reefer container

The reefer container at Lodam Electronics is controlled by a program called Lodam UMO, which can be seen in Figure 8.13. The program also shows the important values in different areas of the cooling system, and it is connected to a Matlab script, that can record these and more values. The Matlab script is where the controller is implemented. Firstly the Matlab script needs to be edited so that the desired control system is the one designed earlier.

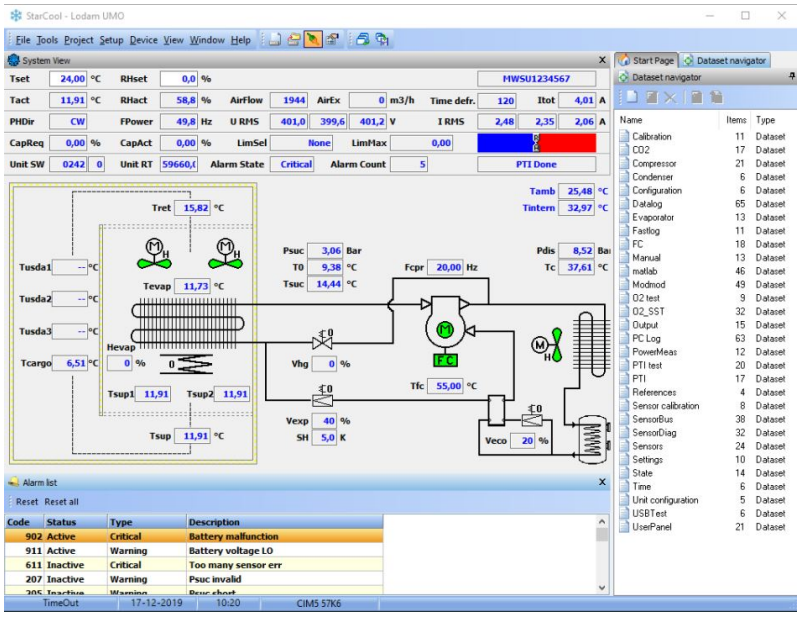

Figure 8.13: The program that connects the reefer container and working computer

In the mentioned matlab script it is edited such that, the only control system is for the superheat. This means that the compressor operates with a constant frequency at 20 Hz, and the air temperature in the container is set to be a constant at a temperature of 10 ℃. As explained earlier about the case of ice appearance on the evaporator coil, the temperature has to be 0 ℃. The reason this is set to 10℃ and not 0 ℃ is to get used to the system, and to test if the H_∞ controller can be stable with almost non disturbances.

Firstly a test where only a P controller is used. The constants for compressor frequency and air temperature in the container are set as mentioned, the superheat reference is set to 10 ℃ and the value of the Proportional gain is set to 3. As seen in Figure 8.14 the P-controller was activated after 5200 seconds and from that point on, it can be seen that the system reacts to the change. From the results it can be concluded that the system

can not be controlled by a regular P-controller, since it has an steady state error, so the Integrator term is necessary.

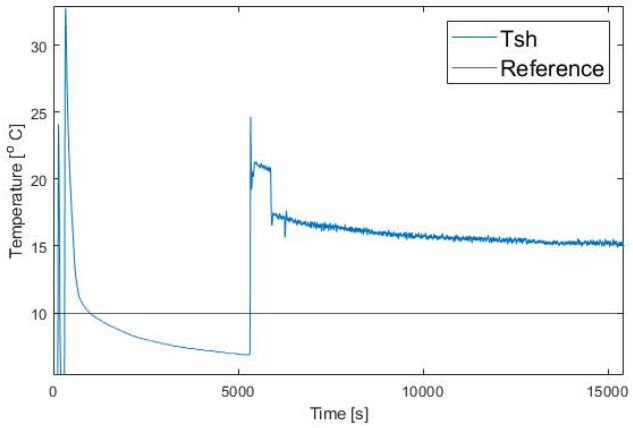

Figure 8.14: A test of superheat control with only a P-controller

H_∞ controller implementation and manual tuning

Now that the system reacts to the edited matlab script, the H_infty controller is now ready to be implemented. Using the same compressor frequency and air temperature constants as the first test, the PID controller with the values Kp = 0.278, Ki = 0.00015, Kd = 108, Tf = 1.07, is now implemented. The results can be seen in Figure 8.15. In this figure the H_∞ controller is running from the beginning until 1800 seconds and is unstable, which can be seen in the control signal in Figure 8.16. After the 1800 seconds, the values of the PID-controller are manually tuned to stabilise.

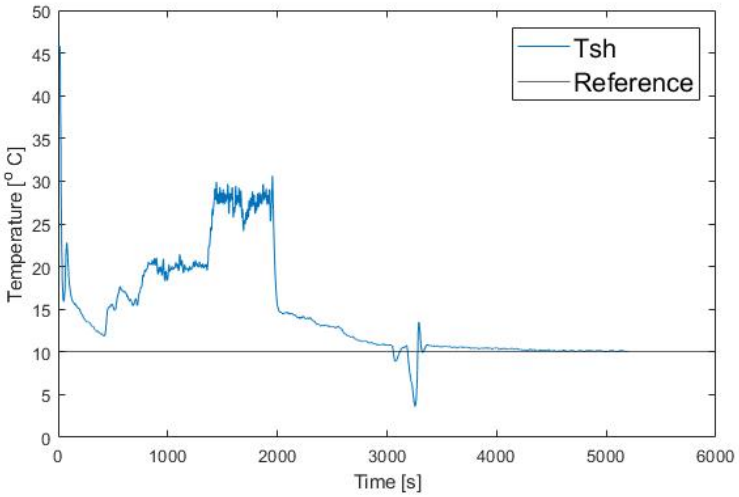

Figure 8.15: Test to stabilise superheat with the H_∞-controller

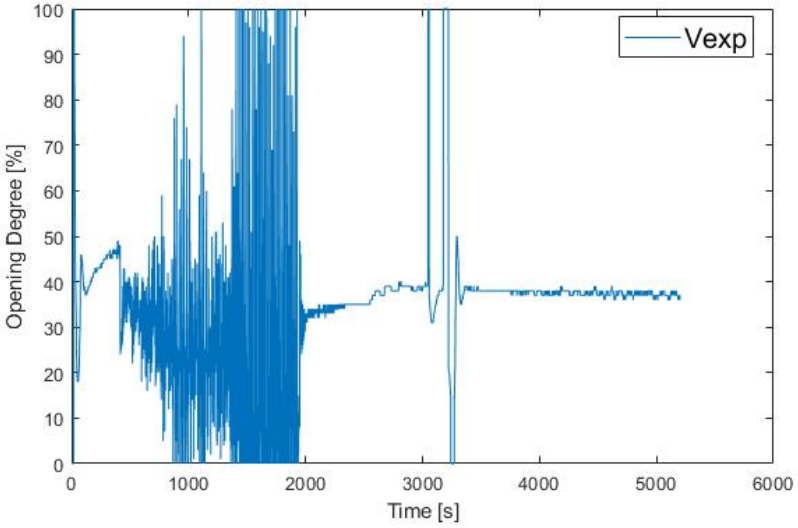

Figure 8.16: The control signal for the H_∞-controller

A third test is done with the new values of the PID-controller where the superheat reference is set to 10 ℃ until 800 seconds and then to 5 ℃. The values of the new PID controller are now : Kp = 2.278, Ki = 0.0185, Kd = 1, Tf = 1.07. As seen in Figure 8.17 the result of the new PID-controller, the system stabilises, with oscillations from 0.1 ℃ - 0.2 ℃. And as seen in Figure 8.18 the control signal is more stable than the H_∞-controller.

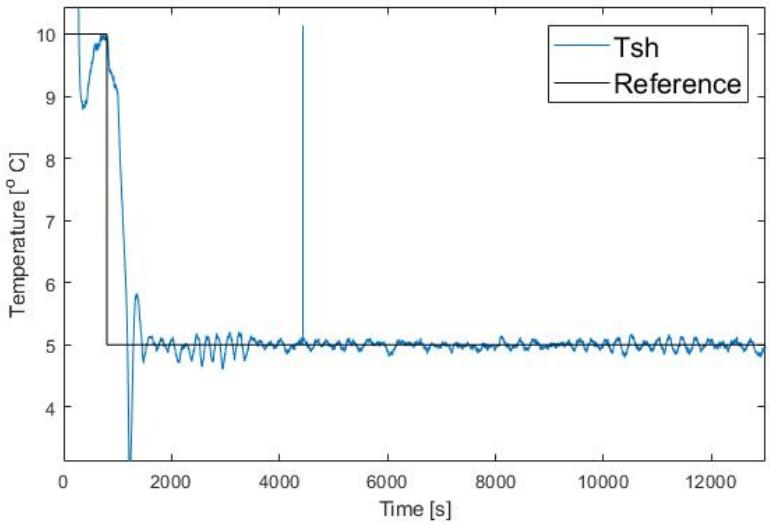

Figure 8.17: Test of superheat control with new values for the PID controller

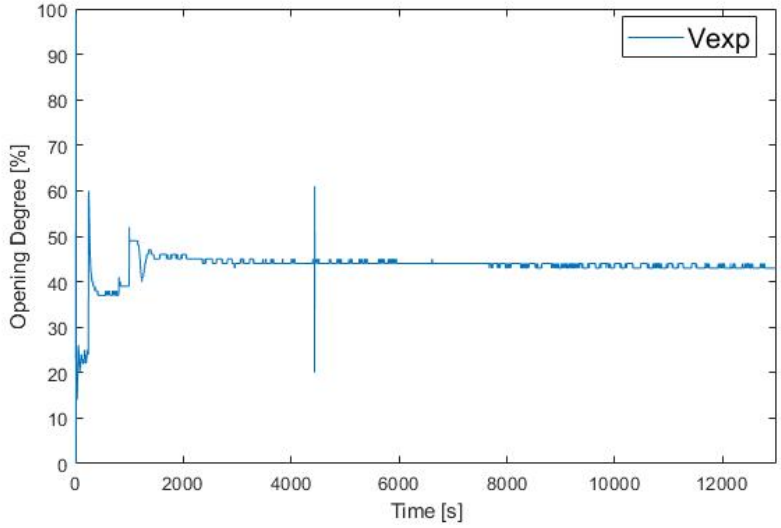

Figure 8.18: Control signal of the test with the new values for the PID controller

Robust Stability and Robust Performance of The New PID-Controller

Now that a new controller is found, the only question is to see if it achieves the robust criteria and is robust towards the worst case. This is done by checking the conditions of nominal performance, robust stability and robust performance as explained earlier:

- Nominal performance $\rightarrow |S(j\omega)W_s(j\omega)| < 1.$
- Robust stability $\rightarrow |T(j\omega)l_m(\omega)| < 1.$
- Robust performance $\rightarrow \quad |S(j\omega)W_s(j\omega)| + |T(j\omega)l_m(\omega)| < 1.$

From figure Figure 8.19 it can be seen that the controller can be stable and reduce the error for the nominal case. But looking at the robust stability in Figure 8.19 and the robust performance in Figure 8.20 it can be concluded that this controller can not stabilise the superheat when ice appears on the evaporator coil.

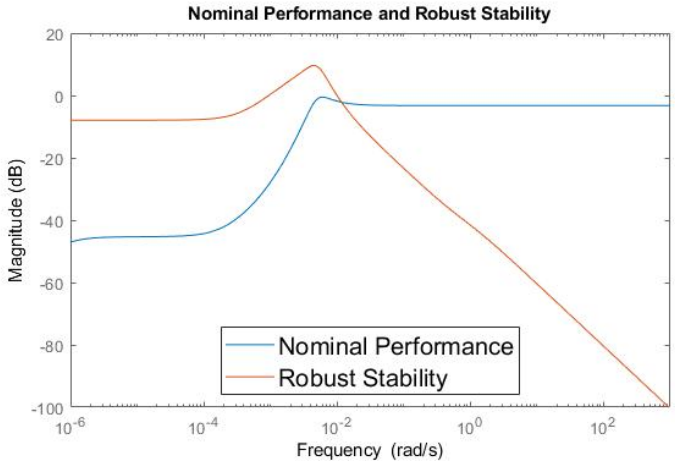

Figure 8.19: Nominal performance and robust stability with the new PID

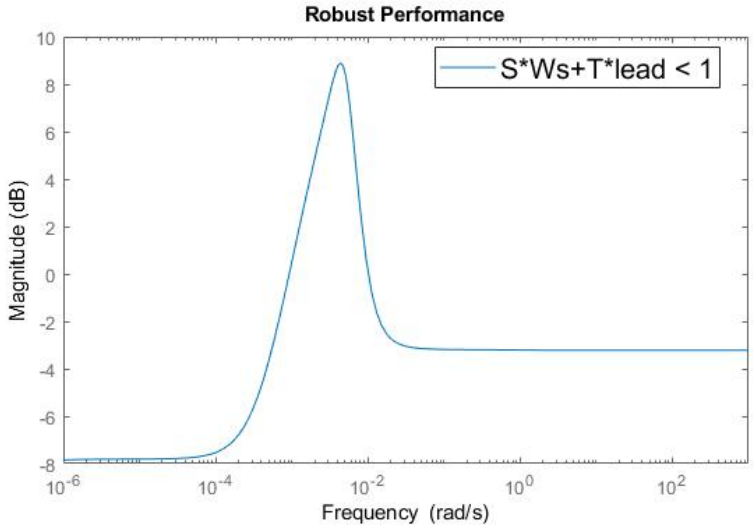

Figure 8.20: Robust performance with the new PID

Conclusion

This part of the report has shown how to decouple a MIMO system, and shown how to design a H_∞ controller, and implement such in a real system. This part has given an example that even though it looks doable through simulations, the end result in the real system might not be exactly the same as in the simulations. This part shows that the solution to the ice appearance on the evaporator might not be to build a robust controller, but might instead be in some other directions. Since the designed H_∞ controller can not be stable in an easy cooling environment and the new controller is not robust towards the worst case. It is therefore decided not to further do tests with this idea on the system, since it might damage some of the components in the system, especially the compressor if any liquid enters the inlet of the compressor. This part has shown some different aspects of the real system compared the simulations, and the whole project is now ready to be concluded.

Part IV

Conclusion

Conclusion 9

In this project, the transport refrigeration system in a reefer container at Lodam Electronics has been studied. The main issue that is focused in this project was presented by the company, which is controlling the system in critical point such as when ice appears on the evaporator coil. This issue has been investigated further with H-X diagram, and a solution to this issue is presented.

With the help of the general moving boundary method, a model for the evaporator and condenser are created, thus the total model was able to be produced. After an estimation of the unknown parameters of the total model, the end result shows that it does not fit the data. This might mean that either some error is present in the model method, or that some values of the parameters are wrong in the Matlab script. Duo to time constraint on this project the error is not found, it was necessary to move on by using the model which was provided by Kresten Sørensen from the company. This model has not been explained in details, but it is designed through similar method and afterwards the order of the MIMO model has been reduced. The reduced MIMO model of the system is then decoupled into two SISO system, where the reference that are focused are the cooling capacity and the superheat.

It was then chosen to only focus on the superheat, since it is important to not get any liquid in the compressor, and at the meantime it is necessary to be efficient at cooling. The controller designed is therefore made to keep a stable superheat.

The chosen controller to solve the ice-appearance issue is a robust H_∞ controller. The reason that this controller is chosen is so that the system can be stable even though some dynamic variations is present in the model. In the worst case of ice appearing on the evaporator coil, it will reduce the heat transfer coefficient by half of the real value.

The H_∞ controller has been designed and proven that it theoretically works, but it is also proven that it does not work practically when it is implemented in the system.

All in all this project has shown that the solution, to the ice appearance on the evaporator coil issue, might not be a robust control, which therefore gives opportunity to investigate other solutions to this problem.

Part V

Appendix

Modelling of the Evaporator and Condenser-Moving Boundary

A

This whole Appendix was written by me, in the last semester project. Since it has been taken directly from my previous report, it will be in appendix instead of in the report. The whole report from my last semester project can be found at [1].

A.1 General Moving Boundary - Dry expansion evaporator

From the **??**, the **Figure 2.4** will be modified so that it only has two phases, the mixed phase and the superheat phase. This will simplify the model and be more accurate comparing it to the real system, since it never appears to start at a sub-cooled phase in the evaporator. The modified model can be seen in **Figure A.1**.

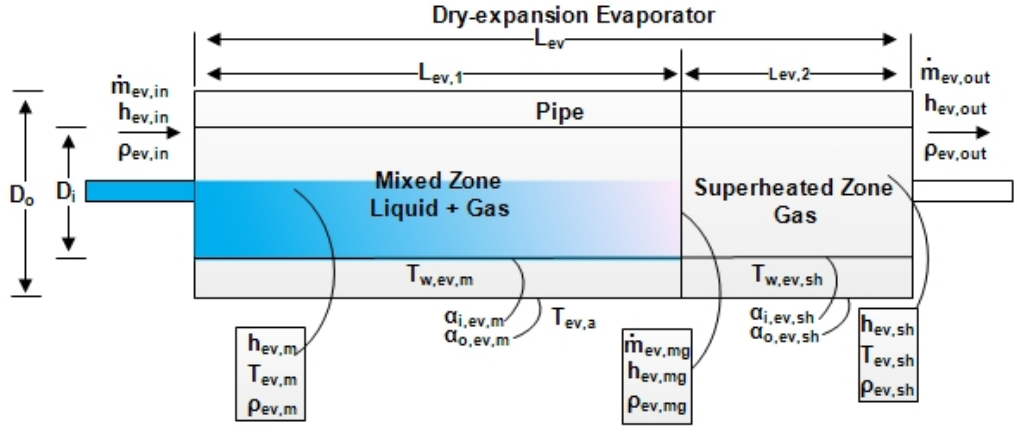

Figure A.1: The dry-expansion evaporator model

The **Figure A.1** is a dry-expansion evaporator model, which means that the inlet of the evaporator is a mixture of liquid and gas with a quality between 0,1 - 0,15 [5]. The quality describes the amount of gas in the refrigerant in percentage, meaning that 0,1, is 10 percent

of the refrigerant is gas. This is the usually interval and from the paper [**?**], it is written that the best estimation of the evaporators inlet quality is 0,1. From the **Figure A.1** there are some constraint such as a geometric constraint as seen in Equation A.1, where L is the total length in [m] of the evaporator and $L_{ev,1}$, $L_{ev,2}$ is the length in [m] of the mixed zone and the superheated zone respectively.

$$L_{ev} = L_{ev,1} + L_{ev,2} \tag{A.1}$$

The following equations are the results of calculations for the mass balance and the energy balance in the different regions. The full calculations can be found in [5] and the way to achieve the dry-expansion evaporator model, the length of the sub-cooled zone is set to zero.

A.1.1 Mass balance and energy balance at mixed zone control volume

The mass balance for the mixed zone control volume can be seen on Equation A.2. In this equation, the average void fraction can be calculated by only knowing the static quality of the refrigerant at the inlet, the outlet of the evaporator and the density ratio [5].

$$\begin{aligned} &A \cdot L_{ev,1} \cdot \left(\bar{\gamma} \cdot \frac{d\rho_{ev,mg}}{dP_{ev}} + (1-\bar{\gamma}) \cdot \frac{d\rho_{ev,l}}{dP_{ev}} \right) \frac{dP_{ev}}{dt} \\ &+ A \cdot (\rho_{ev,l} - \rho_{ev,mg}) \cdot \frac{dL_{ev,1}}{dt} \\ &= \dot{m}_{ev,in} - \dot{m}_{ev,mg} \end{aligned} \tag{A.2}$$

Where:

A	is the cross sectional area of the inner tube of the pipe	$[\mathrm{m}^2]$
$\bar{\gamma}$	is the average void fraction	$[\cdot]$
$\rho_{ev,mg}$	is the density of the refrigerant at the saturated curve	$\left[\frac{\mathrm{kg}}{\mathrm{m}^3}\right]$
$\rho_{ev,l}$	is the density of the refrigerant at the sub cooled saturation curve	$\left[\frac{\mathrm{kg}}{\mathrm{m}^3}\right]$
P_{ev}	is the pressure of the refrigerant	[Bar]
t	is the time	[s]
$\dot{m}_{ev,in}$	is the mass flow of the refrigerant at the inlet of the evaporator	$\left[\frac{\mathrm{kg}}{\mathrm{s}}\right]$
$\dot{m}_{ev,mg}$	is the mass flow of the refrigerant at the saturated curve	$\left[\frac{\mathrm{kg}}{\mathrm{s}}\right]$

The equation for the void fraction can be seen in Equation A.3 [5].

$$\bar{\gamma} = \frac{(X_{out} - X_{in})(1-\mu^{\frac{2}{3}}) - \mu(X_{in}(\mu^{-\frac{1}{3}}-1)+1)(X_{out}(\mu^{-\frac{1}{3}}-1)+1)\beta}{(X_{out} - X_{in})(1-\mu^{\frac{2}{3}})^2} \tag{A.3}$$

Where X_{out}, X_{in} are the refrigerant quality which can be found by thermodynamic functions and β is the volume flow fraction of the gas phase which is defined as in Equation A.4 and μ is the density ratio as in Equation A.5 [5].

$$\beta = ln\left(\frac{(X_{in}(\mu^{-\frac{1}{3}}-1)+1)(X_{out}(1-\mu)+\mu)}{(X_{out}(\mu^{-\frac{1}{3}}-1)+1)(X_{in}(1-\mu)+\mu)}\right) \tag{A.4}$$

$$\mu = \frac{\rho_{ev,mg}}{\rho_{ev,in}} \tag{A.5}$$

Where:

$\rho_{ev,in}$	is the density at the inlet of the evaporator	$\left[\frac{\text{kg}}{\text{m}^3}\right]$

The energy balance for the mixed zone can be seen in Equation A.6.

$$\begin{aligned} &A \cdot L_{ev,1} \cdot \left(\bar{\gamma} \cdot \frac{d\rho_{ev,mg}h_{ev,mg}}{dP_{ev}} + (1-\bar{\gamma}) \cdot \frac{d\rho_{ev,l}h_{ev,l}}{dP_{ev}}\right)\frac{dP_{ev}}{dt} \\ &+ A \cdot (\rho_{ev,l}h_{ev,l} - \rho_{ev,mg}h_{ev,mg}) \cdot \frac{dL_{ev,1}}{dt} \\ &= \dot{m}_{ev,in}h_{ev,in} - \dot{m}_{ev,mg}h_{ev,mg} + \pi D_i \alpha_{i,ev,m} L_{ev,1}(T_{w,ev,m} - \bar{T}_{ev,m}) \end{aligned} \tag{A.6}$$

Where:

$\bar{T}_{ev,m}$	is the temperature of the refrigerant in the mixed zone	[K]
$\bar{T}_{w,ev,m}$	is the temperature of the metal pipe	[K]
$\alpha_{i,ev,m}$	is the transfer heat coefficient from pipe to refrigerant at the mixed zone	[·]
D_i	is the inner diameter of the metal pipe	[m]
$h_{ev,mg}$	is the enthalpy at the saturation curve	$\left[\frac{\text{J}}{\text{kg}}\right]$
$h_{ev,l}$	is the enthalpy at the sub cooled saturation curve	$\left[\frac{\text{J}}{\text{kg}}\right]$

It needs to be noted that the equations are much simpler as they seems like, since some terms can be found by using the thermodynamic functions in matlab and these terms are as seen:

$$\left\{\rho_{ev,mg}, \rho_{ev,l}, h_{ev,mg}, h_{ev,in}, \bar{T}_{ev,m}\right\}$$

A.1.2 Mass balance and energy balance at superheated zone control volume

The mass balance for the superheated zone control volume can be seen on Equation A.7.

$$
\begin{aligned}
&A \cdot (\rho_{ev,mg} - \rho_{ev,sh}) \frac{dL_{ev,1}}{dt} \\
&+ A \cdot L_{ev,2} \left(\frac{1}{2} \left. \frac{d\rho_{ev,sh}}{dh_{ev,sh}} \right|_{P_{ev}} \frac{h_{ev,mg}}{dP_{ev}} + \left. \frac{d\rho_{ev,sh}}{dP_{ev}} \right|_{h_{ev,sh}} \right) \frac{dP_{ev}}{dt} \\
&+ A \cdot L_{ev,2} \cdot \frac{1}{2} \left. \frac{d\rho_{ev,sh}}{dh_{ev,sh}} \right|_{P_{ev}} \frac{dh_{ev,out}}{dt} \\
&= \dot{m}_{ev,mg} - \dot{m}_{ev,out}
\end{aligned}
\tag{A.7}
$$

Where:

$\rho_{ev,sh}$	is the mean density of the refrigerant at the superheat zone	$\left[\frac{\text{kg}}{\text{m}^3}\right]$
$h_{ev,sh}$	is the mean enthalpy at the superheat zone	$\left[\frac{\text{J}}{\text{kg}}\right]$
$h_{ev,out}$	is the enthalpy of the refrigerant at the outlet of the evaporator	$\left[\frac{\text{J}}{\text{kg}}\right]$
$\dot{m}_{ev,out}$	is the mass flow at the outlet of the evaporator	$\left[\frac{\text{kg}}{\text{s}}\right]$

The energy balance for the mixed zone can be seen in Equation A.8.

$$
\begin{aligned}
&A \left(\rho_{ev,mg} h_{ev,mg} - \frac{1}{2} \rho_{ev,sh} (h_{ev,mg} + h_{ev,out}) \right) \frac{dL_{ev,1}}{dt} \\
&+ A \left(\frac{1}{4} L_{ev,2} (h_{ev,mg} + h_{ev,out}) \left. \frac{d\rho_{ev,sh}}{dh_{ev,sh}} \right|_{P_{ev}} + \frac{1}{2} \rho_{ev,sh} \cdot L_{ev,2} \right) \frac{dh_{ev,out}}{dt} \\
&+ A \cdot L_{ev,2} \left(\frac{1}{2} (h_{ev,out} + h_{ev,mg}) \left(\frac{1}{2} \left. \frac{d\rho_{ev,sh}}{dh_{ev,sh}} \right|_{P_{ev}} \frac{h_{ev,mg}}{dP_{ev}} + \left. \frac{\rho_{ev,sh}}{dP_{ev}} \right|_{h_{ev,sh}} \right) + \frac{1}{2} \rho_{ev,sh} \frac{dh_{ev,mg}}{dP_{ev}} - 1 \right) \frac{dP_{ev}}{dt} \\
&= \dot{m}_{ev,mg} h_{ev,mg} - \dot{m}_{ev,out} h_{ev,out} + \pi D_i \alpha_{i,ev,sh} L_1 (T_{w,ev,sh} - \bar{T}_{ev,sh})
\end{aligned}
\tag{A.8}
$$

Where:

$\alpha_{i,ev,sh}$	is the transfer heat coefficient from pipe to refrigerant at the superheat zone	$[\cdot]$
$\bar{T}_{ev,sh}$	is the temperature of the refrigerant at the superheat zone	[K]
$T_{w,ev,sh}$	is the temperature of the metal pipe at the superheat zone	[K]

The terms that can be found by using the thermodynamic functions in matlab, excluding the ones before are as listed:

$$\left\{ \rho_{ev,sh}, h_{ev,out}, \bar{T}_{ev,sh} \right\}$$

A.1.3 Wall energy balance for the mixed and superheated zone control volumes

The wall energy balance for mixed zone control volume can be seen in Equation A.9

$$c_{p,w}\rho_w A_w L_{ev,1}\frac{dT_{w,ev,m}}{dt} = \alpha_{o,ev,m}\pi D_o L_{ev,1}(T_{ev,a}-T_{w,ev,m})-\alpha_{i,ev,m}\pi D_i L_{ev,1}(T_{w,ev,m}-\bar{T}_{ev,m}) \tag{A.9}$$

The wall energy balance for superheated zone control volume can be seen in Equation A.10

$$c_{p,w}\rho_w A_w L_{ev,2}\frac{dT_{w,ev,sh}}{dt} = \alpha_{o,ev,sh}\pi D_o L_{ev,2}(T_{ev,a}-T_{w,ev,sh})-\alpha_{i,ev,sh}\pi D_i L_{ev,2}(T_{w,ev,sh}-\bar{T}_{ev,sh}) \tag{A.10}$$

Where:

$\alpha_{o,ev,m}$	is the transfer heat coefficient from ambient air to refrigerant at mixed zone	$[\cdot]$
$\alpha_{o,ev,sh}$	is the transfer heat coefficient from ambient air to refrigerant at superheated zone	$[\cdot]$
$T_{ev,a}$	is the ambient temperature at the evaporator	[K]

Parameters that are known constants or can be calculated from the equations are:

$$\{A, A_w, L_{ev}, D_i, D_o, \alpha_{i,ev,m}, \alpha_{o,ev,m}, \alpha_{i,ev,sh}, \alpha_{o,ev,sh}, \bar{\gamma}, \rho_w, c_{p,w}\}$$

A.1.4 Section Conclusion

This model gives in total of seven equation with five state variables excluding the equations for average void fraction, beta and μ, meaning the model has an order of five. The state variables are: $x_{ev} = \{L_{ev,1}, h_{ev,out}, P_{ev}, T_{w,ev,m}, T_{w,ev,sh}\}$, with the depended variables: $\{ \dot{m}_{ev,mg}, L_{ev,2} \}$ and the control inputs: $\{ u_{ev} = \dot{m}_{ev,in}, \dot{m}_{ev,out}, h_{ev,in}, T_{ev,a} \}$. Since there are two depended variables, these can be expressed by the other terms, produces a system model with five equation to the ordinary differential equation [5]. For designing a controller to the system, it is important to achieve a model with a low order, and this dry-expansion evaporator model gives an order of five which is low. To be able to use the model, a linearization is necessary.

Model linearization of evaporator

To linearize the model with five differential equations after $\dot{m}_{ev,mg}$ and $L_{ev,2}$ are expressed, it will be set in a compact state space form. This compact state space form can be seen on Equation A.11.

$$D_{ev}\dot{x}_{ev} = f(x_{ev}, u_{ev}) \rightarrow \dot{x}_{ev} = D_{ev}^{-1} f(x_{ev}, u_{ev}) \tag{A.11}$$

where,

$$f(x,u) = \begin{bmatrix} \dot{m}_{ev,in}h_{ev,in} - \dot{m}_{ev,in}h_{ev,mg} + \pi D_i L_{ev,1}\alpha_{i,ev,m}(T_{w,ev,m} - \bar{T}_{ev,m}) \\ \dot{m}_{ev,out}h_{ev,mg} - \dot{m}_{ev,out}h_{ev,out} + \pi D_i (L_{ev} - L_{ev,1})\alpha_{i,ev,sh}(T_{w,ev,sh} - \bar{T}_{ev,sh}) \\ \dot{m}_{ev,in} - \dot{m}_{ev,out} \\ \pi D_o L_{ev,1}\alpha_{o,ev,m}(T_{ev,a} - T_{w,ev,m}) - \pi D_i L_{ev,1}\alpha_{i,ev,m}(T_{w,ev,m} - \bar{T}_{ev,m}) \\ \pi D_o (L_{ev} - L_{ev,1})\alpha_{o,ev,sh}(T_{ev,a} - T_{w,ev,sh}) - \pi D_i (L_{ev} - L_{ev,1})\alpha_{i,ev,sh}(T_{w,ev,sh} - \bar{T}_{ev,sh}) \end{bmatrix} \tag{A.12}$$

,

$$D_{ev} = \begin{bmatrix} d_{ev,11} & d_{ev,12} & 0 & 0 & 0 \\ d_{ev,21} & d_{ev,22} & d_{ev,23} & 0 & 0 \\ d_{ev,31} & d_{ev,32} & d_{ev,33} & 0 & 0 \\ 0 & 0 & 0 & d_{ev,44} & 0 \\ 0 & 0 & 0 & 0 & d_{ev,55} \end{bmatrix}, x_{ev} = \begin{bmatrix} L_{ev,1} \\ P_{ev} \\ h_{ev,out} \\ T_{w,ev,m} \\ T_{w,ev,sh} \end{bmatrix}, u_{ev} = \begin{bmatrix} \dot{m}_{ev,in} \\ h_{ev,in} \\ \dot{m}_{ev,out} \\ T_{ev,a} \end{bmatrix} \tag{A.13}$$

The elements in the dynamic matrix, D_{ev}, can be found in **Appendix B**. By removing the non-linearity of the model the linear form can be achieved. A steady state solution of the system will be used. Since the evaporator is designed to operate at a fixed operating point, the dynamic deviations of that point is small. This can be written as in Equation A.14.

$$x_{ev}(t) = x_{ev}^{ss} + \delta x_{ev}(t), u_{ev}(t) = u_{ev}^{ss} + \delta u_{ev}(t) \tag{A.14}$$

where: $x_{ev}^{ss} = \begin{bmatrix} L_{ev,1}^{ss} & P_{ev}^{ss} & h_{ev,out}^{ss} & T_{w,ev,m}^{ss} & T_{w,ev,sh}^{ss} \end{bmatrix}^T$ and $u_{ev}^{ss} = \begin{bmatrix} \dot{m}_{ev,in}^{ss} & h_{ev,in}^{ss} & \dot{m}_{ev,out}^{ss} & T_{ev,a}^{ss} \end{bmatrix}^T$ are the steady state solution and both $\delta x_{ev}(t)$ and $\delta u_{ev}(t)$ are small dynamic deviations from the fixed operating point. The Taylor series expansion will be used to describe the linear model of the dynamic deviations as seen in

$$\delta \dot{x}_{ev} = A_{ev}\delta x_{ev} + B_{ev}\delta u_{ev} \tag{A.15}$$

where $A_{ev} = D_{ev}^{-1}\frac{\delta f(x_{ev},u_{ev})}{\delta x_{ev}} = D_{ev}^{-1}A'_{ev}$ and $B_{ev} = D_{ev}^{-1}\frac{\delta f(x,u)}{\delta u} = D_{ev}^{-1}B'_{ev}$. The Taylor series expansions A_{ev}' and B_{ev}' can be seen in Equation A.16, and the element expressions can be found in **Appendix B**.

$$A'_{ev} = \begin{bmatrix} a_{ev,11} & a_{ev,12} & 0 & a_{ev,14} & 0 \\ a_{ev,21} & a_{ev,22} & a_{ev,23} & 0 & a_{ev,25} \\ 0 & 0 & 0 & 0 & 0 \\ a_{ev,41} & a_{ev,42} & 0 & a_{ev,44} & 0 \\ a_{ev,51} & a_{ev,52} & a_{ev,53} & 0 & a_{ev,55} \end{bmatrix}, B'_{ev} = \begin{bmatrix} b_{ev,11} & b_{ev,12} & 0 & 0 \\ 0 & 0 & b_{ev,23} & 0 \\ b_{ev,31} & 0 & b_{ev,33} & 0 \\ 0 & 0 & 0 & b_{v44} \\ 0 & 0 & 0 & b_{ev,54} \end{bmatrix} \tag{A.16}$$

Now that the evaporator is modelled with separate nodes of the dynamics, it will be capable to reflect the essential distributed characteristics such as superheat response. This is necessary for the whole model, since the whole point is to have a better performance, and one way to achieve that is to minimize the superheat.

General Moving Boundary - Three Nodes Condenser

From evaporator model, the **Figure A.1** will be modified, so that there are three phases of the refrigerant. While the figure represents an evaporator, the same figure can, as explained, be used for the condenser model, but the flow turned the opposite direction. This gives the figure Figure A.2

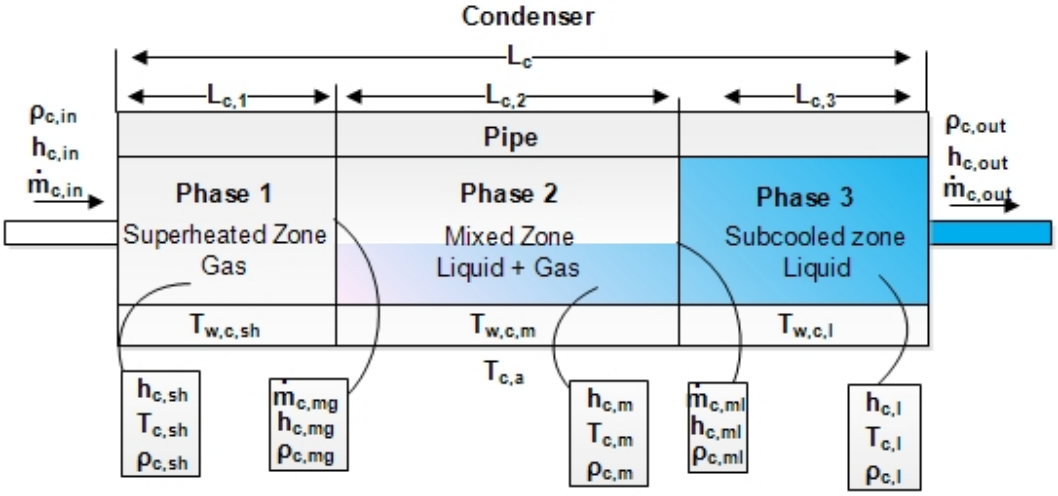

Figure A.2: The dynamic model of the condenser

Just like the evaporator there is also a geometric constraint to this model as well. Here the L_c is the total length in [m] of the condenser and $L_{c,1}$, $L_{c,2}$ and $L_{c,3}$ are the lengths in [m] of the superheated, mixed and the sub-cooled zone respectively:

$$L_c = L_{c,1} + L_{c,2} + L_{c,3} \tag{A.17}$$

The following equations are the results of calculations for the mass balance and the energy balance in the different zones. The full calculations can be found in [6].

A.1.5 Mass Balance And Energy Balance At Superheated Control Volume

The mass balance for the superheated section can be seen on Equation A.18.

$$AL_{c,1}\left(\frac{d\rho_{c,sh}}{dP_c} + \frac{d\rho_{c,sh}}{dh_{c,sh}}\frac{dh_{c,mg}}{dP_c}\right)\frac{dP_c}{dt} + A(\rho_{c,sh} - \rho_{c,mg})\frac{dL_{c,1}}{dt} = \dot{m}_{c,in} - \dot{m}_{c,mg} \tag{A.18}$$

The mean enthalpy of the superheat control volume can be calculated as: $h_{c,sh} = \frac{h_{c,i}+h_{c,mg}}{2}$ and the mean density of the refrigerant at the control volume can be found by use of thermodynamic function: $\rho_{c,sh} = \rho(P_c, h_{c,sh})$.

Where:

A	is the cross-sectional are of the tube	$[\mathrm{m}^2]$
P_c	is the condenser pressure	[bar]
$\rho_{c,sh}$	is the mean density at the superheated zone	$\left[\frac{\mathrm{kg}}{\mathrm{m}^3}\right]$
$\rho_{c,mg}$	is the density at the superheated saturation curve	$\left[\frac{\mathrm{kg}}{\mathrm{m}^3}\right]$
$h_{c,sh}$	is the mean enthalpy at the superheated zone	$\left[\frac{\mathrm{J}}{\mathrm{kg}}\right]$
$h_{c,mg}$	is the enthalpy at the superheated saturation curve	$\left[\frac{\mathrm{J}}{\mathrm{kg}}\right]$
$\dot{m}_{c,in}$	is the mass flow going into the condenser	$\left[\frac{\mathrm{kg}}{\mathrm{s}}\right]$
$\dot{m}_{c,mg}$	is the mass flow at the superheated saturation curve	$\left[\frac{\mathrm{kg}}{\mathrm{s}}\right]$

The energy balance for the superheated section can be seen on Equation A.19.

$$\begin{aligned} & AL_{c,1}(\rho_{c,sh}\frac{dh_{c,mg}}{dP_c} - 1)\frac{dP_c}{dt} \\ & - \frac{1}{2}\rho_{c,mg}A(h_{c,mg} - h_{c,in})\frac{dL_{c,1}}{dt} \\ & = \alpha_{i,c,sh}\pi D_i L_{c,1}(T_{w,c,sh} - T_{c,sh}) - \frac{1}{2}(\dot{m}_{c,in} + \dot{m}_{c,mg})(h_{c,mg} - h_{c,in}) \end{aligned} \tag{A.19}$$

The mean temperature of the refrigerant at the superheated control volume can be found from thermodynamic function like the mean density before : $T_{c,sh} = T(P_c, h_{c,sh})$.

Where:

$\alpha_{i,c,sh}$	is the heat transfer coefficient from refrigerant to pipe at the superheated zone	$[\cdot]$
D_i	is the inner diameter of the metal pipe	[m]
$T_{w,c,sh}$	is the temperature of the metal pipe	[K]
$T_{c,sh}$	is the temperature of the refrigerant in the superheat zone	[K]

A summarized list of all the terms that can be found from thermodynamics functions in this control volume as listed:

$$\{\rho_{c,sh}, \rho_{c,mg}, P_c, h_{c,in}, h_{c,sh}, h_{c,mg}, T_{c,sh}\} \tag{A.20}$$

A.1.6 Mass Balance And Energy Balance At Mixed Control Volume

The mass balance for the mixed section can be seen on Equation A.21.

$$
\begin{aligned}
& ALc_2 \frac{d\rho_{c,m}}{dP_c} \frac{dP_c}{dt} \\
& + A(\rho_{c,mg} - \rho_{c,ml}) \frac{dL_{c,1}}{dt} \\
& + A(\rho_{c,m} - \rho_{c,ml}) \frac{dL_{c,2}}{dt} \\
& = \dot{m}_{c,mg} - \dot{m}_{c,ml}
\end{aligned}
\tag{A.21}
$$

Where:

$\rho_{c,m}$	is the mean density of the refrigerant at the mixed zone	$\left[\frac{\text{kg}}{\text{m}^3}\right]$
$\rho_{c,ml}$	is the density of the refrigerant at the sub-cooled saturation curve	$\left[\frac{\text{kg}}{\text{m}^3}\right]$
$\dot{m}_{c,ml}$	is the mass flow of the refrigerant at the sub-cooled saturation curve	$\left[\frac{\text{kg}}{\text{s}}\right]$

The mean density of the refrigerant of in the mixed section can be estimated as : $\rho_{c,m} = \rho_{c,l}(1-\gamma) + \rho_{c,mg}\gamma$, where γ is the average void fraction, calculated the same way as in evaporator.

The energy balance for the mixed section can be seen on Equation A.22.

$$
\begin{aligned}
& AL_{c,2}\left(\frac{d(\rho_{c,ml}h_{c,ml})}{dP_c}(1-\bar{\gamma}) + \frac{d(\rho_{c,mg}h_{c,mg})}{dP_c}\bar{\gamma} - 1\right) \\
& + A(\rho_{c,mg}h_{c,mg} - \rho_{c,ml}h_{c,ml}) \frac{dL_{c,1}}{dt} \\
& + A\bar{\gamma}(\rho_{c,mg}h_{c,mg} - \rho_{c,ml}h_{c,ml}) \frac{dL_{c,2}}{dt} \\
& = \dot{m}_{c,mg}h_{c,mg} - \dot{m}_{c,ml}h_{c,ml} + \alpha_{i,c,m}\pi D_i L_{c,2}(T_{w,c,m} - T_{c,m})
\end{aligned}
\tag{A.22}
$$

Where:

$h_{c,ml}$	is the enthalpy of the refrigerant at the sub-cooled saturation curve	$\left[\frac{\text{J}}{\text{kg}}\right]$
$\alpha_{i,c,m}$	is the transfer heat coefficient from refrigerant to pipe at the mixed zone	$[\cdot]$
$T_{w,c,m}$	is the temperature of the pipe at the mixed zone	[K]
$T_{c,m}$	is the mean temperature of the refrigerant at the mixed zone	[K]

A summarized list of all the terms, that can be found from thermodynamics functions in this control volume, excluding the same terms from previous control volume, is as listed:

$$
\{\rho_{c,m}, \rho_{c,ml}, T_{c,m}\} \tag{A.23}
$$

A.1.7 Mass Balance And Energy Balance At Sub-Cooled Control Volume

In the control volume the refrigerant is fully liquefied which means the the mass will not change through this phase. The mass balance for the sub-cooled section can be seen on Equation A.24.

$$\dot{m}_{c,ml} = \dot{m}_{c,out} \tag{A.24}$$

Where:

$\dot{m}_{c,out}$	is the mass flow of the refrigerant at the outlet of the condenser	$\left[\frac{\text{kg}}{\text{s}}\right]$

The energy balance for the sub-cooled section can be seen on Equation A.25.

$$\begin{aligned} &AL_{c,3}\left(\left(\frac{\rho_{c,ml}}{2}\frac{dh_{c,ml}}{dP_c}-1\right)\frac{dP_c}{dt}+\frac{\rho_{c,ml}}{2}\frac{dh_{c,out}}{dt}\right) \\ &+A\rho_{c,ml}\frac{h_{c,ml}-h_{c,out}}{2}\left(\frac{dL_{c,1}}{dt}+\frac{dL_{c,2}}{t}\right) \\ &=\dot{m}_{c,out}(h_{c,ml}-h_{c,out})+\alpha_{i,c,l}\pi D_i L_{c,3}(T_{w,c,l}-T_{c,l}) \end{aligned} \tag{A.25}$$

Where:

$h_{c,out}$	is the enthalpy of the refrigerant at the outlet of the condenser	$\left[\frac{\text{J}}{\text{kg}}\right]$
$\alpha_{i,c,l}$	is the transfer heat coefficient from refrigerant to pipe at the sub-cooled zone	$[\cdot]$
$T_{w,c,l}$	is the temperature of the wall at the sub-cooled zone	[K]
$T_{c,l}$	is the mean temperature of the refrigerant at the sub-cooled zone	[K]

A.1.8 Wall energy balance for all the control volumes

The wall energy balance for the superheat control volume can be seen in Equation A.26

$$(c_{p,w}\rho_w A_w)(\frac{dT_{w,c,sh}}{dt}+\frac{T_{w,c,sh}-T_{w,c,m}}{L_{c,1}}\frac{dL_{c,1}}{dt}) = \alpha_{i,c,sh}\pi D_i(T_{c,sh}-T_{w,c,sh})+\alpha_{o,c,sh}\pi D_o(T_{c,a}-T_{w,c,sh}) \tag{A.26}$$

The wall energy balance for the superheat control volume can be seen in Equation A.27

$$(c_{p,w}\rho_w A_w)\frac{dT_{w,c,m}}{dt} = \alpha_{i,c,m}\pi D_i(T_{c,m}-T_{w,c,m})+\alpha_{o,c,m}\pi D_o(T_{c,a}-T_{w,c,m}) \tag{A.27}$$

The wall energy balance for the superheat control volume can be seen in Equation A.28

$$(c_{p,w}\rho_w A_w)(\frac{dT_{w,c,l}}{dt}+\frac{T_{w,c,m}-T_{w,c,l}}{L_{c,3}}(\frac{dL_{c,1}}{dt}+\frac{dL_{c,2}}{dt})) = \alpha_{i,c,l}\pi D_i(T_{c,l}-T_{w,c,l})+\alpha_{o,c,l}\pi D_o(T_{c,a}-T_{w,c,l}) \tag{A.28}$$

Where:

$\alpha_{o,c,sh}$	is the transfer heat coefficient from pipe to ambient air at the superheated zone	$[\cdot]$
$\alpha_{o,c,m}$	is the transfer heat coefficient from pipe to ambient air at the mixed zone	$[\cdot]$
$\alpha_{o,c,l}$	is the transfer heat coefficient from pipe to ambient air at the sub-cooled zone	$[\cdot]$
$T_{c,a}$	is the ambient temperature at the condenser	[K]

Parameters that are known constants or can be calculated from the equations are :

$$\{A, A_w, \rho_w, c_{p,w}, L_c, D_i, D_o, \alpha_{i,c,sh}, \alpha_{o,c,sh}, \alpha_{i,c,m}, \alpha_{o,c,m}, \alpha_{i,c,l}, \alpha_{o,c,l}\} \tag{A.29}$$

A.1.9 Section conclusion

This model gives in total of ten equation with seven state variables, which means this model has an order of seven. The state variables are: $x_c = \{L_{c,1}, L_{c,2}, P_c, h_{c,out}, T_{w,c,sh}, T_{w,c,m}, T_{w,c,l}\}$, with the depended variables: $\{\ \dot{m}_{c,mg}, \dot{m}_{c,ml}, L_{c,3}\ \}$ and the control inputs: $u_c = \{\dot{m}_{c,in}, \dot{m}_{c,out}, h_{c,in}, T_{c,a}\ \}$. Since there are three depended variables, that can be expressed by the other terms, a system model with seven equation to the ordinary differential equation can be achieved [6]. For designing a controller to the system, this model will be a part of the whole model.

Model linearization of condenser

The linearization structure and method of the model is made the same way as the evaporator:

$$D_c\dot{x}_c = f(x_c, u_c) \rightarrow \dot{x}_c = D_c^{-1} f(x_c, u_c) \tag{A.30}$$

where,

$$f(x,u) = \begin{bmatrix} \dot{m}_{c,in}h_{c,in} - \dot{m}_{c,in}h_{c,mg} + \pi D_i L_{c,1}\alpha_{i,c,sh}(T_{w,c,sh} - T_{c,sh}) \\ \dot{m}_{c,out}h_{c,mg} - \dot{m}_{c,out}h_{c,l} + \pi D_i L_{c,2}\alpha_{i,c,m}(T_{w,c,m} - T_{c,m}) \\ \dot{m}_{c,out}h_{c,l} - \dot{m}_{c,out}h_{c,out} + \pi D_i L_{c,3}\alpha_{i,c,m}(T_{w,c,l} - T_{c,l}) \\ \dot{m}_{c,in} - \dot{m}_{c,out} \\ \alpha_{o,c,sh}\pi D_o(T_{c,a} - T_{w,c,sh}) - \alpha_{i,c,sh}\pi D_i(T_{w,c,sh} - T_{c,m}) \\ \alpha_{o,c,m}\pi D_o(T_{c,a} - T_{w,c,m}) - \alpha_{i,c,m}\pi D_i(T_{w,c,m} - T_{c,m}) \\ \alpha_{o,c,l}\pi D_o(T_{c,a} - T_{w,c,l}) - \alpha_{i,c,l}\pi D_i(T_{w,c,l} - T_{c,l}) \end{bmatrix} \tag{A.31}$$

,

$$D_c = \begin{bmatrix} d_{c,11} & 0 & d_{c,c,13} & 0 & 0 & 0 & 0 \\ d_{c,21} & d_{c,22} & d_{c,23} & 0 & 0 & 0 & 0 \\ d_{c,31} & d_{c,32} & d_{c,33} & d_{c,34} & 0 & 0 & 0 \\ d_{c,41} & d_{c,42} & d_{c,43} & 0 & 0 & 0 & 0 \\ d_{c,51} & 0 & 0 & 0 & d_{55} & 0 & 0 \\ 0 & 0 & 0 & 0 & 0 & d_{c,66} & 0 \\ d_{c,71} & d_{c,72} & 0 & 0 & 0 & 0 & d_{c,77} \end{bmatrix}, x_c = \begin{bmatrix} L_{c,1} \\ L_{c,2} \\ P_c \\ h_{c,out} \\ T_{w,c,sh} \\ T_{w,c,m} \\ T_{w,c,l} \end{bmatrix}, u_c = \begin{bmatrix} \dot{m}_{c,in} \\ h_{c,in} \\ \dot{m}_{c,out} \\ T_{c,a} \end{bmatrix} \tag{A.32}$$

To achieve the seven differential equations as seen in Equation A.31, the expressions of $\dot{m}_{c,mg}$ and $\dot{m}_{c,ml}$ needs to be expressed by rearranging the model equations earlier.

The Taylor series expansion will be used to remove the non-linearity of the system, and achieve the linear model with the dynamic deviations as seen in Equation A.33.

$$\delta \dot{x}_c = A_c \delta x_c + B_c \delta u_c \tag{A.33}$$

Where $A_c = D_c^{-1} \frac{\delta f(x_c, u_c)}{\delta x_c} = D_c^{-1} A_c'$ and $B_c = D_c^{-1} \frac{\delta f(x_c, u_c)}{\delta u_c} = D_c^{-1} B_c'$. The Taylor series expansions A_c' and B_c' can be seen in Equation A.34, where the element expressions can be found in **Appendix C** [6].

$$A_c' = \begin{bmatrix} a_{c11} & 0 & a_{c13} & 0 & a_{c15} & 0 & 0 \\ 0 & a_{c22} & a_{c23} & 0 & 0 & a_{c26} & 0 \\ a_{c31} & a_{c32} & a_{c33} & a_{c34} & 0 & 0 & 0 \\ 0 & 0 & 0 & 0 & 0 & 0 & 0 \\ 0 & 0 & a_{c53} & 0 & a_{c55} & 0 & 0 \\ 0 & 0 & a_{c63} & 0 & 0 & a_{c66} & 0 \\ 0 & 0 & a_{c73} & a_{c74} & 0 & 0 & a_{c77} \end{bmatrix}, B_c' = \begin{bmatrix} b_{c11} & b_{c12} & 0 & 0 \\ 0 & 0 & b_{c23} & 0 \\ 0 & 0 & b_{c33} & 0 \\ b_{c41} & 0 & b_{c43} & 0 \\ 0 & 0 & 0 & b_{c54} \\ 0 & 0 & 0 & b_{c64} \\ 0 & 0 & 0 & b_{c74} \end{bmatrix} \tag{A.34}$$

This concludes the finished model of the condenser, and this model will be included later in the whole dynamic together.

Evaporator matrix elements

B

This Appendix was written by me, in the last semester project. Since it has been taken directly from my previous report, it will be in appendix instead of in the report. The whole report from my last semester project can be found at [1].

This appendix will be describing the expressions of the elements in the matrices of the dynamic model of the evaporator.

B.1 The dynamic matrix, D

$$D = \begin{bmatrix} d_{11} & d_{12} & 0 & 0 & 0 \\ d_{21} & d_{22} & d_{23} & 0 & 0 \\ d_{31} & d_{32} & d_{33} & 0 & 0 \\ 0 & 0 & 0 & d_{44} & 0 \\ 0 & 0 & 0 & 0 & d_{55} \end{bmatrix} \tag{B.1}$$

$d_{11} = A(\rho_l h_l - \rho_l h_{mg})$
$d_{12} = AL_1 \left((1-\bar{\gamma}) \frac{\delta \rho_l h_l}{\delta P} - (1-\bar{\gamma}) \frac{\delta \rho_l h_{mg}}{\delta P} \right)$
$d_{21} = -\frac{1}{2} A \bar{\rho}_{sh} h_{out}$
$d_{22} = A(L-L_1) \left(\frac{1}{2} h_{out} \left. \frac{\delta \bar{\rho}_{sh}}{\delta \bar{h}_{sh}} \right|_P \frac{\delta h_{mg}}{\delta P} + \left. \frac{\delta \bar{\rho}_{sh}}{\delta P} \right|_h + \frac{1}{2} \bar{\rho}_{sh} \frac{\delta h_{mg}}{\delta P} - 1 \right)$
$d_{23} = A(L-L_1) \left(\frac{1}{4} (h_{out} - h_{mg}) \left. \frac{\delta \bar{\rho}_{sh}}{\delta \bar{h}_{sh}} \right|_P + \frac{1}{2} \bar{\rho}_{sh} \right)$
$d_{31} = A(\rho_l - \bar{\rho}_{sh})$
$d_{32} = A((L-L_1)(\frac{1}{2} \left. \frac{\delta \bar{\rho}_{sh}}{\delta \bar{h}_{sh}} \right|_P \frac{\delta h_{mg}}{\delta P} + \left. \frac{\delta \bar{\rho}_{sh}}{\delta P} \right|_h) + L_1 \left(\bar{\gamma} \frac{\delta \rho_{mg}}{\delta P} + (1-\bar{\gamma}) \frac{\delta \rho_l}{\delta P} \right))$
$d_{33} = \frac{1}{2} A(L-L_1) \frac{\delta \bar{\rho}_{sh}}{\delta \bar{h}_{sh}}|_P$
$d_{44} = c_{p,w} \rho_w A_w$
$d_{55} = c_{p,w} \rho_w A_w$

B.2 The Taylor series expansion matrices, A' and B'

$$A' = \begin{bmatrix} a_{11} & a_{12} & 0 & a_{14} & 0 \\ a_{21} & a_{22} & a_{23} & 0 & a_{25} \\ 0 & 0 & 0 & 0 & 0 \\ a_{41} & a_{42} & 0 & a_{44} & 0 \\ a_{51} & a_{52} & a_{53} & 0 & a_{55} \end{bmatrix}, B' = \begin{bmatrix} b_{11} & b_{12} & 0 & 0 \\ 0 & 0 & b_{23} & 0 \\ b_{31} & 0 & b_{33} & 0 \\ 0 & 0 & 0 & b_{44} \\ 0 & 0 & 0 & b_{54} \end{bmatrix} \tag{B.2}$$

$a_{11} = \pi D_i \alpha_{i,m}(T_{w,m} - \bar{T}_m)$
$a_{12} = -\dot{m}_{in}\frac{\delta h_{mg}}{\delta P} - \pi D_i L_1 \alpha_{i,m}\frac{\delta \bar{T}_m}{\delta P}$
$a_{14} = \pi D_i L_1 \alpha_{i,m}$
$a_{21} = -\pi D_i \alpha_{i,sh}(T_{w,sh} - \bar{T}_{sh})$
$a_{22} = \dot{m}_{out}\frac{\delta h_{mg}}{\delta P} - \pi D_i \alpha_{i,sh}\frac{\delta \bar{T}_{sh}}{\delta P}$
$a_{23} = \dot{m}_{out} - \pi D_i \alpha_{i,sh}\frac{\delta \bar{T}_{sh}}{\delta P}$
$a_{25} = \alpha_{i,sh}\pi D_i(L - L_1)$
$a_{41} = \alpha_o \pi D_o(T_{amb} - T_{w,m}) - \alpha_{i,m}\pi D_i(T_{w,m} - \bar{T}_m)$
$a_{42} = \alpha_{i,m}\pi DiL_1\frac{\delta \bar{T}_m}{\delta P}$
$a_{44} = \alpha_{i,m}\pi D_i L_1 - \alpha_o \pi D_o L_1$
$a_{51} = \alpha_{i,sh}\pi D_i T_{w,m} - \alpha_{i,sh}\pi D_i \bar{T}_m - \alpha_o \pi D_o T_{amb} + \alpha_o \pi D_o T_{w,m}$
$a_{52} = \alpha_{i,sh}\pi D_i(L - L_1)\frac{\delta \bar{T}_{sh}}{\delta P}$
$a_{53} = \alpha_{i,sh}\pi D_i(L - L_1)\frac{\delta \bar{T}_{sh}}{\delta h_{out}}$
$a_{52} = -\alpha_{i,sh}\pi D_i(L - L_1) - \alpha_o \pi D_o(L - L_1)$

$b_{11} = h_{in} - h_{mg}$
$b_{12} = \dot{m}_{in}$
$b_{23} = h_{mg} - h_{out}$
$b_{31} = 1$
$b_{33} = -1$
$b_{44} = \pi L_1 D_o(T_{amb} - T_{w,m})\frac{\delta \alpha_o}{\delta V_a}$
$b_{54} = \pi(L - L_1)D_o(T_{amb} - T_{w,sh})\frac{\delta \alpha_o}{\delta V_a}$

Condenser matrix elements

C

This Appendix was written by me, in the last semester project. Since it has been taken directly from my previous report, it will be in appendix instead of in the report. The whole report from my last semester project can be found at [1].

This appendix will be describing the expressions of the elements in the matrices of the dynamic model of the condenser.

C.1 The dynamic matrix, D

$$d_c = \begin{bmatrix} d_{c,11} & 0 & d_{c,13} & 0 & 0 & 0 & 0 \\ d_{c,21} & d_{c,22} & d_{c,23} & 0 & 0 & 0 & 0 \\ d_{c,31} & d_{c,32} & d_{c,33} & d_{c,34} & 0 & 0 & 0 \\ d_{c,41} & d_{c,42} & d_{c,43} & 0 & 0 & 0 & 0 \\ d_{c,51} & 0 & 0 & 0 & d_{c,55} & 0 & 0 \\ 0 & 0 & 0 & 0 & 0 & d_{c,66} & 0 \\ d_{c,71} & d_{c,72} & 0 & 0 & 0 & 0 & d_{c,77} \end{bmatrix} \tag{C.1}$$

$d_{c,11} = 0.5A\rho_{sh}(h_{c,in} - h_{c,mg})$
$d_{c,13} = AL_{c,1}(\rho_{c,sh}\frac{dh_{c,mg}}{dP_c} + 0.5(h_{c,in} - h_{c,mg})(\frac{d\rho_{c,sh}}{dP_c} + \frac{d\rho_{c,sh}}{dh_{c,sh}}\frac{dh_{c,mg}}{dP_c} - 1)$
$d_{c,21} = A\rho_{c,l}h_{c,fg}$
$d_{c,22} = A\gamma\rho_{c,l}h_{c,fg}$
$d_{c,23} = AL_{c,2}(-(1-\gamma)\frac{d(\rho_{c,l}h_{c,fg})}{dP_c} + \rho_{c,m}\frac{dh_{c,mg}}{dP_c} - 1)$
$d_{c,31} = 0.5A\rho_{c,l}(h_{c,l} - h_{c,out})$
$d_{c,32} = 0.5A\rho_{c,l}(h_{c,l} - h_{c,out})$
$d_{c,33} = AL_{c,3}(0.5\rho_{c,l}\frac{dh_{c,l}}{dP_c} - 1)$
$d_{c,34} = 0.5AL_{c,3}\rho_{c,l}$
$d_{c,41} = A(\rho_{c,sh} - \rho_{c,l})$
$d_{c,42} = A(\rho_{c,m} - \rho_{c,l})$
$d_{c,43} = AL_{c,1}(\frac{d\rho_{c,sh}}{dP_c} + \frac{d\rho_{c,sh}}{h_{c,sh}}\frac{dh_{c,mg}}{dP_c}) + AL_{c,2}\frac{d\rho_{c,m}}{dP_c})$
$d_{c,51} = c_{p,w}\rho_w A_w(\frac{T_{w,c,sh} - T_{w,c,m}}{L_{c,1}})$
$d_{c,55} = c_{p,w}\rho_w A_w$
$d_{c,66} = c_{p,w}\rho_w A_w$
$d_{c,71} = c_{p,w}\rho_w A_w(\frac{T_{w,c,m} - T_{w,c,l}}{L_{c,3}})$

$d_{c,72} = c_{p,w}\rho_w A_w(\frac{T_{w,c,m}-T_{w,c,l}}{L_{c,3}})$
$d_{c,77} = c_{p,w}\rho_w A_w$

C.2 The Taylor series expansion matrices, A' and B'

$$A'_c = \begin{bmatrix} a_{c,11} & & a_{c,13} & 0 & a_{c,15} & 0 & 0 \\ 0 & a_{c,22} & a_{c,23} & 0 & 0 & a_{c,26} & 0 \\ a_{c,31} & a_{c,32} & a_{c,33} & a_{c,34} & 0 & 0 & a_{c,37} \\ 0 & 0 & 0 & 0 & 0 & 0 & 0 \\ 0 & 0 & a_{c,53} & 0 & a_{c,55} & 0 & 0 \\ 0 & 0 & a_{c,63} & 0 & 0 & a_{c,66} & 0 \\ 0 & 0 & a_{c,73} & a_{c,74} & 0 & 0 & a_{c,77} \end{bmatrix}, B'_c = \begin{bmatrix} b_{c,11} & b_{c,12} & 0 & 0 \\ 0 & 0 & b_{c,23} & 0 \\ 0 & 0 & b_{c,33} & 0 \\ b_{c,41} & 0 & b_{c,43} & 0 \\ 0 & 0 & 0 & b_{c,54} \\ 0 & 0 & 0 & b_{c,64} \\ 0 & 0 & 0 & b_{c,74} \end{bmatrix} \tag{C.2}$$

$a_{11} = \alpha_{i,c,sh}\pi D_i L_{c,1}$
$a_{13} = -(\dot{m}_{c,in}\frac{dh_{c,mg}}{dP_c} + \alpha_{i,c,sh}\pi D_i L_{c,1}(\frac{dT_{c,sh}}{dP_c} + \frac{dT_{c,sh}}{dh_{c,sh}}\frac{dh_{c,mg}}{dP_c}))$
$a_{15} = \alpha_{c,i,sh}\pi D_i L_{c,1}$
$a_{22} = \alpha_{i,c,m}\pi D_i(T_{w,c,m} - T_{c,m})$
$a_{23} = \dot{m}_{c,out}\frac{dh_{c,mg}}{dP_c} - m_{c,out}\frac{dh_{c,l}}{dP_c} - \alpha_{i,c,m}\pi D_i L_{c,2}\frac{T_{c,m}}{dP_c}$
$a_{26} = \alpha_{i,c,m}\pi D_i L_{c,2}$
$a_{31} = -\alpha_{i,c,l}\pi D_i(T_{i,c,l} - T_{c,l})$
$a_{32} = -\alpha_{i,c,l}\pi D_i(T_{i,c,l} - T_{c,l})$
$a_{33} = \dot{m}_{c,out}\frac{dh_{c,mg}}{dP_c} - alpha_{i,c,l}\pi D_i L_{c,3}\frac{T_{c,l}}{dP_c}$
$a_{34} = -\dot{m}_{c,out} - \alpha_{i,c,l}\pi D_i L_{c,3}\frac{dT_{c,l}}{dh_{c,out}}$
$a_{37} = \alpha_{i,c,l}\pi D_i L_{c,3}$
$a_{53} = \alpha_{i,c,sh}\pi D_i(\frac{dT_{c,sh}}{dP_c} + \frac{dT_{c,sh}}{dh_{c,sh}}\frac{dh_{c,mg}}{dP_c})$
$a_{55} = -(\alpha_{i,c,sh}\pi D_i + \alpha_{o,c,sh})$
$a_{63} = \alpha_{i,c,m}\pi D_i\frac{T_{dc,m}}{dP_c})$
$a_{66} = -(\alpha_{i,c,m}\pi D_i + \alpha_{o,c,m}\pi D_o)$
$a_{73} = \alpha_{i,c,l}\pi D_i\frac{dT_{c,l}}{dP_c}$
$a_{74} = \alpha_{i,c,l}\pi D_i\frac{dT_{c,l}}{dh_{c,out}}$
$a_{77} = -(\alpha_{i,c,l}\pi D_i + \alpha_{o,c,l}\pi D_o)$

$b_{c,11} = h_{c,in} - h_{c,mg}$
$b_{c,12} = \dot{m}_{c,in}$
$b_{c,23} = h_{c,mg} - h_{c,l}$
$b_{c,33} = h_{c,l} - h_{c,out}$
$b_{c,41} = 1$
$b_{c,43} = -1$
$b_{c,54} = \pi D_o$
$b_{c,64} = \pi D_o$
$b_{c,57} = \pi D_o$

Transfer functions for the system model

D

All of the system models transfer function, that are used in the report and in simulink are listed in zero, pole, gain form :

```
>> zpk(H(1,1))

ans =

  From input "ctrl.cpr_speed" to output "SysMon.QCool":
             0.44399 (s+1.169) (s+1) (s+0.9992) (s+0.7272) (s+0.3947) (s+0.0009876)
  ---------------------------------------------------------------------------------------------
  (s+11.63) (s+1)^3 (s+0.8386) (s+0.3495) (s+0.05659) (s+0.01) (s+0.00253) (s^2 + 2.018s + 1.021)
```

```
>> zpk(H(2,1))

ans =

  From input "ctrl.cpr_speed" to output "SysMon.Tsh":
          0.38705 (s+1) (s+1) (s+0.945) (s+0.8983) (s+0.3189) (s+0.214) (s+0.00753)
  ---------------------------------------------------------------------------------------
  (s+11.63) (s+1) (s+1) (s+0.8386) (s+0.3495) (s+0.05659) (s+0.00253) (s^2 + 2.018s + 1.021)
```

```
>> zpk(H(1,2))

ans =

  From input "ctrl.evap_vexp" to output "SysMon.QCool":
            -0.029741 (s+1.451) (s+1) (s+0.9179) (s-0.03195) (s^2 + 0.8946s + 0.3161)
  ---------------------------------------------------------------------------------------------
  (s+11.63) (s+1)^3 (s+0.8386) (s+0.3495) (s+0.05659) (s+0.01) (s+0.00253) (s^2 + 2.018s + 1.021)
```

```
>> zpk(H(2,2))

ans =

  From input "ctrl.evap_vexp" to output "SysMon.Tsh":
      -0.025927 (s+0.7781) (s+1) (s+1.001) (s+0.4277) (s+0.03733) (s^2 + 1.14s + 0.6956)
  ---------------------------------------------------------------------------------------
  (s+11.63) (s+1) (s+1) (s+0.8386) (s+0.3495) (s+0.05659) (s+0.00253) (s^2 + 2.018s + 1.021)
```

```
>> zpk(D1)

ans =

  From input "SysMon.Tsh" to output "SysMon.Tsh":

  14.929 (s+11.63) (s+1.018) (s+0.9773) (s+0.9461) (s+0.8983) (s+0.8386) (s+0.3495) (s+0.3189)

           (s+0.214) (s+0.05659) (s+0.00753) (s+0.00253) (s^2 + 2.004s + 1.005) (s^2 + 2.018s + 1.02)

  ---------------------------------------------------------------------------------------------------

  (s+11.63) (s+1.009) (s+0.9913) (s+0.8386) (s+0.7781) (s+0.4277) (s+0.3495) (s+0.05659) (s+0.03733)

                      (s+0.00253) (s^2 + 2.001s + 1.001) (s^2 + 2.018s + 1.021) (s^2 + 1.14s + 0.6956)
```

```
>> zpk(D2)

ans =

  From input "SysMon.QCool" to output "SysMon.QCool":

  0.066985 (s+11.63) (s+1.451) (s+1.014) (s+0.9856) (s+0.9179) (s+0.8386) (s+0.3495) (s+0.05659)

           (s-0.03195) (s+0.01) (s+0.00253) (s^2 + 2.001s + 1.001) (s^2 + 2.018s + 1.021) (s^2 + 0.8946s + 0.3161)

  ---------------------------------------------------------------------------------------------------------------

      (s+11.63) (s+1.169) (s+0.9654) (s+0.8386) (s+0.7272) (s+0.3947) (s+0.3495) (s+0.05659) (s+0.01)

              (s+0.00253) (s+0.0009876) (s^2 + 2.062s + 1.063) (s^2 + 1.968s + 0.9693) (s^2 + 2.022s + 1.025)
```

```
>> zpk(Hqcool)

ans =

  From input to output "SysMon.QCool":

  2.0073e-16 (s+1.313e14) (s+11.5) (s+0.2945) (s+0.1656) (s+0.9747) (s+0.6756) (s+0.06354)

           (s+0.01002) (s+0.002719) (s^2 + 0.004866s + 5.947e-06) (s^2 + 0.1065s + 0.00286)

           (s^2 + 23.4s + 136.9) (s^2 + 0.3568s + 0.05041) (s^2 + 0.3959s + 0.1146) (s^2 + 5.129s + 6.726)

           (s^2 + 0.4685s + 0.2662) (s^2 + 0.6863s + 0.5815) (s^2 + 1.072s + 1.098) (s^2 + 1.629s + 1.92)

                                                    (s^2 + 4.144s + 5.634) (s^2 + 2.614s + 3.437)

  -----------------------------------------------------------------------------------------------------------

  (s+11.63)^3 (s+1.469) (s+0.5861) (s+0.4277) (s+0.3527) (s+0.05659)^3 (s+0.03733) (s+0.01)^2

           (s+0.00253)^3 (s^2 + 0.696s + 0.1211) (s^2 + 1.217s + 0.3829) (s^2 + 2.859s + 2.076)

           (s^2 + 1.337s + 0.4903) (s^2 + 1.515s + 0.6266) (s^2 + 1.539s + 0.6928) (s^2 + 2.648s + 1.856)

           (s^2 + 1.765s + 0.9366) (s^2 + 2.361s + 1.558) (s^2 + 2.052s + 1.237) (s^2 + 1.14s + 0.6957)
```

```
>> zpk(Htsh)

ans =

  From input to output "SysMon.Tsh":

  -1.1721e-17 (s+1.313e14) (s+11.7) (s+0.06723) (s+0.00995) (s+0.002851) (s^2 + 0.004752s + 5.695e-06)

          (s^2 + 0.1034s + 0.002721) (s^2 + 0.3266s + 0.02953) (s^2 + 23.2s + 134.6) (s^2 + 0.363s + 0.06237)

          (s^2 + 0.4313s + 0.1405) (s^2 + 4.899s + 6.157) (s^2 + 0.5673s + 0.303) (s^2 + 1.191s + 0.622)

          (s^2 + 0.8291s + 0.6263) (s^2 + 1.269s + 1.262) (s^2 + 3.915s + 4.843) (s^2 + 2.753s + 3.044)

                                                                                  (s^2 + 2.062s + 2.244)

  ----------------------------------------------------------------------------------------------------------------------

     (s+11.63)^3 (s+1.405) (s+1.149) (s+0.3947) (s+0.3474) (s+0.05659)^3 (s+0.01) (s+0.00253)^3

             (s+0.0009876) (s^2 + 0.7012s + 0.1229) (s^2 + 1.222s + 0.3755) (s^2 + 1.282s + 0.4314)

             (s^2 + 2.758s + 1.924) (s^2 + 1.394s + 0.5386) (s^2 + 2.585s + 1.752) (s^2 + 1.554s + 0.6984)

                                    (s^2 + 1.767s + 0.9151) (s^2 + 2.32s + 1.482) (s^2 + 2.03s + 1.185)
```

List of References

[1] Ajdin Kovacevic. Model of a transport refrigeration systems for future designs of robust control. https://projekter.aau.dk/projekter/da/studentthesis/model-of-a-transport-refrigeration-systems-for-future-designs-of-robust-control(4383.html. Last seen: 22-02-2018.

[2] Kresten Kjær Sørensen. Model based control of reefer container systems. http://kom.aau.dk/~jakob/phdStudents/krestenSoerensenThesis.pdf. Last seen: 07-01-2020.

[3] The Engineering ToolBox. Mollier diagram. https://www.engineeringtoolbox.com/psychrometric-chart-mollier-d_27.html. Last seen: 07-01-2020.

[4] Palle Andersen Steen Tøffner-Clausen and Jakob Stoustrup. Robust control. https://www.moodle.aau.dk/pluginfile.php/1154906/mod_resource/content/2/Notes%20Robust%20Control.pdf. Last seen: 07-01-2020.

[5] Jakob Munch Jensen. Dynamic modeling of thermo-fluid systems - with focus on evaporators for refrigeration, march, 2003. https://www.moodle.aau.dk/pluginfile.php/1154626/mod_folder/content/0/Munch_Dynamic_Modeling_of_ThermoFluid_Systems_web.pdf?forcedownload=1. Last seen: 07-01-2020.

[6] Xiang-Dong He. Dynamic modeling and multivariable control of vapor compression cycles in air conditioning systems. http://hdl.handle.net/1721.1/10725. Last seen: 07-01-2020.